

Development of Bioengineering Strategies for Periodontal Tissue Regeneration

Laura Sofia Alves

Thesis to obtain the Master of Science Degree in

Biological Engineering

Supervisor: Dr. Marta Monteiro Silva Carvalho

Examination Committee

Chairperson: Prof. Frederico Castelo Alves Ferreira

Supervisor: Dr. Marta Monteiro Silva Carvalho

Members of the Committee: Dr. João Carlos Fernandes da Silva

December 2021

DECLARATION

I declare that this document is an original work of my own authorship and that it fulfills all the requirements of the Code of Conduct and Good Practices of the Universidade de Lisboa.

PREFACE

The work presented in this thesis was performed at the Institute for Bioengineering and Biosciences of Instituto Superior Técnico (Lisbon, Portugal), during the period March-November 2021, under the supervision of Dr. Marta Monteiro Silva Carvalho.

ACKNOWLEDGEMENTS

First, I would like to thank my supervisor, Dr. Marta Silva Carvalho, for her guidance and support. Marta's mentoring was paramount in the making and presenting of this work. Her valuable advice taught me not only how to write a MSc thesis, but also how to understand scientific research and ask research questions.

I would also like to express my gratitude to Prof. Joaquim Sampaio Cabral, Prof. Frederico Ferreira and Prof. Cláudia Lobato da Silva for the opportunity to join the Stem Cell Engineering Research Group in iBB (IST, Portugal). I would like to give a special thanks to Prof. Cláudia Lobato da Silva for her support and readiness to help in the first steps of this final chapter to attain a Master of Science Degree.

I would like to thank the funding received from FCT - Fundação para a Ciência e a Tecnologia, I.P., in the scope of the project DentalBioMatrix (PTDC/BTM-BTM/3537/2020) of the Research Unit Institute for Bioengineering and Biosciences-iBB. I also would like to express my gratitude for the funding received from FCT to iBB (UIDB/04565/2020 and UIDP/04565/2020) and to i4HB - the Associate Laboratory Institute for Health and Bioeconomy (LA/P/0140/2020).

ABSTRACT

Periodontitis is an inflammatory disease caused by dental plaque accumulation that can damage the periodontium. Periodontium is composed by hard (cementum and alveolar bone) and soft (periodontal ligament) tissues. In this work, a novel strategy for periodontal tissue regeneration, namely alveolar bone, was explored by combining human periodontal ligament stem cells (PDLSCs) with 3D-printed polycaprolactone (PCL) scaffolds with different pore sizes (100 μm , 300 μm and 600 μm). Thus, we isolated and characterized PDLSCs from human teeth of healthy donors and compared the osteogenic potential of these cells with mesenchymal stromal cells (MSCs) derived from bone marrow (BMMSCs) and adipose tissue (ATMSCs). Results demonstrated that PDLSCs presented MSC-like morphology, MSC-related marker expression and multilineage differentiation capacity (adipogenic, chondrogenic and osteogenic). Despite this, immunocytochemistry assays showed that PDLSCs expressed osteopontin, osteocalcin, asporin and Stro-1, while BMMSCs and ATMSCs did not. Moreover, only PDLSCs expressed CD146 and presented higher proliferative potential than BMMSCs and ATMSCs. Furthermore, results demonstrated that, after osteogenic differentiation, PDLSCs exhibited higher calcium content and an enhanced upregulation of osteogenic/periodontal genes compared to ATMSCs and BMMSCs. However, alkaline phosphatase activity of PDLSCs did not increase. Lastly, PDLSCs were successfully cultured in PCL scaffolds with different pore sizes. Results suggested that lower pore sizes (100 μm and 300 μm) favored PDLSC proliferation. Future studies should evaluate the osteogenic potential of PDLSCs in PCL scaffolds for alveolar bone regeneration applications. Overall, the results showed that PDLSCs are a promising cell source for periodontal regeneration, presenting enhanced proliferative and osteogenic potential.

Keywords: Alveolar Bone, Mesenchymal Stromal Cells, Periodontal Ligament Stem Cells, Periodontium, Polycaprolactone

RESUMO

Periodontite é uma doença inflamatória causada por acumulação de placa dentária, podendo danificar o periodonto. O periodonto é composto por tecido mineralizado (cimento e osso alveolar) e fibroso (ligamento periodontal). Neste trabalho, explora-se uma nova estratégia para regeneração de osso alveolar, combinando células estaminais do ligamento periodontal humano (CELPDs) com suportes de policaprolactona (PCL) impressos em três-dimensões com diferentes tamanhos de poro (100 μm , 300 μm e 600 μm). Para tal, isolámos e caracterizámos CELPDs de dentes humanos saudáveis e comparámos o potencial osteogénico destas com células estromais mesenquimais (CEMs) de medula óssea (CEMMOs) e tecido adiposo (CEMTAs). CELPDs exibiram morfologia típica de CEMs, expressão de marcadores relacionados com CEMs e capacidade de diferenciação multilinhagem. Contudo, ensaios de imunocitoquímica mostraram que as CELPDs expressaram osteopontina, osteocalcina, asporina e Stro-1, enquanto os CEMMOs e CEMTAs não. Além disso, apenas CELPDs expressaram CD146 e apresentaram maior potencial proliferativo do que CEMMOs e CEMTAs. Após diferenciação osteogénica, as CELPDs exibiram maior concentração de cálcio e sobre-expressão superior de genes osteogénicos/periodontais comparando com CEMTAs e CEMMOs. Contudo, a atividade da fosfatase alcalina das CELPDs não aumentou. Por último, as CELPDs foram cultivadas em suportes de PCL. Resultados mostram que menores tamanhos de poro (100 μm e 300 μm) favorecem a proliferação de CELPDs. Estudos futuros devem avaliar o potencial osteogénico de CELPDs em suportes de PCL para aplicações em regeneração óssea alveolar. No geral, os resultados mostraram que as CELPDs são uma fonte celular promissora para regeneração periodontal, apresentando potencial proliferativo e osteogénico superior.

Palavras-Chave: Células Estaminais do Ligamento Periodontal, Células Estromais Mesenquimais, Osso Alveolar, Periodonto, Policaprolactona

CONTENTS

- 1. Aims and Objectives..... 1
- 2. Introduction..... 3
 - 2.1. The Periodontium..... 3
 - 2.1.1. Cementum..... 3
 - 2.1.2. Alveolar Bone..... 4
 - 2.1.3. Periodontal Ligament 4
 - 2.2. Periodontitis..... 8
 - 2.2.1. Disease Mechanism and Inflammatory Response 8
 - 2.2.2. Risk Factors 9
 - 2.3. Treatment of Periodontitis 10
 - 2.3.1. Non-surgical Treatment 10
 - 2.3.2. Surgical Treatment..... 10
 - 2.3.2.1. Bone Grafts 11
 - 2.3.2.2. Scaffolds 12
 - 2.3.2.3. Membrane Guided Tissue Regeneration 13
 - 2.4. Periodontal Ligament Stem Cells 15
 - 2.4.1. Characteristics of PDLSCs 16
 - 2.4.2. Identification and Isolation of PDLSCs 18
 - 2.4.3. Culture Methods and Conditions..... 19
 - 2.5. New Strategies for Periodontal Regenerative Therapy and Alveolar Bone Regeneration 20
 - 2.5.1. Stem Cell-based Therapies 20
 - 2.5.2. Three-Dimensional Scaffold Manufacturing..... 21
 - 2.5.3. 3D Printed PCL Scaffolds for Periodontal Regeneration 22
- 3. Materials and Methods 25
 - 3.1 PDLSC Isolation and Culture 25
 - 3.2 ATMSC and BMMSCs Cell Culture..... 25
 - 3.3 Multilineage Differentiation and Stainings 26
 - 3.4 Flow Cytometry Analysis 27
 - 3.5 Immunocytochemistry Analysis..... 27

3.6 Cell morphology assay	28
3.7 Kinetics Assay	28
3.8 Quantitative Assessment of Osteogenic Differentiation	29
3.9 Fabrication of 3D printed PCL Scaffolds by FDM	30
3.10 PCL Scaffold Sterilization and PDLSC Seeding	31
3.11 Metabolic Activity and Morphology of PDLSCs cultured in 3D printed PCL Scaffolds.....	32
4. Results.....	33
4.1. Isolation and Characterization of Periodontal Ligament Stem Cells	33
4.1.1. Expression of Mesenchymal Stromal Markers	33
4.1.1.1. Flow Cytometry	33
4.1.1.2. Immunocytochemistry Analysis.....	35
4.1.2. Multilineage Differentiation.....	36
4.1.3. PDLSC Growth Kinetics	36
4.2. Comparison of MSCs derived from Adipose Tissue, Bone Marrow and Periodontal Ligament .	38
4.2.1. Expression of Mesenchymal Stromal Markers	38
4.2.1.1. Flow Cytometry	38
4.2.1.2. Immunocytochemistry Analysis.....	38
4.2.2. Multilineage Differentiation.....	41
4.2.3. Growth Kinetics and Morphology	41
4.3. Osteogenic Potential of MSCs derived from Adipose Tissue, Bone Marrow and Periodontal Ligament	45
4.3.1. Calcium and Alkaline Phosphatase Activity Quantification.....	46
4.3.2. Gene Expression.....	46
4.3.3. Immunocytochemistry Analysis.....	46
4.4. PDLSC Culture on 3D Printed PCL Scaffolds.....	48
4.4.1. Cell Proliferation.....	48
4.4.2. Cell Morphology	48
5. Discussion	51
5.1. Isolation and Characterization of Periodontal Ligament Stem Cells (PDLSCs).....	51
5.2. Comparison of Periodontal Ligament Stem Cells with MSCs derived from Adipose Tissue and Bone Marrow.....	53

5.3. Osteogenic Potential of MSCs derived from Adipose Tissue, Bone Marrow and Periodontal Ligament	56
5.4. PDLSC Culture on 3D Printed PCL Scaffolds.....	59
6. Conclusions	61
7. Future Work.....	63
8. References	65

LIST OF FIGURES

Figure 1. Structures of the periodontium: alveolar bone, periodontal ligament, and cementum.....	5
Figure 2. Illustration of periodontal ligament (PDL) and its collagenous fibers that connect the root cementum to the alveolar bone..	6
Figure 3. Longitudinal section of the periodontium illustrating Sharpey fibers within both the alveolar bone and cementum, and principal fiber subgroups of the periodontal ligament: alveolar crest group, horizontal group, oblique group, apical group, and interradicular group.....	8
Figure 4. Illustration of healthy gingiva, gingivitis, early-to-moderate periodontitis and advanced periodontitis..	10
Figure 5. Illustration of healthy periodontium, periodontitis, and current surgical regenerative treatment options..	13
Figure 6. Multipotency of PDLSCs. PDLSCs have been successfully differentiated into osteoblasts, adipocytes, chondrocytes, fibroblasts, pancreatic islet cells, endothelial cells, retinal ganglion cells, neural cells, myocytes, and cementoblasts.....	18
Figure 7. Mesenchymal stromal cell (MSC) ability to self-renew and differentiate into the mesodermal lineage..	20
Figure 8. 3D scaffold printing technologies. .	23
Figure 9. Schematic diagram of FDM extrusion 3D printing with PCL filament.....	33
Figure 10. Models and dimensions of polycaprolactone scaffolds generated with CAD for 3D printing by fused deposition modelling with different pore sizes (100 µm, 300 µm and 600 µm).....	33
Figure 11. PDLSC isolation..	35
Figure 12. Characterization of PDLSCs by immunophenotypic analysis.	36
Figure 13. Characterization of PDLSCs by immunocytochemistry analysis..	37
Figure 14. <i>In vitro</i> multilineage differentiation of PDLSCs. Adipogenic differentiation was detected by Oil red o staining showing the lipid vacuoles in red. Alcian blue stains proteoglycans in blue synthesized by chondrocytes. Alkaline phosphatase (ALP) and von Kossa (VK) stainings show ALP activity in red and mineralized extracellular matrix deposits in black. Alizarin red stains the calcium deposited in the extra-cellular matrix in red.	38
Figure 15. Proliferation of PDLSCs cultured in expansion conditions (DMEM + 10%FBS + 1% A/A) seeded at 1.5×10^2 , 1.5×10^3 and 3.0×10^3 cells/cm ² in 12-well plates.....	39
Figure 16. Bright field images depicting different zones of a 12-well plate bottom with PDLSC cultured for 12 days in expansion conditions (DMEM +10% FBS + 1% A/A) at 1.5×10^2 cells/cm ² ..	39
Figure 17. Immunophenotypic analysis of PDLSCs, ATMSCs and BMMSCs cultured in expansion conditions (DMEM + 10%FBS + 1% A/A) at passages 3, 5 and 7 by flow cytometry.)	41
Figure 18. Comparison of immunofluorescent staining images for PDLSCs, BMMSCs and ATMSCs for the expression of fibronectin (Fib, green), laminin (Lam, red), stro-1 (STRO-1, red), asporin (ASPN, red), osteopontin (OPN, red) and osteocalcin (OC, red).	42

Figure 19. *In vitro* multilineage differentiation of PDLSCs, ATMSCs and BMMSCs. Adipogenic differentiation was detected with Oil red o staining showing the lipid vacuoles in red. Alcian blue stained sulfated glycosaminoglycans in blue. Alkaline phosphatase (ALP) and von Kossa (VK) stainings showed ALP activity in red and mineralized extracellular matrix deposits in black. Alizarin red stained calcium deposits in the extracellular matrix in red. 44

Figure 20. Growth curves for PDLSCs, BMMSCs and ATMSCs cultured in expansion conditions (DMEM + 10%FBS + 1% A/A) for 9 days at two different cell seeding densities: 1.5×10^3 and 3.0×10^3 cells/cm².. 45

Figure 21. Proliferation of PDLSCs, ATMSCs and BMMSCs cultured in expansion conditions (DMEM + 10%FBS + 1% A/A) seeded at 1.5×10^2 , 1.5×10^3 and 3.0×10^3 cells/cm² in 12-well plates.. 45

Figure 22. Morphology of PDLSCs, ATMSCs and BMMSCs at days 1, 3, 5 and 7 of culture in expansion conditions (DMEM + 10% FBS + 1% A/A) at 3×10^3 cells/cm²..... 46

Figure 23. Quantitative assessment of calcium content and alkaline phosphatase (ALP) activity of PDLSCs, BMMSCs and ATMSCs cultured for 21 days under expansion (DMEM) and osteogenic differentiation (OSTEO) conditions, normalized to metabolic activity. 47

Figure 24. qRT-PCR analysis of PDLSCs, BMMSCs and ATMSCs after 21 days of osteogenic differentiation. 48

Figure 25. Immunocytochemistry analysis of PDLSCs, BMMSCs and ATMSCs cultured under osteogenic differentiation conditions for 21 days. 50

Figure 26. A. Proliferation of PDLSCs cultured for 10 days in expansion conditions (DMEM + 10% FBS + 1% A/A) on polycaprolactone scaffolds with different pore sizes (100 μm, 300 μm and 600 μm)..... 50

Figure 27. Bright field images of 3D printed polycaprolactone scaffolds after 1 day of PDLSC culture in expansion conditions (DMEM +10% FBS + 1% A/A)..... 51

Figure 28. PDLSC morphology in 3D printed polycaprolactone scaffolds with different pore sizes (100 μm, 300 μm and 600 μm). 51

LIST OF TABLES

Table 1. Forward and reverse primer sequences used in qRT-PCR analysis.....	32
--	----

LIST OF ABBREVIATIONS

3D	Three Dimensional
ALP	Alkaline Phosphatase
AR	Alizarin Red
ASP	Asporin
ATMSC	Adipose Tissue Mesenchymal Stromal Cells
BMMSC	Bone Marrow Mesenchymal Stromal Cells
BSA	Bovine Serum Albumin
CAD	Computer Aided Design
cDNA	Complementary Deoxyribonucleic Acid
CEMP-1	Cementum Protein 1
CNC	Cranial Neural Crest
CO₂	Carbon Dioxide
DMEM	Dulbecco's Minimum Essential Medium
DNA	Deoxyribonucleic acid
ECM	Extra-cellular Matrix
ERM	Epithelial Cell Rests of Malassez
ESC	Embryonic Stem Cells
FBS	Fetal Bovine Serum
FGF	Fibroblast Growth Factor
FMD	Fused Deposition Modelling
GAG	Glycosaminoglycan
GTR	Guided Tissue Regeneration
HCl	Hydrochloric acid
HERS	Hertwig's Ephythelial Root Sheath
HSC	Hematopoietic Stem Cell
IFN-γ	Inflammatory Cytokine Interferon Gamma
ISCT	International Society for Cellular Therapy
IST	Instituto Superior Técnico
JE	Junctional Ephythelium
LIFT	Laser-induced Forward Transfer
LPS	Lipopolysaccharides
MCAM	Melanoma Cell Adhesion Molecule
α-MEM	alpha-Minimum Essential Medium
MHC	Major Histocompatibility Complex
MMP	Matrix Metalloproteinases
MSC	Mesenchymal Stromal Cell
OC	Osteocalcin
OPN	Osteopontin
PBMNC	Peripheral Blood Mononuclear Cells

PCL	Polycaprolactone
PD	Population Doubling
PDL	Periodontal Ligament
PDLSC	Periodontal Ligament Stem Cells
PFA	Paraformaldehyde
PGA	Polyglycolic Acid
PGLA	Poly(lactic-co-glycolic) Acid
PLA	Poly(lactic) Acid
PLAP	Periodontal Ligament-Associated Protein 1
PLGA	Poly(lactic-co-glycolic) Acid
PMN	Polymorphonuclear Leukocytes
iPSC	Induced Pluripotent Stem Cell
PTFE	Polytetrafluorethylene
RM	Regenerative Medicine
qRT-PCR	Quantitative Reverse Transcription-Polymerase Chain Reaction
RUNX2	RUNX Family Transcription Factor 2
SCERG	Stem Cell Engineering Research Group
SD	Standard Deviation
TE	Tissue Engineering
TGF-β1	Transforming Growth Factor beta 1
TNF-α	Tumour Necrosis Factor-alpha
VCAM	Vascular Cell Adhesion Molecule 1
VK	Von Kossa

1. AIMS AND OBJECTIVES

Since Seo and colleagues (Seo *et al.* 2004) first isolated PDLSCs in 2004, several additional reports have confirmed the presence of MSC-like cells in the human PDL. This discovery opened exciting applications since the use of these cells may constitute an advantage in novel strategies for regenerative periodontal therapy. However, aiming to develop successful novel periodontal tissue regeneration strategies, it is crucial to establish a reproducible isolation protocol from PDL samples and to assess the PDLSC *in vitro* properties, such as cell proliferation and differentiation. Furthermore, it is important to evaluate the capacity of PDLSCs incorporated into scaffold-based TE approaches.

The aims of the MSc thesis work herein presented can be summarized in the following goals:

1. *Isolation and characterization of PDLSCs*

The work carried out in this MSc thesis intends to implement an efficient and reproducible PDLSC isolation protocol in the Stem Cell Engineering Research Group (SCERG, iBB-IST, Portugal). The identity of isolated cells was assessed by flow cytometry analysis of surface marker expression, immunofluorescent stainings and multilineage differentiation assays. Considering the critical need for optimization of *ex vivo* cell expansion, due to low numbers of harvested cells from PDL samples, proliferative capacity of PDLSCs was evaluated and the effect of cell passaging was also assessed.

2. *Comparison of MSCs derived from adipose tissue, bone marrow and periodontal ligament*

Definition of specific markers for PDLSC identification is crucial for stem cell-based periodontal regeneration applications. Thus, this MSc thesis aims to investigate an alternative source of accessible MSCs, PDL, that can be harvested without invasive surgical procedures. In this context, PDLSCs were compared with MSCs derived from bone marrow (BMMSCs) and from adipose tissue (ATMSCs), regarding cell surface marker expression analyzed by flow cytometry, immunocytochemistry, multilineage differentiation potential, morphology, and growth kinetics.

3. *Comparison of osteogenic potential of MSCs derived from adipose tissue, bone marrow and periodontal ligament*

The therapeutic potential of MSCs may vary according to the tissue of origin. Thus, differences in osteoblast phenotype expression may be observed in MSCs derived from different tissues.

For periodontal tissue regeneration, the differentiation of progenitor cells into osteoblasts is a key step to regenerate alveolar bone that is lost during root resorption processes triggered by periodontitis. In this context, this MSc thesis aims to evaluate the osteogenic potential of MSCs derived from PDL and to compare with MSCs derived from bone marrow and adipose tissue, aiming to determine the best source to be applied for periodontal tissue regeneration strategies. Therefore, several techniques and assays were performed to assess the osteogenic *in vitro*

differentiation potential of PDLSCs, BMSCs and ATMSCs, focusing on calcium content, alkaline phosphatase quantification, transcript relative expression and immunocytochemistry analysis.

4. PDLSC culture on 3D printed PCL scaffolds

Aiming to contribute to the development of new bioengineering strategies for periodontal tissue regeneration, this MSc thesis aims to assess PDLSCs proliferation capacity in 3D printed PCL scaffolds with different pore sizes. PDLSCs were seeded onto 3D printed PCL scaffolds with different pore sizes (100, 300 and 600 μm). Cell adhesion, morphology and proliferation were evaluated for scaffolds with different pore sizes. Finally, the effect of mean pore size on PDLSC proliferation was assessed.

2. INTRODUCTION

2.1. THE PERIODONTIUM

The periodontium is a dynamic structure composed by specialized tissues that surround the tooth and provide attachment to the bone of the jaw. Periodontium has an important role by allowing the teeth to withstand the forces of mastication. Periodontium is composed by several tissues: alveolar bone, cementum and periodontal ligament (PDL) (Fehranbat and Popowics, 2015) (Figure 1).

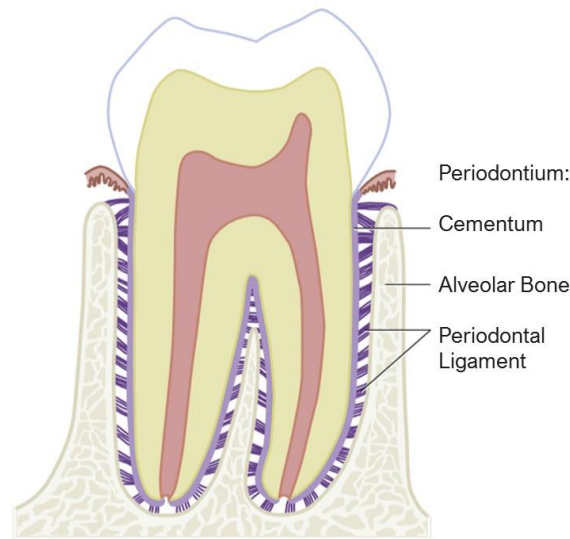


Figure 1. Structures of the periodontium: alveolar bone, periodontal ligament, and cementum. Adapted from Fehranbat and Popowics, 2015.

2.1.1.1. *Cementum*

Cementum is a hard, avascular connective tissue that covers the roots of teeth. Cementum is located between the tooth root and the PDL. Thus, its primary function is to attach PDL fibers.

Two types of cementum can be identified by the presence or absence of cells and by the origin of the collagen fibers of the matrix. Acellular cementum provides attachment for the tooth, while cellular cementum has an adaptive role in response to tooth wear and movement and is associated with repair of periodontal tissues (Cho and Garant, 2000; Nanci and Bosshardt, 2006).

Cementum composition is similar to bone with about 65% of its weight composed of inorganic material, 23% of organic material and 12% of water (Fehranbat and Popowics, 2015). The main organic component is type I collagen, constituting up to 90% of the organic matrix (Nanci and Bosshardt, 2006). Interestingly, almost all non-collagenous matrix proteins identified in cementum are also found in bone, including fibronectin, osteocalcin, osteonectin, osteopontin (Bosshardt, 2005).

Periodontal regeneration requires the formation of new cementum from precursor cells, cementoblasts. However, the origin of cementoblasts and the molecular factors regulating their recruitment and differentiation are not yet fully understood. Still, reports have suggested that PDL may

be a source of cementoblast progenitors in adult humans (Liu *et al.*, 1997; Grzesik and Narayanan, 2002).

2.1.2. Alveolar Bone

The alveolar bone arises from the maxilla or mandible and is the part of the bone that contains the sockets for the teeth. Alveolar bone is a hard, mineralized tissue being composed by 60% of inorganic material, 25% of organic material, and 15% of water (Fehranbat and Popowics, 2015). Alveolar bone has an important role in anchoring the roots of teeth by attaching the PDL fibers to the teeth sockets. Additionally, alveolar bone is responsible for blood vessel supply to the PDL. Moreover, since the tooth is continuously making minor movements, alveolar bone is always remodeling to meet the functional demand placed by the forces of mastication (Kumar, 2019). In fact, during tooth migration, alveolar bone is maintained healthy by a constant remodeling of the matrix. Bone remodeling allows the balance between bone resorption and bone deposition and a failure in this balance can lead to several pathologies, such as osteoporosis (Carvalho *et al.*, 2021). Similarly to what has been proposed for cementum maintenance and repair, evidence suggests that alveolar bone balance is maintained by progenitor cells that can differentiate into osteoblasts and osteoclasts (Nanci and Bosshardt, 2006; Kumar, 2019).

2.1.3. Periodontal Ligament

PDL is a highly cellular, fibrous connective tissue placed in the periodontal space between the alveolar bone and the cementum covering the root (Figure 2). The width of the PDL typically ranges from 0.15 to 0.38 mm, showing a progressive decrease in thickness with age (Kumar, 2019). This specialized tissue comprises several heterogenous cell populations and an extracellular compartment of collagenous fibers. PDL cell populations include osteoblasts, osteoclasts, fibroblasts, epithelial cell rests of Malassez (ERMs), macrophages, PDL stem cells (PDLSCs), and cementoblasts, making it a cell reservoir for tissue homeostasis and repair/regeneration. The extracellular compartment consists of well-defined collagen fibers bundles, mainly composed by glycosaminoglycans, glycoproteins, and glycolipids (Nanci and Bosshardt, 2006; Nanci, 2017).

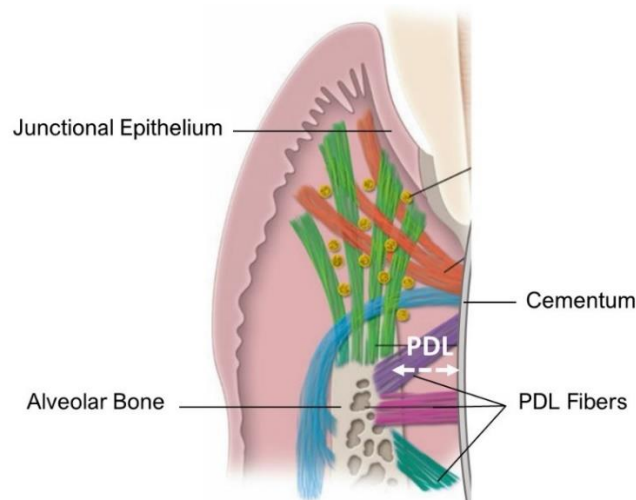


Figure 2. Illustration of periodontal ligament (PDL) and its collagenous fibers that connect the root cementum to the alveolar bone. Adapted from Nanci, 2017.

PDL has been reported to have several important functions, such as supportive, sensory, nutritive, and remodeling (Chiego, 2019):

- i) Supportive: The principal function of the PDL is to attach the teeth to the alveolar bone, allowing the teeth to withstand changes in physical forces during mastication, speech, and orthodontic tooth movement.
- ii) Sensory: PDL is an innervated tissue. The nerve receptors assure proper positioning of the jaw and contribute to the sensations of touch and pressure on the teeth.
- iii) Nutritive: Blood vessels that are present in the PDL provide essential nutrients for the ligament's vitality and for the hard tissues, cementum and alveolar bone.
- iv) Remodeling: Maintenance of the masticatory apparatus. PDL is composed by progenitor cells that differentiate into osteoblasts and osteoclasts, allowing the maintenance and repair of alveolar bone.

Moreover, the PDL's ability to maintain its width over time suggests the existence of a finely regulated control over cellular organization and signaling in the local site, allowing for an appropriate balance between formation and maintenance of hard (alveolar bone and cementum) and soft tissues (McCulloch, Lekic and McKee, 2000; Nanci, 2017). Furthermore, during development and regeneration, cells present in the PDL secrete molecules, such as osteocalcin, that can regulate the extent of mineralization and prevent the fusion of the tooth root with surrounding bone (Brito, 2013). Moreover, at the genetic level, it has been reported that the transcription factor *Msx2* (a known tendon and ligament mineralization inhibitor) prevents the osteogenic differentiation of PDL fibroblasts by repressing *Runx2* (the main transcription factor for osteogenic differentiation) transcriptional activity (Yoshizawa *et al.*, 2004). Lastly, the PDL also has the capacity to adapt to functional changes. When the functional demand increases, the width of the PDL can increase by as much as 50% and the fiber bundles also increase greatly in thickness (Nanci and Bosshardt, 2006). On the other hand, a decrease in function leads to narrowing of the ligament and a decrease in number and thickness of the fiber bundles. These functional modifications of the PDL also implicate adaptive changes in the bordering cementum and alveolar bone (Nanci and Bosshardt, 2006).

2.1.3.1. Periodontal Ligament Fibers

The collagen fibers of the PDL are critical for tooth support and attachment to bone (McCulloch, Lekic and McKee, 2000). The vast majority of collagen fibrils in the PDL are organized into groups or bundles according to their specific function and orientation to the tooth (Figure 3). These fibers consist of collagen type I, which accounts for ~80% of the total collagen present in the PDL, and are referred to as principal fibers (Berkovitz, 1990; Fehranbat and Popowics, 2015). At the end, each principal fiber is anchored by their insertion into either the wall of the alveolar bone or the tooth cementum. The embedded portion calcifies to a substantial degree, forming Sharpey fibers, and ensuring the attachment of the teeth to the hard tissues of the periodontium (McCulloch, Lekic and McKee, 2000; Nanci, 2017). In addition to collagen fibers, elastic-like oxytalan fibers have also been identified in human PDL, constituting around 3% of the total PDL fibers (Berkovitz, 2004). These fibers are parallel to the

cementum surface and form a branching network that surrounds the root. The function of these elastic fibers is not fully understood, however they have been associated with the neural and vascular network of the PDL and may regulate vascularization (Sims, 1975; Strydom *et al.*, 2012; de Jong *et al.*, 2017; Nanci, 2017)

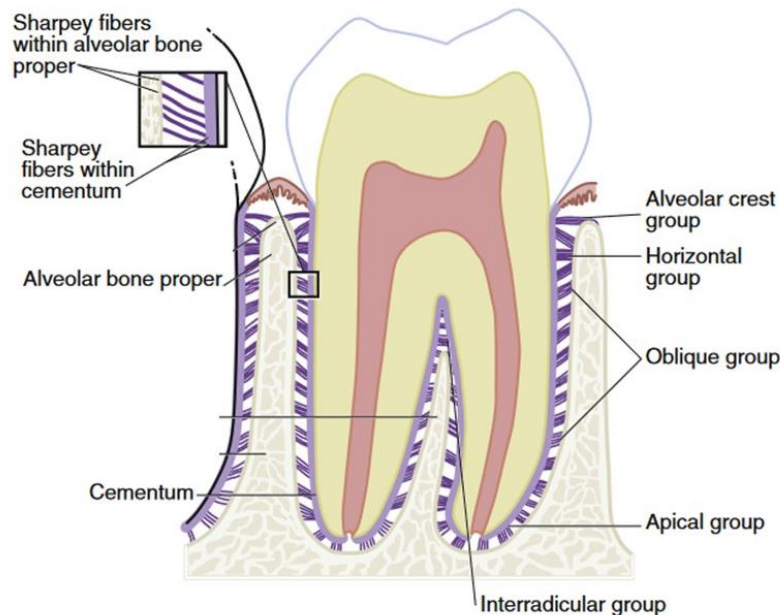


Figure 3. Longitudinal section of the periodontium illustrating Sharpey fibers within both the alveolar bone and cementum, and principal fiber subgroups of the periodontal ligament: alveolar crest group, horizontal group, oblique group, apical group, and interradicular group. Adapted from Fehranbat and Popowics, 2015.

2.1.3.2. Periodontal Ligament Cells

As mentioned above, the PDL contains an heterogeneous cell population, including fibroblasts, epithelial cells, precursor and resorptive cells, macrophages and periodontal ligament stem cells (PDLSCs).

Fibroblasts: The primary cells of the PDL are fibroblasts, which constitute between 50 and 60% of total PDL cellularity (Jiang *et al.*, 2016) and are responsible for the synthesis of collagen, elastin fibers and the intercellular substance present in the connective tissue. Moreover, several reports revealed that fibroblasts present an extensive cytoplasm containing an abundance of organelles associated with protein synthesis and secretion (Lekic and Mcculloch, 1996). PDL fibroblasts also have a well-developed cytoskeleton with a particularly prominent actin network (Lekic and Mcculloch, 1996; Berkovitz, 2004; Nanci, 2017). Furthermore, fibroblasts are responsible for collagen degradation associated with PDL continuous remodeling with a high rate of collagen turnover (Lekic and Mcculloch, 1996). Reports demonstrated that PDL fibroblasts appear to function as mechanosensing entities that regulate extracellular matrix (ECM) homeostasis through collagen-secretory and collagen-remodeling activities according to the level of strain in the ligament (Ziegler *et al.*, 2010).

Epithelial Cells: The epithelial cells in the PDL are remnants of Hertwig's epithelial root sheath (HERS) and known as the epithelial cell rests of Malassez (ERM). These groups of epithelial cells are present in mature PDL after the disintegration of HERS during the formation of the root (Fehranbat and Popowics, 2015). Until recently, these remnants were thought to be latent or quiescent structures

associated with pathological processes, but new evidences showed that the ERM is a major tissue structure, maintaining PDL homeostasis through its potential for differentiation and capacity to repair the periodontium (Silva *et al.*, 2017). The ERM is located close to the cementum as a cluster of cells that form an epithelial network and have been reported to express a number of bone and cementum-related proteins, growth factors, and cytokines important for periodontal regeneration (Nanci and Bosshardt, 2006; Nanci, 2017; Silva *et al.*, 2017).

Precursor and Resorptive Cells: In the “pressure-tension theory”, proposed to address orthodontic tooth movement, the PDL acts a sensor for changes in mechanical forces or stresses (Henneman, Von den Hoff and Maltha, 2008). In this theory, the biomechanical and biological responses of the periodontium to mechanical stimuli culminate in remodeling of bone and PDL on the compression side and in root resorption on the tension side. This requires the action of precursor cells, such as osteoblasts and cementoblasts, and resorptive cells, namely osteoclasts and cementoclasts (Jiang *et al.*, 2016; Li *et al.*, 2021; Yamaguchi and Mishima, 2021). In fact, the removal and deposition of bone is carried out by osteoclasts and osteoblasts, respectively. Osteoblasts are bone-forming cells that are placed in the periodontal surface of the alveolar bone. Osteoclasts are cells that resorb bone. In healthy periodontium, the surface of the bone is covered largely by osteoblasts in various stages of differentiation and by osteoclasts (Kumar, 2019). Cementoblasts produce root cementum and are typically found lining the surface of cementum covering the tooth. Cementoclasts are less common and only occasionally found in normal functioning PDL. Interestingly, cementum is not resorbed like bone under physiological conditions, but it undergoes continual deposition during life. However, resorption of cementum can still occur under certain circumstances (Kumar, 2019).

Macrophages: These immune cells present in the PDL have a critical role in microenvironment homeostasis. Reports suggest that PDL macrophages are predominantly located adjacent to blood vessels, playing a dual role in phagocytosing dead cells and secreting growth factors that regulate the proliferation of adjacent cells (Gordon and Martinez, 2010). In fact, macrophages synthesize a range of molecules with important functions, like interferon, prostaglandins and factors that enhance the growth of fibroblasts and endothelial cells (Nanci, 2017; Liu *et al.*, 2019).

Periodontal Ligament Stem Cells (PDLSCs): Current knowledge on periodontium homeostasis and regeneration revealed that it recapitulates the main periodontium development processes, including differentiation, ECM production and mineralization (Nanci and Bosshardt, 2006). In fact, Melcher and colleagues proposed a theory that undifferentiated cells reside in the PDL (Melcher, 1985; Bartold, Shi and Gronthos, 2006). These cells are a source of renewable progenitor cells producing cementoblasts, osteoblasts and fibroblasts throughout adult life (Melcher, 1985; Bartold, Shi and Gronthos, 2006). In 2004, Seo and colleagues successfully isolated cells with stem cell characteristics from the human PDL (Seo *et al.*, 2004). In fact, the identification of stem cell populations in the periodontium has raised interest in the potential use of stem cell-based therapies to treat defects caused by trauma or periodontal disease.

2.2. PERIODONTITIS

Periodontitis is an inflammatory disease that affects the periodontium (Figure 4) – the complex system that includes the specialized epithelial, connective and bone tissues that surround and support the teeth (Pihlstrom, Michalowicz and Johnson, 2005). The disease is initiated and sustained by pathogenic microorganisms that arise from dental plaque accumulation. In early stages, the inflammation affects the gingiva and is referred to as gingivitis. Despite being reversible by effective oral hygiene, if left untreated gingivitis progresses to periodontitis (Figure 4). Severe periodontitis can result in occasional pain and discomfort, impaired mastication, and eventual tooth loss (Pihlstrom, Michalowicz and Johnson, 2005; Kinane, Stathopoulou and Papapanou, 2017).

Periodontitis is prevalent in adults but may also occur in children and adolescents. Periodontitis prevalence is estimated to vary between 10 to 50% (Preshaw, Seymour and Heasman, 2004; Sanz *et al.*, 2010). The large variation of the estimation is due to lack of clear and consensual thresholds for both disease extent (the number of affected teeth) and disease severity (the magnitude of pocket depth, clinical attachment loss and alveolar bone loss at the affected teeth) (Kinane, Stathopoulou and Papapanou, 2017).

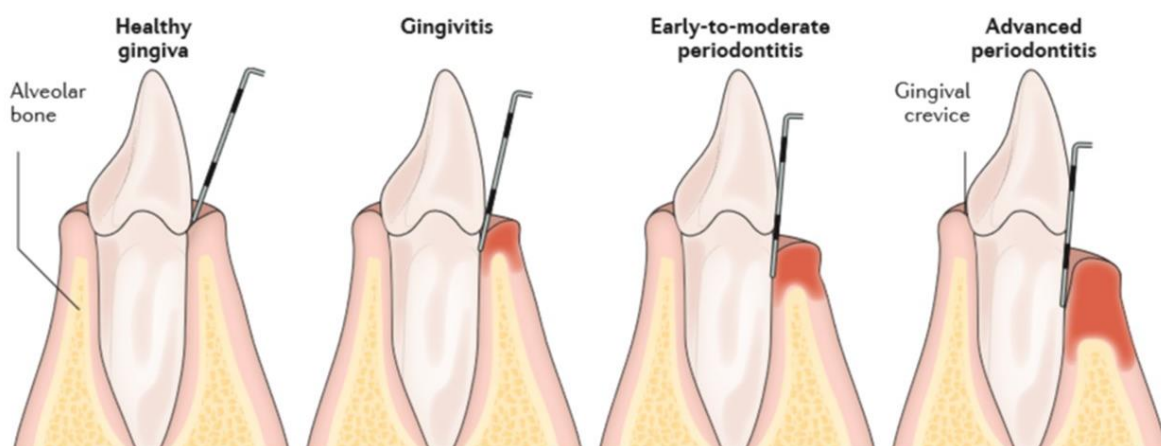


Figure 4. Illustration of healthy gingiva, gingivitis, early-to-moderate periodontitis and advanced periodontitis. Adapted from Kinane, Stathopoulou and Papapanou, 2017.

2.2.1. Disease Mechanism and Inflammatory Response

Dental plaque accumulation at the gingival margin results in the release of microbial substances, such as lipopolysaccharides and microbial peptides. As these molecules cross the junctional epithelium and enter in the gingival connective tissues, fluid accumulates in the tissues (Preshaw, Seymour and Heasman, 2004). Host-derived defense cells, such as neutrophils (polymorphonuclear leukocytes, PMNs), plasma cells, monocytes/ macrophages and lymphocytes also infiltrate in the connective tissue, migrating from the capillaries (Preshaw, Seymour and Heasman, 2004). These events lead to the disruption of the normal anatomy of the connective tissues, with degradation of collagen fibers to create space to accommodate the infiltrating defense cells (Preshaw, Seymour and Heasman, 2004).

Gingival inflammation worsens because the microbial challenge is not contained by the primary host defenses, leading to increased permeability of the junctional epithelium. Furthermore, large numbers of PMNs migrate into the tissues, secreting large quantities of destructive enzymes and inflammatory mediators (Preshaw, Seymour and Heasman, 2004). To accommodate the inflammatory and immune cells, destruction of structural components of the periodontium occurs by the action of matrix metalloproteinases (MMPs, synthesized by PMNs), including collagenases, which degrade collagen fibers in the periodontal tissues. Further tissue damage results from the release of large quantities of destructive enzymes and oxygen radicals into the extracellular environment by PMNs (Preshaw, Seymour and Heasman, 2004).

During later stages of periodontitis, macrophages are also recruited and activated (by binding to lipopolysaccharides) to produce prostaglandins, interleukins and tumor necrosis factor- α (TNF- α) (Preshaw, Seymour and Heasman, 2004). High levels of these molecules stimulate osteoclasts, bone degrading cells that are important for alveolar bone resorption (Preshaw, Seymour and Heasman, 2004). Finally, the pocket deepens even further, and plaque bacteria migrate along the root surface into the pocket where the physical conditions allow gram-negative anaerobic species to proliferate (Preshaw, Seymour and Heasman, 2004).

Overall, periodontitis pathogenesis is initiated by bacteria accumulation, however the key destructive events are caused by host-derived mediators and enzymes released by inflammatory cells that leads to tooth attachment loss and bone loss (Preshaw, Seymour and Heasman, 2004).

2.2.2. Risk Factors

As stated above, host susceptibility plays a relevant role in disease progression. Despite this, additional risk factors have been identified, including genetic and environmental risk factors. Previous studies have shown that smoking is a major risk factor for periodontitis (Nociti, Casati and Duarte, 2015). Clinical studies in diverse populations demonstrated that smokers present increased susceptibility to periodontitis and greater severity and progression of periodontal disease compared with non-smokers (Do *et al.*, 2008; Bergstrom, 2014; Eke *et al.*, 2016). In addition, diabetes has been associated to severe periodontal disease (Soskolne and Klinger, 2001; Taylor, 2001). Results demonstrated that although patients with well-controlled diabetes do not present increased risk of periodontal disease, patients with poorly controlled diabetes have increased risk of periodontitis and progressive bone loss. Additionally, chronic periodontitis can have a negative effect on metabolic control in patients with diabetes, being responsible for increased inflammatory burden and enhanced insulin resistance (Lalla and Papapanou, 2011).

Genetic factors have an important role in determining risk for the onset and the progression of periodontitis, accounting as much as 50% (Michalowicz *et al.*, 2000). Moreover, reports showed that genetic variations in or near cytokine genes could affect the systemic inflammatory response in patients with periodontitis (D'Aiuto *et al.*, 2004).

2.3. TREATMENT OF PERIODONTITIS

2.3.1. Non-surgical Treatment

Generally, gingivitis treatment is non-surgical aiming at controlling the biofilm and other prominent risk factors. The non-surgical treatment consists in professional removal of plaque from teeth, followed by daily home care (Kinane, Stathopoulou and Papapanou, 2017). The patient's healing response is usually assessed after one or two months of treatment. To enhance treatment outcomes, several adjuncts treatments have been proposed, such as local delivery of drugs, systemic antibiotics and systemic host modulation agents. Host modulatory therapies aim to modulate destructive components of the host response, significantly responsible for periodontitis progression, and include (Preshaw, Seymour and Heasman, 2004): (i) non-steroidal anti-inflammatory drugs, which block the production of prostaglandins; (ii) doxycycline, which downregulates MMPs in periodontal tissues; and (iii) bisphosphonates, which reduce osteoclast activity and bone resorption.

Non-surgical periodontal therapy, with or without adjunctive therapies, has been shown to reduce pocket depth and results in the formation of new tooth attachment, often being sufficient for patients with early or moderate disease (Pihlstrom, Michalowicz and Johnson, 2005). However, surgical therapy is frequently required to fully eliminate dental plaque or to restore lost periodontal structures.

2.3.2. Surgical Treatment

For patients with advanced disease, periodontal surgery is used to reduce the depth of periodontal pockets, to remove residual dental plaque, and to stimulate regeneration of lost periodontal tissues. Several surgical procedures are used, such as grafting materials and biological substances. Most of the surgical interventions involved in the reconstruction of periodontal defects are based on autologous tissue grafts and/or artificial implants. However, these surgical approaches have limited success due to insufficient biocompatibility, resorption of bone, limited graft quantity and donor-site morbidity (Hynes *et al.*, 2012).

Several studies have investigated the use of biomaterials for surgical treatment of periodontal regeneration (Sculean *et al.*, 2015) and various products are currently available on the market including bone grafts, scaffolds and membranes

Figure 5).

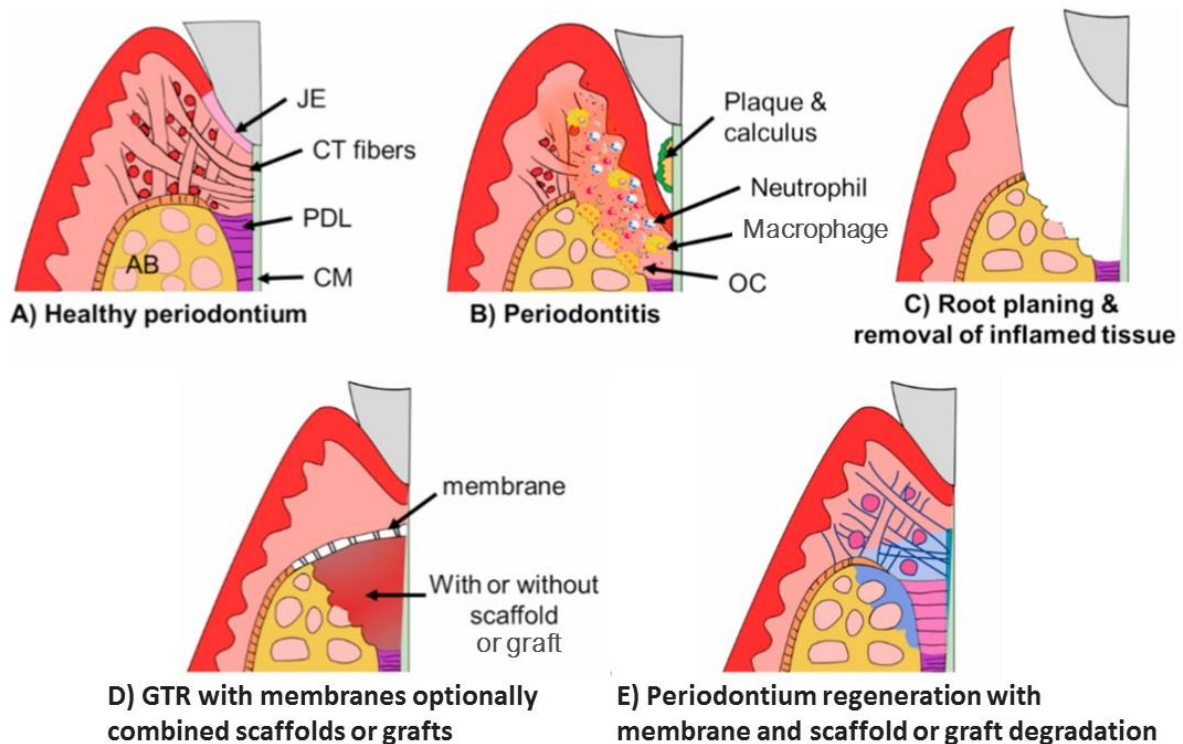


Figure 5. Illustration of healthy periodontium, periodontitis, and current surgical regenerative treatment options. **A)** Healthy periodontium composed by junctional epithelium (JE), connective tissue (CT) fibers, cementum (CM), periodontal ligament (PDL) and alveolar bone (AB). **B)** Periodontitis disease resulting in bone resorption by activated osteoclasts (OC), formation dental plaque, and epithelial down growth associated with increased number of neutrophil and macrophages. **C)** Outcome of surgical root planing and removal of inflamed tissue. **D)** Guided Tissue Regeneration (GTR) therapy with contact inhibition membrane that can be combined with scaffolds or grafts. **E)** Scaffold and membrane degradation and simultaneous periodontium regeneration. Adapted from Woo *et al.*, 2021.

2.3.2.1. Bone Grafts

Bone grafts can be transplanted into a bony defect and are capable of promoting bone healing, either alone or in combination with other materials (Zhao *et al.*, 2021). The main function of bone grafts is to provide mechanical support and stimulate regeneration, with the ultimate goal of bone replacement (Bhatt and Rozental, 2012).

Successful bone graft regeneration depends on four fundamental biological properties (Zhao *et al.*, 2021):

- i. Osseointegration: Ability of a grafting material to bond to the surface of the bone.
- ii. Osteogenesis: Formation of new bone by osteoblasts or progenitor cells present within the grafting material.
- iii. Osteoconduction: Ability of a bone grafting material to generate a bioactive scaffold on which host cells can grow.
- iv. Osteoinduction: Recruitment of host stem cells into the grafting site, where local proteins and other factors (i.e. platelet-derived growth factors (PDGFs), fibroblast growth factors (FGFs), transforming growth factors- β (TGFs- β)) induce the differentiation of stem cells into osteoblasts.

Additional properties such as biocompatibility, bioresorbability, sterility, structural integrity, adequate porosity for vascular ingrowth, plasticity, ease of handling, cost, and compressive strength contribute to the success rate of a bone graft-based periodontal regeneration therapy (Kolk *et al.*, 2012).

Studies have found that almost all current bone graft materials only satisfy one of the four essential properties, such as osteoconductivity, serving primarily as a structural support for bone regeneration (Buser *et al.*, 1998; Horch *et al.*, 2006; Kolk *et al.*, 2012). Additionally, limitations associated with graft *versus* host responses are present in most of the materials that are not derived from the patients (autografts) (Zhao *et al.*, 2021).

There are three types of bone grafts:

- **Autografts:** Composed by grafting material surgically removed from one part of the body to another within the same patient (Elsalanty and Genecov, 2009). Autografts are considered the gold standard for graft materials, to which all other grafting materials are measured, since autografts have the lowest risk of immunological rejection and present high osteoconductive, osteoinductive, and osteogenic properties (Baldwin *et al.*, 2019). Despite their advantages, the amount of autologous bone graft available varies with each patient, so large defects may require a large amount of graft that may not be safely harvested from the patient (Baldwin *et al.*, 2019). Moreover, autografts need a second surgical procedure and can cause donor site pain and morbidity (Carvalho *et al.*, 2021).
- **Allografts:** Grafts obtained from either a compatible living donor or a cadaveric bone source (Roberts and Rosenbaum, 2012) that can be delivered in three primary forms: fresh, frozen, or freeze-dried (Zhao *et al.*, 2021). Fresh and frozen allografts possess superior osteoinductive properties but are rarely used due to the higher risk of host immunogenic response, limited shelf life, and increased risk of disease transmission (Zhao *et al.*, 2021). Freeze dried allografts possess longer shelf life and lower risk of disease transmission when compared with fresh and frozen grafts, but decreased structural strength and osseointegration (Baldwin *et al.*, 2019).
- **Xenografts:** Grafting materials derived from a different species than that of the receiving organism (Zhao *et al.*, 2021). Xenogeneic grafts available for periodontal regeneration can be from bovine, porcine, or equine origin. Xenografts undergo deproteinization and demineralization through thermal and chemical treatment with the utilization of sodium hydroxide (Ausenda *et al.*, 2019). After processing, the final graft product is solely constituted by the remaining mineral components that form a network of calcium phosphate and calcium carbonate (Ausenda *et al.*, 2019).

2.3.2.2. Scaffolds

To overcome potential immunogenicity and morbidity at donor sites associated with bone-grafting surgical approaches and limitations related to graft availability, artificial scaffolds are emerging as an alternative to grafts in bone tissue regeneration.

The ability to provide both temporary mechanical support and volumetric space maintenance in regenerating tissues makes scaffolds particularly adequate for periodontal Tissue Engineering (TE), particularly in the field of alveolar bone regeneration. When periodontal lesion results in alveolar bone resorption, large bone volumes can be irreversibly resorbed if alveolar bone space is not maintained. Thus, scaffolds with the ability to maintain robust and highly porous structures can potentially favor

osteogenesis in periodontal TE/ Regenerative Medicine (RM). (Bartnikowski, Vaquette and Ivanovski, 2020)

The basic premise of TE is that biologics, including cells, genes, and proteins, can be delivered by a degradable scaffold that provides structural support while promoting tissue regeneration (Hollister, 2009). The ideal scaffold should be biodegradable, biocompatible and highly porous with an interconnected network and surface characteristics suited for cell adhesion and tissue regeneration (Galli *et al.*, 2021). Additionally, scaffold design should fulfill the following requirements (Hollister, 2009):

- i. Match the geometry of complex 3D defects to guide the tissue shape to match the original 3D anatomy.
- ii. Support the functional and biomechanical demands during healing until sufficient tissue has formed to take over these demands.
- iii. Enhance tissue regeneration through the delivery of appropriate biologics and by providing an appropriate mass transport environment.
- iv. Integrate with the surrounding tissues.

Scaffolds materials for periodontal TE are commonly fabricated from natural or synthetic materials and can be tailored to films, fibers, sheets, gels, and sponges (Shimauchi *et al.*, 2013). Natural biomaterials are derived from a living source without modification (Zhao *et al.*, 2021) and offer a wide variety of functional cues that regulate cell adhesion, proliferation, phenotype, matrix production and enzyme activity (Hubbell, 2003). These materials often exhibit similarities to ECM components and have strong biological characteristics and biocompatibility (Yang and El Haj, 2006). Collagen and chitosan are two commonly used natural biomaterials for regeneration of periodontal tissues (Woo *et al.*, 2021). Collagen is known to influence cell motility (Ashworth *et al.*, 2018) and has been widely used as a biomaterial for bone and periodontal TE (Murphy, Haugh and O'Brien, 2010; Kato *et al.*, 2015; Kämmerer *et al.*, 2017; Ashworth *et al.*, 2018; Nakamura *et al.*, 2019). In fact, Ashworth and colleagues (Ashworth *et al.* 2018) fabricated 3D collagen scaffolds with aligned pores (size of 50-100 μm) and showed a promising effect on induction of dynamic and rapid migration of PDL fibroblasts.

Chitosan has also been widely used for periodontal TE because of its good biocompatibility, biodegradability, non-immunogenicity, and anti-microbial properties against bacteria or fungi (Di Martino, Sittinger and Risbud, 2005; Perinelli *et al.*, 2018; Zang *et al.*, 2019; Lauritano *et al.*, 2020; Tang *et al.*, 2020). Despite its advantages, chitosan has been frequently mixed with another type of scaffold material to address its limitations, such as limited water solubility and aggregation of particles (Woo *et al.*, 2021). Recently, Sukpaita and colleagues fabricated chitosan scaffolds combined with dicarboxylic acid (a dissolving and cross-linking agent) that significantly promoted *in vivo* bone regeneration after 6 and 12 weeks (Sukpaita *et al.*, 2019).

Synthetic polymers are widely used in TE applications as they offer the ability to provide controllable and reproducible structural properties allowing mass production. Despite poor potential in providing cell adhesion/migration and proliferation, synthetic polymers show good mechanical properties, and their mechanical strength and degradation rate can be adjusted in order to reach the most favorable outcome. Polyester-based polymers such as polylactic acid (PLA), polyglycolic acid (PGA), polylactic-co-glycolic

acid (PLGA) and polycaprolactone (PCL) have been frequently used for periodontal applications (Carmagnola *et al.*, 2017). Previous studies showed that delivery of cementoblasts through a 3D PLGA scaffold promoted mineral formation and had no toxic effect on the other cells (Jin *et al.*, 2003). Electrospun PLGA/PCL composite scaffolds with FGF-2 and bone marrow-derived mesenchymal stromal cells (BMMSCs) resulted in improved periodontal tissue healing by 6 weeks *in vivo* in a rat model (Cai *et al.*, 2015). Additionally, a recent study that combined 3D printed PLGA/PCL composite scaffolds with human PDLSCs showed significantly increased adhesion, proliferation, and osteogenic capacity of human PDLSCs *in vitro* (Peng *et al.*, 2018).

2.3.2.3. Membrane Guided Tissue Regeneration

Membranes have been used in periodontal surgical treatment since the introduction of guided tissue regeneration (GTR) (Nyman *et al.*, 1982; Gottlow *et al.*, 1986). GTR is based on the implementation of cell-occlusive barrier membranes to selectively exclude relatively rapid epithelial and fibroblastic downgrowth, while promoting repopulation of defect sites with slower migrating cells from the periodontal ligament, bone and cementum (Giannobile, 2014).

The ideal membrane should be (Mancini, Fratini and Marchetti, 2021):

- i. Biocompatible: The membrane should not activate an immune response or acute inflammation.
- ii. Cell-exclusive: Acting as a barrier capable of excluding specific types of cells.
- iii. Space-making: Creating and maintaining space adjacent to the root surface for ingrowth of tissue from the PDL.
- iv. Easy to use: Membranes must be easy to handle in clinical setting.

Membranes can be divided into two categories according to biodegradability. Non-resorbable membranes are considered first-generation membranes (Carmagnola *et al.*, 2017) and are no longer used in periodontal regeneration (Mancini, Fratini and Marchetti, 2021). Typical materials used in non-resorbable membranes are polytetrafluorethylene (PTFE) and titanium (Mancini, Fratini and Marchetti, 2021). Resorbable membranes are second-generation membranes and currently the most widely used in periodontal GTR approaches, as there is no need for second surgery to remove the membrane. Common materials for resorbable membranes include PCL, PGA and PLA, used alone or in combination (Carmagnola *et al.*, 2017). Although polyester biodegradation occurs through hydrolysis, releasing potentially toxic by-products, it has been considered safe given the insignificant amount of residual particles that are released at a very slow rate (Shue, Yufeng and Mony, 2012).

However, the use of membranes raises the potential for complications such as exposure, which could reduce the regenerative potential and allow the infiltration of bacteria and possible infection of the site (Bosshardt and Sculean, 2009).

2.4. PERIODONTAL LIGAMENT STEM CELLS

Stem cells have been isolated from a number of dental tissues, namely, dental pulp, exfoliated deciduous teeth, dental follicle and PDL (Zhai *et al.*, 2019).

The neural crest is a pluripotent cell population originated in the ectoderm at the margins of the neural tube, known to contribute extensively to embryo development and give rise to various cell and tissue types (Sommer, 2010). During craniofacial development, cranial neural crest (CNC) cells migrate and originate the dental tissues (Le Douarin, Ziller and Couly, 1993; Xu *et al.*, 2013) as tooth development is triggered by mutually inductive signaling between the primitive oral epithelium and the CNC-derived ectomesenchyme (Pispa and Thesleff, 2003; Maeda *et al.*, 2011). Subsequently, the concentration of CNC-derived ectomesenchymal cells gives rise to the dental follicle, a loose connective tissue that surrounds the enamel and the dental papilla of the developing tooth germ before tooth eruption. Moreover, dental follicle contains progenitors of osteoblasts, cementoblasts and PDL cells (Cho and Garant, 2000; Handa *et al.*, 2002; Luan *et al.*, 2006).

In line with the findings discussed above, studies showed that PDL tissue derives from CNC-derived ectomesenchymal cells (Chai *et al.*, 2000; Coura *et al.*, 2008; Huang *et al.*, 2009; Mitsiadis and Graf, 2009; Dangaria *et al.*, 2011a; Kaku *et al.*, 2012). Additionally, increasing knowledge on PDL characteristics and function, including evidence of the presence of progenitor cells provided by histological and *in vivo* studies (Gould, Melcher and Brunette, 1980; McCulloch *et al.*, 1987), led to speculation that this tissue might contain stem cells that contribute to periodontal tissue homeostasis and regeneration.

In 2004, Seo and colleagues successfully isolated an unique population of multipotent stem cells from PDL tissue of extracted human third molar teeth and named these cells PDLSCs (Seo *et al.* 2004). In order to identify PDLSCs, Seo and co-workers applied several techniques typically used to characterize BMMSCs, including magnetic and fluorescence activated cell sorting, immunocytochemistry, quantitative reverse transcription-polymerase chain reaction (qRT-PCR), and western and northern blot analyses. Results demonstrated that the isolated cells have a phenotypic profile similar to BMMSCs and the capacity to develop into cementoblast-like cells, osteoblasts and adipocytes *in vitro*, and cementum/PDL-like tissue *in vivo* (Seo *et al.*, 2004).

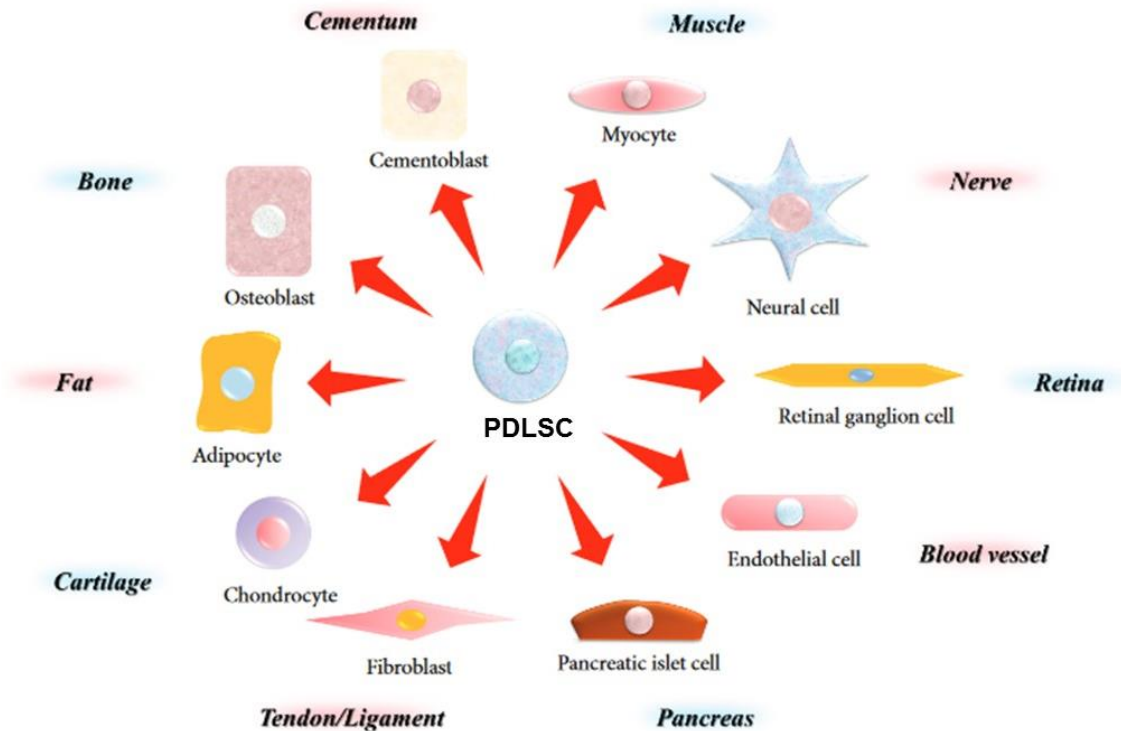


Figure 6. Multipotency of PDLSCs. PDLSCs have been successfully differentiated into osteoblasts, adipocytes, chondrocytes, fibroblasts, pancreatic islet cells, endothelial cells, retinal ganglion cells, neural cells, myocytes, and cementoblasts. Adapted from Tomokiyo *et al.*, 2018.

2.4.1. Characteristics of PDLSCs

Stem cells are defined by their ability to self-renew and to differentiate into multiple lineages that produce a range of specialized daughter cells (Smith, 2006). PDLSC self-renewal capacity has been demonstrated by Menicanin and colleagues. These PDLSCs exhibited an immunophenotype and multipotential capacity similar to primary PDLSCs (Menicanin *et al.*, 2014). Moreover, the multilineage differentiation potential of PDLSCs has been demonstrated in various studies (Seo *et al.*, 2004; Nagatomo *et al.*, 2006; Iwata *et al.*, 2010; Kaku *et al.*, 2012). PDLSCs have been successfully differentiated *in vitro* (Figure 6) into osteoblasts, adipocytes, chondrocytes, fibroblasts, pancreatic islet cells, endothelial cells, retinal ganglion cells, neural cells, myocytes and cementoblasts (Seo *et al.*, 2004; Gay, Chen and MacDougall, 2007; Techawattanawisal *et al.*, 2007; Xu *et al.*, 2009; Okubo *et al.*, 2010; Dapeng *et al.*, 2014; J. S. Lee *et al.*, 2014; Menicanin *et al.*, 2014; Ng *et al.*, 2015; Pelaez *et al.*, 2017; Shinagawa-Ohama *et al.*, 2017).

Mesenchymal stromal cells (MSCs) derived from various tissues have been reported to have immunoregulatory properties promoted by inflammatory cytokines (Krampera, 2011). Thus, the interactions between immune cells that produce inflammatory cytokines and MSCs are believed to be intimately related with tissue homeostasis, inflammation and repair (Tomokiyo, Wada and Maeda, 2019). Consistent with these findings, PDLSCs exhibit immunomodulatory properties with the ability to suppress immune reactions (Wada *et al.*, 2009). *Ex-vivo* expanded PDLSCs have been reported to suppress the proliferation of activated peripheral blood mononuclear cells (PBMNCs) via soluble factors partly dependent on the inflammatory cytokine interferon gamma (IFN- γ), synthesized by activated

PBMNCs. Similarly to BMMSCs (Bartholomew *et al.*, 2002; Di Nicola *et al.*, 2002; Meisel *et al.*, 2004), PDLSC inhibitory factors include: indoleamine 2, 3-dioxygenase (IDO) that is dependent on IFN- γ , and transforming growth factor beta 1 (TGF- β 1) and hepatocyte growth factor (HGF) that are independent on IFN- γ (Wada *et al.*, 2009). Additionally, PDLSCs represent a distinctive potential to form cementum- and PDL-like tissues *in vivo*, suggesting that PDLSCs might belong to a unique population of MSCs (Seo *et al.*, 2004; Tran *et al.*, 2014).

2.4.1.1. Mesenchymal Stromal Cells

MSCs are adult multipotent stromal cells that were first described in the 1960s and 1970s (Friedenstein, Piatetzky-Shapiro and Petrakova, 1966; Friedenstein, Chailakhjan and Lalykina, 1970; Friedenstein, Gorskaja and Kulagina, 1976). Friedenstein and colleagues initially discovered MSCs in bone marrow, observing a cell population that adhered to plastic and developed into fibroblastic colony forming cells. Additionally, these cells also exhibited the capacity to self-renew and differentiate into a number of mesenchymal phenotypes, including bone, cartilage, muscle, fat and other connective tissues (Figure 7). Furthermore, MSCs exhibited great potential for clinical applications in cell-based therapies and TE due to their role in the regulation of immune (M. Kaplan, E. Youd and A. Lodie, 2011) and inflammatory responses (Shi *et al.*, 2018). However, cell's ability to adhere and grow on plastic was not considered sufficient to classify them as MSCs. The Mesenchymal and Tissue Stem Cell Committee of the International Society for Cellular Therapy has proposed three minimal criteria for defining multipotent mesenchymal stromal cells (Dominici *et al.*, 2006). These include: (i) adhesion to plastic; (ii) positive expression of specific immunophenotypic marker combinations (CD73, CD90 and CD105), and lack of expression of hematopoietic markers (CD14, CD34 and CD45) and class-II major histocompatibility complex (MHC) molecules (i.e. HLA-DR); (iii) capability of differentiating into mesodermal lineages (adipocytes, osteoblasts and chondrocytes).

Although MSCs were originally isolated from bone marrow, similar populations have been isolated from other adult and perinatal tissues, including adipose tissue (Zuk *et al.*, 2002), endometrium (Gargett *et al.*, 2009), menstrual blood (Chen, Qu and Xiang, 2019), lung (Fang *et al.*, 2019), dental tissues (Liu *et al.*, 2015), synovial tissues (de Sousa *et al.*, 2014), umbilical cord blood (Goodwin *et al.*, 2001), umbilical cord (Nagamura-Inoue, 2014), placenta (in 't Anker *et al.*, 2004) and amniotic fluid (in 't Anker *et al.*, 2003). When compared with pluripotent embryonic stem cells (ESCs) and induced pluripotent stem cells (iPSCs), MSCs demonstrated lower developmental potential. In fact, only ESCs and iPSCs hold the potential to differentiate into all cell types derived from the three primary germ layers (ecto-, meso-, and endoderm) (Hynes *et al.*, 2012). Moreover, MSCs present a shorter lifespan, since MSCs, unlike ESCs and iPSCs, are not able to proliferate indefinitely *in vitro* (Gronthos *et al.*, 2003). Nonetheless, MSCs derived from post-natal tissues are an attractive candidate for TE/RM applications since these cells are not subject to the ethical and legal concerns related to isolation and application as ESCs and iPSCs. Moreover, isolation of MSCs from adult tissues enables the development of autologous transplantation-based therapies, by decreasing the complications derived from immune rejection.

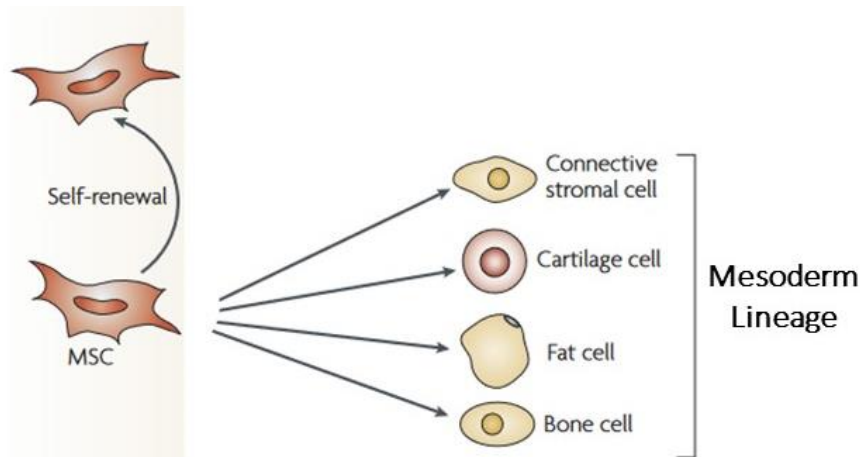


Figure 7. Mesenchymal stromal cell (MSC) ability to self-renew and differentiate into the mesodermal lineage. Adapted from Uccelli, Moretta and Pistoia, 2008.

2.4.2. Identification and Isolation of PDLSCs

A significant challenge in the characterization of PDLSCs is to find specific markers associated with either PDL or cementum. Human PDLSCs were firstly isolated from PDL heterogeneous cell populations using two early MSCs-related cell surface molecules: Stro-1 (putative stem cell marker) and CD146/MUC18 (perivascular cell marker) that are also present in BMMSCs and dental pulp stem cells (Seo *et al.*, 2004). Stro-1 surface antigen has been shown to be nonreactive to hematopoietic stem cells (HSCs) (Simmons and Torok-Storb, 1991). Stro-1⁺ MSCs were shown to be capable of forming clonogenic fibroblast colonies *in vitro* (Simmons and Torok-Storb, 1991). However, the use of Stro-1 alone is not sufficient to obtain pure populations of stem cells because of its cross-reaction with glycoprotein-A-positive nucleated red cells and a small subset of B lymphocytes (Simmons and Torok-Storb, 1991; Chen *et al.*, 2006). Moreover, the reported percentage of Stro-1⁺ cells in the PDL tissue varies widely between 1.2% and 33.5% (Nagatomo *et al.*, 2006; Gay, Chen and MacDougall, 2007; Lindroos *et al.*, 2008; Itaya *et al.*, 2009; Iwata *et al.*, 2010).

Since the first successful isolation in 2004, studies have reported the expression of several additional cell surface markers. These include stromal and endothelial cell surface markers CD44, CD90, CD105, CD166, and Stro-3 (Trubiani *et al.*, 2005; Nagatomo *et al.*, 2006; Wada *et al.*, 2009); MSC-related markers such as CD10, CD26, CD29, CD44, CD73, CD90, CD105, CD166 and CD349/FZD9 (Trubiani *et al.*, 2010; Banavar *et al.*, 2020); neural crest markers including Nestin, Slug, p75NTR, and SOX10 (Huang *et al.*, 2009); and embryonic stem cell markers OCT4, NANOG, SOX2, KLF4, SSEA-1, SSEA-3, SSEA-4, TRA-1-60, TRA-1-81, and REX1 (Huang *et al.*, 2009; Kawanabe *et al.*, 2010). In contrast, but in line with the MSC phenotype, PDLSCs lack the expression of hematopoietic cell markers, CD14, CD19, CD34, CD40, CD45, CD80, and CD86 (Wada *et al.*, 2009; Vasandan *et al.*, 2014). Additionally, two related markers have been identified for PDLSCs. Studies suggested that periostin – an ECM protein predominantly expressed in collagen-rich fibrous connective tissues – is critically required for maintenance of PDL integrity in response to mechanical stresses, contributing to PDL homeostasis and regeneration (Rios *et al.*, 2005; Dangaria *et al.*, 2009). Genetic expression and immunohistochemical results showed that periostin is strongly expressed specifically in PDLSCs (Iwata *et al.*, 2010). Moreover, Yamada and colleagues identified a novel human isoform of periostin, predominantly expressed in the

PDL with much lower expression in other tissues and organs (Yamada *et al.*, 2014). Hence, periostin is a PDL function related marker that can be used to identify PDLSCs.

PDL shares some morphological and functional bundles and the ability to absorb mechanical forces of stress and strain (Pöschke *et al.*, 2018). Therefore, scleraxis, a tendon-specific protein, was reported to be a marker for PDLSC identification. Reports showed that PDLSCs present higher level of expression of scleraxis when compared to BMMSCs (Seo *et al.*, 2004; Bartold, Shi and Gronthos, 2006; Liu *et al.*, 2006).

2.4.3. Culture Methods and Conditions

Although PDLSCs demonstrate interesting properties, the amount of PDL tissue that can be recovered from teeth is limited, making it difficult to harvest enough PDLSCs for applications in periodontal tissue regeneration. Therefore, to obtain a sufficient amount of PDLSCs, optimization of cell culture expansion protocols is required.

Recent research demonstrated that human PDLSCs can be isolated by outgrowth or enzymatic dissociation methods and expanded *in vitro* (Gay, Chen and MacDougall, 2007; Xu *et al.*, 2009; Tamaki *et al.*, 2013; Tran *et al.*, 2014). Enzymatic dissociation is a common method to obtain single cell suspensions from primary tissues which consists in exposing the tissue to enzymes for a minimal period of time in order to preserve maximum cell viability. In the outgrowth method, PDL fragments are placed directly into a culture plate so that cells will outgrow from the tissue explants. Recent findings suggested that PDLSCs isolated by the outgrowth method present unique cementogenic properties and form cellular cementum-like hard tissue *in vivo* (Shinagawa-Ohama *et al.*, 2017). Thus, these isolated cells may be promising candidates for root-defect repair/regeneration that requires formation of the cellular cementum. Regarding the enzymatic digestion method, studies showed a greater success rate of cell expansion with a combination of type I collagenase and dispase, when compared to using trypsin and EDTA for the digestion step (Iwata *et al.*, 2010).

One drawback of PDLSC clinical application is the low number of cells acquired from each donor tooth, which makes *ex vivo* expansion a key step in the development of future PDLSC dependent therapies. Cellular characteristics and functions must be maintained even in extended expansions, and this requires a time- and cost-effective technique for obtaining a sufficient number of cells. For this, additional research is needed to understand the impact of passaging in PDLSC quality and the best suited culture media should be established. The most common media formulations for the primary expansion of PDLSCs are α -minimum essential medium (α -MEM) and Dulbecco's minimum essential medium (DMEM) (Jung *et al.*, 2013). Results from a comparative study (Jung *et al.*, 2013) showed that both media formulations can maintain stem cell phenotypes until passage 8, namely the expression of Stro-1, CD146, CD105, and CD44. However, PDLSCs cultured in α -MEM had greater proliferation rates and stronger osteogenic potential than PDLSCs cultured in DMEM (Jung *et al.*, 2013). Lastly, study results (Iwata *et al.*, 2010) showed that PDLSCs seeded at low density (50 cells/cm²) proliferated at a higher rate than those seeded at relatively high densities (500 and 5000 cells/cm²). Additionally, the colony-forming efficiency of the PDLSCs seeded at 50 cells/cm² increased with every passage until the 5th passage. This suggests that seeding cells at a low cell seeding densities may exclusively select highly proliferative PDLSCs (Iwata *et al.*, 2010).

2.5. NEW STRATEGIES FOR PERIODONTAL REGENERATIVE THERAPY AND ALVEOLAR BONE REGENERATION

Disease progression to advanced periodontitis and the consequential deepening of the tissue pockets results in damage of all periodontal tissues, ultimately leading to loss of tooth attachment (Galli *et al.*, 2021). Successful periodontal regeneration involves the healing of all periodontal components, composed by soft and hard connective tissues with numerous cell types and tissue interfaces. Additionally, this process needs to be coordinated since the alveolar bone regeneration precedes the differentiation of the remaining mineralized and soft connective tissues.

Due to the complexity of periodontium, research and development of new TE/RM therapeutic approaches include the use of signaling molecules/growth factors, scaffolds, and cells with particular focus on promoting osteogenesis, angiogenesis, as well as controlling inflammation (Galli *et al.*, 2021).

2.5.1. *Stem Cell-based Therapies*

Therapeutic application of stem cells has offered a new solution for periodontal regeneration. These cells have an increased proliferative and differentiative capacity being suited to replenish destroyed cells and regenerate lost tissues. Current stem cell-based therapies rely mainly on the delivery of *in vitro* cultured-expanded cells to the periodontal defect with the aim of enhancing wound healing (Xu *et al.*, 2019). Single-cell suspensions prepared *in vitro* can be directly injected into the site of injury, being a simple and minimally invasive procedure (Mooney and Vandenberg, 2008). Several studies have investigated BMSCs delivery into various periodontal-defect animal models (Yamada *et al.*, 2004; Chen *et al.*, 2008; Pieri *et al.*, 2009; Qiu *et al.*, 2020). Results have shown that BMSCs have the capacity to enhance periodontal regeneration by promoting bone formation and neovascularization (Hynes *et al.*, 2012). Despite this, there are some limitations regarding the isolation and expansion of BMSCs to use for periodontal regeneration in the clinical context.

Recently, a population of PDLSCs has been identified (Seo *et al.*, 2004) and research has been conducted to assess the regenerative capacity of these cells in dental defects using several animal models (Liu *et al.*, 2008; Kim *et al.*, 2009; Ji *et al.*, 2010; Park, Jeon and Choung, 2011). Collectively, results consistently showed that PDLSCs hold the potential to form soft and mineralized periodontal-like structures and to enhance periodontal regeneration. Therefore, PDLSCs are important for periodontal regeneration and some studies have suggested a greater capacity to generate all periodontium tissues.

Despite promising treatment outcomes, several limitations have been reported regarding stem-cell therapies application in periodontal defects. Some of these limitations are: insufficient cell numbers after cell implantation, poor engraftment, spread of injected cells to surrounding healthy tissue, and loss of cell fate control (Mooney and Vandenberg, 2008). Another possible stem-cell based approach is the delivery of monolayer or stacked cell sheets. This technique is notably easier to be implemented and results in minimal cell loss/damage (Iwata *et al.*, 2015). Interestingly, a comparative study of cell injection and cell sheet transplantation in swine periodontitis bone defects showed that despite both approaches being able to significantly regenerate periodontal bone, the cell sheet transplantation exhibited higher bone regeneration capacity (Hu *et al.*, 2016).

Considering the combined evidence discussed above, PDLSC-based periodontal regeneration approaches are very promising, addressing the accessibility constraints of BMMSCs and demonstrating favorable treatment outcomes in several animal disease models.

2.5.2. Three-Dimensional Scaffold Manufacturing

In recent decades, three-dimensional (3D) printing has emerged as a promising approach for the manufacture of customized scaffolds with fine-tuned architecture. 3D printing with layer-by-layer deposition enables the creation of personalized scaffolds with specific shape and dimensions. These scaffolds are designed according to alveolar bone defect anatomy and can be combined with osteogenic cells and/or osteoinductive molecules to promote bone tissue regeneration (C. H. Lee *et al.*, 2014).

The printed structures are designed using computer-aided design (CAD) software or from images obtained via computed tomography (CT), magnetic resonance imaging, or X-ray. Traditionally, 3D printing has been primarily used to fabricate scaffolds constituted of synthetic biomaterials, which are then seeded with living cells and tested *in vivo* after implantation (Obregon *et al.*, 2015).

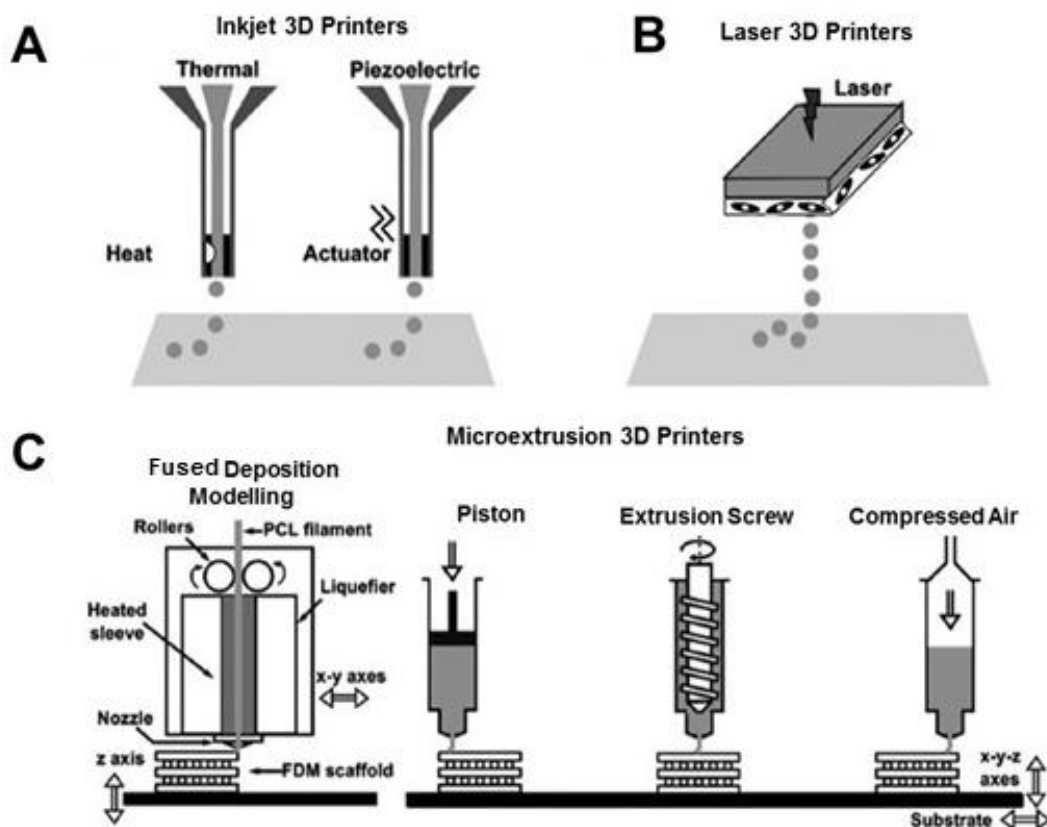


Figure 8. 3D scaffold printing technologies. **A)** Inkjet printing. **B)** Laser printing. **C)** Extrusion printing, including fused deposition modelling, mechanical extrusion (piston and extrusion screw) and pneumatic extrusion (compressed air). Adapted from Obregon *et al.*, 2015.

Although several commercial printers are available in the market and have been reported in the literature, most current systems are inkjet, laser-based and microextrusion printers (Figure 8):

- **Inkjet printers:** In this system, volumes of liquid or low-viscosity inks, such as hydrogels or cell slurries, are ejected using acoustic, thermal, or electromagnetic forces. Despite reports of high cell viability, the shear stress caused by extrusion through small orifices of the print head can be a limiting factor (Xu *et al.*, 2005; Obregon *et al.*, 2015).

- **Laser-based printers:** Printing technology commonly used for defined deposition of cells with a technique based on laser-induced forward transfer. Generally, laser printers are constituted by 3 components: a pulsed laser source, a transparent glass slide (generally coated with an absorbing layer of metal such as gold) covered with a ribbon (layer of cells and biomaterials from which a biological material is printed), and a receiving substrate that collects the printed material. The laser pulses are focused through the glass slide into the gold layer, leading to the vaporization of the metal film and resulting in the production of a jet of liquid solution which is deposited onto receiving substrate (Guillotin *et al.*, 2010; Koch *et al.*, 2010; Obregon *et al.*, 2015).

- **Microextrusion printers:** This category includes a great variety of systems with different extrusion methods. In fused deposition modeling (FDM) systems, a small temperature-controlled extruder forces out a thermoplastic filament material and deposits the semi-molten polymer onto a platform in a layer-by-layer process. The monofilament is moved by two rollers and acts as a piston to drive the semi-molten extrudate. At the end of each finished layer, the base platform is lowered and the next layer is deposited (Zein *et al.*, 2002; Obregon *et al.*, 2015). FDM allows the use of high density and stiffness polymers. Furthermore, FDM is highly reproducible, with a relatively moderate speed, and enables control over mechanical properties, porosity, and pore shape (Hutmacher *et al.*, 2001). In other extrusion printers, inks of low viscosity, molten polymers, injectable shear-thinning biomaterials, or cellular aggregates are dispensed using either mechanical action or a pneumatic system (compressed air). The mechanical properties of these inks can vary considerably, depending on their composition. Hydrogels tend to have relatively low viscosity, cell aggregates will depend on the extent of cell-cell interactions and ECM secretion, and prepolymerized inks are typically dispensed as solidified and stiffer gels. (Khalil, Nam and Sun, 2005; Obregon *et al.*, 2015)

Common to all of these systems is coordinated motion of stages in the X, Y, and Z directions, while an automated system dispenses a bioink via different mechanisms.

2.5.3. 3D Printed PCL Scaffolds for Periodontal Regeneration

Literature review reveals PCL is one of the most commonly studied biomaterials applied to periodontal TE (C. H. Lee *et al.*, 2014; Carmagnola *et al.*, 2017; Galli *et al.*, 2021; Woo *et al.*, 2021). PCL is a synthetic bioresorbable polymer with favorable properties for thermoplastic processing that has been approved by the U. S. Food and Drug Administration. Its melting point ranging between 59 and 64 °C (above body temperature), and a high decomposition temperature of 350 °C allow for a wide range of extrusion temperatures. (Hutmacher *et al.*, 2001; Dwivedi *et al.*, 2020). At physiological temperature, PCL exhibits a rubbery state with high toughness and superior mechanical properties (high strength, elasticity depending on its molecular weight) (Dwivedi *et al.*, 2020). This polymer has been extensively studied *in vitro* and *in vivo* and results confirmed its biocompatibility, biodegradability, non-toxicity and

biocompatibility (Engelberg and Kohn, 1991; Sant *et al.*, 2011; Siddiqui *et al.*, 2018, Silva *et al.*, 2020, Moura *et al.*, 2020).

PCL is known to exhibit a much slower degradation rate (Gavasane, 2014) than PLA and PGLA, two other widely used synthetic materials for scaffold-based TE medical applications (Agrawal and Ray, 2001; Shue, Yufeng and Mony, 2012; Carmagnola *et al.*, 2017; Galli *et al.*, 2021). This makes it an attractive candidate for long term controlled drug release systems (Abudula *et al.*, 2020).

The combination of PCL's physical and mechanical properties makes it a suited biomaterial for alveolar bone regeneration, which requires a robust and resilient material. Moreover, PCL is particularly suitable for the regeneration of resorbed alveolar bone because the biomaterial is not required to significantly enhance the existing load-bearing capacity of the resident bone. (Bartnikowski, Vaquette and Ivanovski, 2020) Thus, PCL has emerged as a promising option for periodontal TE/RM.

In line with the evidence discussed above, previous studies showed PCL scaffolds with perpendicularly oriented micro-channels improved collagen attachment in mineralized structures within the periodontium (Park *et al.*, 2012). Moreover, a pilot randomized controlled trial showed that the surgical insertion of a PCL scaffold 3D printed with FDM technology in fresh extraction sockets allowed bone healing and a better maintenance of ridge height after 6 months as compared to extraction sockets without the scaffold (Goh *et al.*, 2015). A study designed to investigate the ability of an osteoconductive biphasic scaffold to simultaneously regenerate alveolar bone, PDL and cementum, showed significant new bone formation in athymic rats implanted with calcium phosphate coated PCL scaffolds 3D printed by extrusion with FDM (Costa *et al.*, 2014).

Among the various extrusion 3D printing techniques, FDM is one of the most commonly utilized low-cost processes due to its simplicity and availability of machines at affordable prices. The characteristics of FDM 3D printed scaffolds can be tailored by altering printing parameters, such as layer thickness, printing orientation (Zhang, Fan and Liu, 2020). Therefore, this technique allows the development of structures with fully interconnected channel networks, controllable porosity and channel size (Zein *et al.*, 2002). In addition, FDM allows the design of patient-specific scaffolds from computer tomography scans that match defect anatomy. In comparison with other commercially available bioresorbable polymers, PCL is an ideal material for the FDM fabrication process since its flexible, easy to process and structurally stable in FDM working conditions. Previous studies have confirmed the efficacy of the FDM technique in the fabrication and design of PCL scaffolds with mechanical properties dependent on its porosity (Zein *et al.*, 2002).

Importantly, the structure of the periodontal tissues demands the fabrication of scaffolds with optimal pore size. Understanding the effect of mean pore size on PDLSC activity is crucial. Scaffolds need to remain intact as newly tissue is being formed within the porous scaffold, allowing the balance between degradation and regeneration (Ivanovski *et al.*, 2014). The ideal pore size for periodontal TE scaffolds has not been found yet. Several reports have investigated pore sizes from 50 to 600 μm . Ashworth and colleagues have fabricated a 3D collagen scaffold with aligned pores in size of 50-100 μm and showed enhanced PDL fibroblast migration (Ashworth *et al.*, 2018). Costa and co-workers investigated the ability of a biphasic scaffold to simultaneously regenerate alveolar bone, PDL and cementum. Thus, the scaffold was fabricated by attaching a fused deposition modelled bone compartment to an electrospun

periodontal compartment. The bone compartment was produced by FDM composed by PCL containing β -tricalcium phosphate with pore sizes ranging from 100 to 400 μm (Costa *et al.*, 2014). In a different study, PCL-hydroxyapatite scaffolds were fabricated by FDM in three phases with different pore size: 100 μm designed for the cementum interface, 600 μm for the PDL compartment and 300 μm for the alveolar bone (C. H. Lee *et al.*, 2014). Therefore, optimization of pore size of scaffolds for periodontal regeneration still needs to be evaluated.

3. MATERIALS AND METHODS

3.1 PDLSC ISOLATION AND CULTURE

Healthy human third molars were extracted for orthodontic reasons from two healthy patients (20 and 28 years old) from the Dental Clinic at Instituto Universitário Egas Moniz, with written informed consent, following approved guidelines set by the Directive 2004/23/EC of the European Parliament and of the Council of 31 March 2004 on setting standards of quality and safety for the donation, procurement, testing, processing, preservation, storage and distribution of human tissues and cells (Portuguese Law 22/2007, June 29), with the approval of the Ethics Committee of the respective clinical institution.

Isolation of PDLSCs: Similarly to the previously established protocol by Mrozik *et al.* in 2017, samples were washed with wash buffer (and the PDL was gently separated from the surface of the root with the aid of a surgical blade and plated into a 6-well plate containing wash buffer. The wash buffer containing PDL tissue was transferred into a 15 mL conical bottom tube and centrifuged at 1500 rpm for 10 min at 18 °C. After discarding the supernatant, cells were digested in a solution of 3 mg/mL collagenase type I (Sigma-Aldrich) and 4 mg/mL dispase (Sigma-Aldrich) for 1 h at 37 °C. To neutralize enzyme activity, an excess volume of wash buffer was added to the digested tissue and was then strained through a 70 µm cell strainer to remove undigested tissue from periodontal ligament cells. PDL cells were finally separated by centrifugation at 1500 rpm for 10 min at 18 °C, resuspended in 2 mL of 10% FBS-containing DMEM growth media and plated in 6 well-plates.

Adherent Cell Culture of PDLSCs: After PDLSC isolation, adherent PDLSCs colonies were harvested after reaching confluency. Cells were washed once with phosphate-buffered saline solution (PBS, Gibco), harvested using a solution of 0.05% trypsin (Gibco) and counted using the Trypan Blue exclusion method (Gibco). Cells were then plated on T-75 flasks using low-glucose Dulbecco's modified Eagle's medium (DMEM, Gibco) supplemented with 10% fetal bovine serum (FBS MSC qualified, Gibco) and 1% antibiotic-antimycotic (A/A, Gibco) and kept at 37°C, 5% CO₂ in a humidified atmosphere. Medium renewal was performed every 3 days. Isolated cells were kept frozen in liquid/vapor nitrogen tanks until further use.

3.2 ATMSC AND BMMSCS CELL CULTURE

ATMSCs and BMMSCs used in this work are part of the cell bank available at the Stem Cell Engineering Research Group (SCERG), Institute for Bioengineering and Biosciences (iBB) at Instituto Superior Técnico (IST) (32-40 years old). These MSCs were previously isolated/expanded according to previously established protocols (Gimble, Katz and Bunnell, 2007; dos Santos *et al.*, 2009). Originally, human tissue samples were obtained from local hospitals under collaboration agreements with iBB-IST (bone marrow: Instituto Português de Oncologia Francisco Gentil, Lisboa; adipose tissue: Clínica de Todos-os-Santos, Lisboa). All human samples were obtained from healthy donors after written informed

consent according to the Directive 2004/23/EC of the European Parliament and of the Council of 31 March 2004 on setting standards of quality and safety for the donation, procurement, testing, processing, preservation, storage and distribution of human tissues and cells (Portuguese Law 22/2007, June 29), with the approval of the Ethics Committee of the respective clinical institution. Isolated cells were kept frozen in liquid/vapour nitrogen tanks until further use.

Human MSCs from different sources were thawed and plated on T-75 flasks using low-glucose DMEM supplemented with 10% FBS and 1% (A/A) and kept at 37 °C and 5% CO₂ in a humidified atmosphere. Medium renewal was performed every 3-4 days.

3.3 MULTILINEAGE DIFFERENTIATION AND STAININGS

To investigate the multipotency of MSCs derived from different sources (adipose tissue, bone marrow and periodontal ligament), *in vitro* multilineage differentiation studies (adipogenic, chondrogenic and osteogenic lineages) were performed. All samples were stained and imaged and cells that were not cultured with differentiation medium were used as controls.

Osteogenic Differentiation: For osteogenic differentiation, ATMSCs, BMMSCs and PDLSCs were cultured at 3×10^3 cells/cm² on 24-well plates with DMEM + 10% FBS + 1% A/A. At 80% confluence, cells were incubated with osteogenic medium composed by low glucose DMEM supplemented with 10% FBS and 1% A/A, 10 mM β -glycerophosphate (Sigma-Aldrich), 10 nM dexamethasone (Sigma-Aldrich), and 50 μ g/ml ascorbic acid (Sigma-Aldrich). Medium renewal was performed every 3-4 days. After 21 days of osteogenic differentiation, cultures were stained with alkaline phosphatase (ALP), von Kossa (VK), and Alizarin Red (AR) stainings.

ALP and VK stainings identify ALP activity (a known by-product of osteoblast activity) and mineralization, respectively, indicating the presence of active osteoblasts. Medium was removed and cells were washed with PBS. Cells were then fixed with 4% paraformaldehyde (PFA) (Sigma-Aldrich) solution for 15 min. Then, for the ALP staining, cells were rinsed with milliQ water and incubated with a Fast Violet solution (Sigma-Aldrich) and Naphthol AS-MX Phosphate alkaline solution (Sigma-Aldrich) in a final concentration of 4% for 45 min, at room temperature in the dark. Lastly, cells were washed and incubated with a 2.5% silver nitrate solution (Sigma-Aldrich) for 30 min at room temperature in the dark (von Kossa staining), followed by cell washing and imaging.

Alizarin Red staining was also performed to visualize calcium deposits. Cells were stained with a 2% AR solution (Sigma-Aldrich) by incubation for 1 h at room temperature. Afterwards, cells were washed with PBS and imaged.

Adipogenic Differentiation: For adipogenic differentiation, ATMSCs, BMMSCs and PDLSCs were cultured at 3×10^3 cells/cm² on 24-well plates with DMEM + 10% FBS + 1% A/A. After reaching 80% confluency, adipogenic differentiation medium (StemPro™ Adipogenesis Differentiation Kit, Gibco) was added to the culture to induce differentiation into adipocytes. Medium was changed every 3-4 days and after 21 days of adipogenic differentiation, cells were fixed with 4% PFA for 15 min and stained with Oil

Red O solution (0.3% in isopropanol) (Sigma-Aldrich) for 1 h at room temperature. Oil Red O stains accumulated lipids, allowing the detection of intracellular lipid droplet accumulation resulting from adipogenic differentiation. After staining, cells were washed with PBS and imaged.

Chondrogenic Differentiation: For chondrogenic differentiation, ATMSCs, BMSCs and PDLSCs were cultured as cell aggregates. Cells were plated as small droplets (10 μ L) at a cell density of 1×10^7 cells/ml on ultra-low attachment multi-well plates (Corning). Plates were placed in the incubator for 30 min and chondrogenic differentiation media (MesenCult™ Chondrogenic Differentiation Kit, Stemcell Technologies) was added. Medium was changed every 3-4 days and after 21 days of chondrogenic differentiation cells were fixed in 4% PFA for 15 min. These aggregates were stained with 1% Alcian Blue solution (Sigma-Aldrich) for 1 h, at room temperature. Alcian Blue stains glycosaminoglycans (GAGs), a known by-product of chondrocyte activity. Finally, aggregates were washed with PBS and imaged.

3.4 FLOW CYTOMETRY ANALYSIS

Immunophenotypic analysis of BMSCs, ATMSCs and PDLSCs was performed by flow cytometry using a panel of mouse anti-human monoclonal antibodies for the expression of CD14, CD19, CD29, CD34, CD44, CD45, CD73, CD80, CD90, CD105, CD106, CD146, CD166, HLA-DR and STRO-1 (BioLegend).

PDLSCs were analyzed from passages 1 to 7. ATMSCs and BMSCs were analyzed in passages 3, 5, and 7. Briefly, cells (1×10^6 cells/ml) were incubated with each antibody for 20 min in the dark at room temperature. Afterwards, cells were washed with PBS and centrifuged at 1500 rpm for 5 min. Finally, cells were fixed using a solution of 4% PFA. A minimum of 10 000 events were collected for each sample. Flow cytometric analysis was performed using FACScalibur flow cytometer (Becton Dickinson) and CellQuest™ software (Becton Dickinson) was used for acquisition. For data analysis, Flowing Software (University of Turku, Finland) was used.

3.5 IMMUNOCYTOCHEMISTRY ANALYSIS

The presence and distribution of several ECM proteins, such as collagen I (Col I), asporin, fibronectin, laminin, osteopontin, osteocalcin, cementum protein 1 and Stro-1, was analyzed in BMSCs, ATMSCs and PDLSCs cultured under expansion (with DMEM growth media, Section 3.3) and osteogenic differentiation conditions (with osteogenic differentiation media, Section 3.3).

Cells were plated on 24-well plates and were fixed at two different timepoints: after reaching confluency (DMEM + 10% FBS + 1% A/A) and after 21 days of osteogenic differentiation. Briefly, cells were washed with PBS and fixed with 4% PFA for 20 min at room temperature. Then, cells were washed with 1% bovine serum albumin (BSA, Sigma-Aldrich) in PBS and incubated for 45 min with a solution composed by 1% BSA, 10% FBS and 0.3% Triton X-100 in PBS to block and permeabilize cells. Primary antibodies (dilution 1:500 in 1% BSA, 10% FBS and 0.3% Triton X-100) including rabbit anti-human

collagen I (Thermo Fisher Scientific), asporin (Abcam), laminin (Thermo Fisher Scientific), osteopontin (Abcam), osteocalcin (Sigma-Aldrich) and cementum protein 1 (Abcam) and mouse anti-human (dilution 1:500 in 1% BSA, 10% FBS and 0.3% Triton X-100) collagen IV (Thermo Fisher Scientific), fibronectin (Thermo Fisher Scientific) and stro-1 (Thermo Fisher Scientific) were added followed by overnight incubation at 4°C. After washing with 1% BSA in PBS, goat anti-mouse IgG Alexa Fluor 546, goat anti-rabbit IgG Alexa Fluor 546 and goat anti-mouse IgG Alexa Fluor 488 (Thermo Fisher Scientific, dilution 1:200 in 1% BSA PBS solution) were used as secondary antibodies and incubated in the dark for 1 h at room temperature. Finally, the cell nuclei were counterstained with DAPI (Thermo Fisher Scientific, 1.5 µg/ml) for 5 min and then washed with PBS. Immunofluorescence staining was confirmed by fluorescence microscopy (Leica DMI3000B, Wetzlar, Germany).

3.6 CELL MORPHOLOGY ASSAY

Cells were seeded on 24-well plates at a density of 3×10^3 cells/cm², and cell morphology was assessed after 1, 3, 5 and 7 days of culture under expansion conditions (with DMEM media, Section 3.3). Cells were washed twice with PBS, fixed with 4% PFA for 15 min and then permeabilized with a 0.1% Triton X-100 solution (Sigma-Aldrich) for 10 min. After permeabilization, cells were incubated with Phalloidin-TRITC (Sigma-Aldrich; dilution 1:250, 2 µg/ml) for 45 min in the dark. Afterwards, cells were washed twice with PBS and counterstained with DAPI 1.5 µg/ml for 5 min and then washed with PBS. Cells were imaged by fluorescence microscope (Leica DMI3000B).

3.7 KINETICS ASSAY

ATMSCs, BMMSCs, and PDLSCs were plated onto 12-well plates at different cell densities: 1.5×10^2 cells/cm² (PDLSCs), 1.5×10^3 cells/cm² and 3×10^3 cells/cm² using DMEM + 10% FBS + 1% A/A as growth medium. Cells were kept at 37°C and 5% CO₂ in a humidified atmosphere and culture medium was changed every 3-4 days. At days 1, 3, 5, 7, 9 and 12, cells were harvested using a solution of 0.05% trypsin (Gibco). Cells were incubated with trypsin for 7 min at 37 °C and 5% CO₂. The reaction was stopped by adding DMEM + 10% FBS + 1% A/A. Cells were centrifuged at 1250 rpm for 7 min and resuspended in DMEM + 10% FBS + 1% A/A. Cells were counted using the Trypan Blue exclusion method (Gibco) to determine cell growth curves. Cell number was determined by applying Eq. 1 with a dilution factor of 2.

$$\text{Total number of cells} = \frac{(\text{Total cells counted} \times \text{Dilution factor} \times 10^4 \text{ cells} \times \text{volume})}{\text{Number of squares counted}} \quad \text{Eq. 1}$$

Fold increase (FI) in total cell number was calculated using Eq. 2 where N is the number of viable cells and N_0 is the number of viable cells plated at day 0. Population doublings (PD) were calculated using Eq. 3.

$$FI = \frac{N}{N_0} \quad \text{Eq. 2}$$

$$PD = \frac{\log FI}{\log 2} \quad \text{Eq. 3}$$

3.8 QUANTITATIVE ASSESSMENT OF OSTEOGENIC DIFFERENTIATION

After 21 days of osteogenic differentiation (Section 3.3), metabolic activity, calcium content and ALP activity assays were performed on ATMSCs, BMMSCs and PDLSCs cultured under osteogenic differentiation conditions.

Metabolic Activity: After 21 days of osteogenic differentiation, medium was removed, cells were washed with PBS and the metabolic activity of MSCs was evaluated using AlamarBlue® cell viability reagent (Thermo Fischer Scientific) following the manufacturer's guidelines. Briefly, a 10% AlamarBlue® solution in culture medium was added to cells and incubated at 37°C for 3 h. Fluorescence intensity was measured in a microplate reader (Infinite M200 Pro, Tecan) at an excitation/emission wavelength of 560/590 nm. Three samples were used for each condition and fluorescence was measured in triplicates.

ALP Activity Assay: After 21 days of osteogenic differentiation, ALP activity was detected using a colorimetric ALP kit (BioAssays Systems) according to the manufacturer's protocol. Samples were washed with PBS and incubated in lysis buffer composed by 0.1% Triton X-100 in PBS by shaking for 30 minutes at room temperature. The lysate was added to p-nitrophenyl phosphate solution (10 mM) provided with the ALP kit. Lastly, the absorbance was measured on a plate reader (Infinite M200 Pro, Tecan) at 405 nm and normalized to the metabolic activity. Three different samples were used for each condition and absorbance was measured in triplicates.

Calcium Quantification Assay: For determination of total calcium content, samples were washed with PBS and incubated with a 0.5 M HCl solution (Sigma-Aldrich). Accumulated calcium was removed from the cellular component by shaking overnight at 4°C. The supernatant was used for calcium determination according to the manufacturer's instructions in the calcium colorimetric assay kit (Sigma-Aldrich). Total calcium was calculated from calcium standard solutions prepared in parallel. Absorbance at 575 nm was measured for each condition on a plate reader (Infinite M200 Pro, Tecan) and normalized to the metabolic activity. Three samples were used for each condition and absorbance values were measured in triplicates.

Quantitative Reverse Transcription-Polymerase Chain Reaction (qRT-PCR) Analysis: Total RNA was extracted using the RNeasy Mini Kit (QIAGEN, Germany). cDNA was synthesized from the purified RNA using High-Capacity cDNA Reverse Transcription kit (Life Technologies). Reaction

mixtures were incubated in a thermal cycler (96-well T-100 Thermal Cycler, Biorad) and the primer sequences used in the qRT-PCR analysis are summarized in Table 1. The qRT-PCR was performed using NZYSpeedy qPCR Green Master Mix (2x), ROX plus (NZYTech) and StepOnePlus real-time PCR system (Applied Biosystems). All reactions were carried out at 95 °C for 10 min, followed by 40 cycles of 95 °C for 15 sec and 60°C for 1min; all were performed in triplicate. Target genes expression was primarily normalized to the housekeeping gene glyceraldehyde 3-phosphate dehydrogenase (GAPDH) and then determined as a fold-change relative to the baseline expression of the target genes measured at day 0 (undifferentiated cells) as internal control to normalize differences in total RNA levels in each sample. A threshold cycle (Ct) was observed in the exponential phase.

Table 1. Forward and reverse primer sequences used in qRT-PCR analysis.

<i>Gene</i>	<i>Primer Sequences</i>
Col I	Fwd: 5'-CATCTCCCCTTCGTTTTTGA-3' Rev: 5'-CCA AAT CCG ATG TTT CTG CT-3'
Runx2	Fwd: 5'-AGATGATGACTGCCACCTCTG-3' Rev: 5'-GGGATGAAATGCTTGGGAACT-3'
ALP	Fwd: 5'-ACCATTCCCACGTCTTCACATTT Rev: 5'-AGACATTCTCTCGTTCACCGCC-3'
OPN	Fwd: 5'-TGTGAGGTGATGTCCTCGTCTGTAG-3' Rev: 5'-5'-ACACATATGATGGCCGAGGTGA-3'
OC	Fwd: 5'-TGCCTCAGAAGAGCTGAAAAC-3' Rev: 5'-CACAGACTCCCTGCTTTTGCT-3'
CEMP-1	Fwd: 5'-ACATCAAGCACTGACAGCCA-3' Rev: 5'-GTTGATCTCCGCCATAAGC-3'
POSTN	Fwd: 5'-ACATCAAGCACTGACAGCCA Rev: 5'-GCCTCCAATATGTCCGATGT-3'

3.9 FABRICATION OF 3D PRINTED PCL SCAFFOLDS BY FDM

The scaffolds were fabricated using a 3D printing system (Prusa, i3 MK3) by fused deposition modelling technology as shown in Figure 9. Three PCL (MW 50000 Da, TM 6500, Perstorp Caprolactones) scaffolds with different sizes (100 µm, 300 µm and 600 µm) were designed by CAD in the form of squared prisms. Dimensions of each scaffold according to pore size are illustrated in Figure 10. Briefly, the PCL filament material was heated at 80° C (a temperature above PCL's melting point of 60° C) and extruded through a nozzle guided by a robotic device with computer-controlled motion. Each layer has a 0.15 mm height, and all layers were printed in a squared grid pattern.

3.10 PCL SCAFFOLD STERILIZATION AND PDLSC SEEDING

Similarly to previous protocols (Silva, Carvalho, *et al.*, 2020), before cell culture, PCL scaffolds were sterilized by ultraviolet radiation exposure for 1 h on each side of the scaffold. Then, scaffolds were washed with 70% ethanol and rinsed three times with washing buffer (PBS + 1% A/A). Lastly, to improve cell binding to scaffold surface, scaffolds were incubated with culture media (DMEM + 10% FBS + 1% A/A) for 1 h.

Cells were seeded by manually dispensing 10 μ L of a PDLSC suspension (in DMEM + 10% FBS + 1% A/A) with adequate concentration to fulfill a seeding density of 5×10^4 cells per scaffold. To promote initial cell attachment, the 3D printed PCL scaffolds were incubated for 2 h at 37 $^{\circ}$ C and 5% CO₂, before adding culture media. Cells were cultured under expansion conditions (DMEM + 10% FBS + 1% A/A) and medium renewal was performed every 3-4 days.

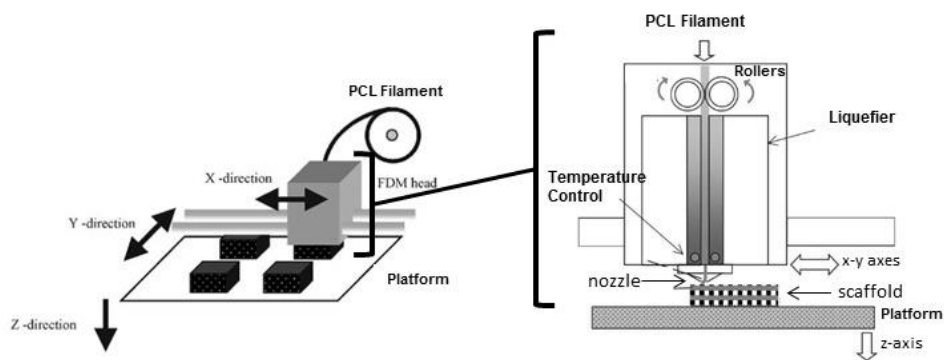


Figure 9. Schematic diagram of FDM extrusion 3D printing with PCL filament. Adapted from Zein *et al.*, 2002.

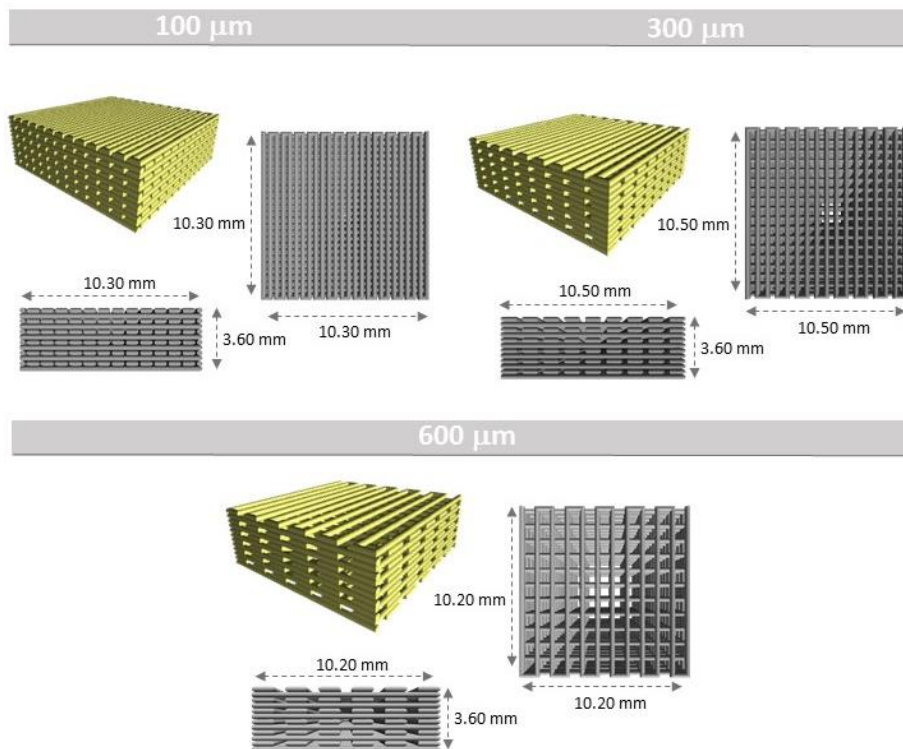


Figure 10. Models and dimensions of polycaprolactone scaffolds generated with CAD for 3D printing by fused deposition modelling with different pore sizes (100 μ m, 300 μ m and 600 μ m).

3.11 METABOLIC ACTIVITY AND MORPHOLOGY OF PDLSCs CULTURED IN 3D PRINTED PCL SCAFFOLDS

The metabolic activity of PDLSCs in the different experimental scaffold groups (pore size: 100 μm , 300 μm and 600 μm) was evaluated on days 1, 3, 7 and 10 using AlamarBlue® cell viability reagent (Thermo Fischer Scientific) following the manufacturer's guidelines. Briefly, a 10% AlamarBlue® solution in culture medium was added to the scaffolds and incubated at 37° C for 3 h. Fluorescence intensity was measured in a microplate reader (at an excitation/emission wavelength of 560/590 nm and compared to a calibration curve to assess the equivalent number of cells present in each scaffold. Scaffolds without seeded cells (for each experimental group) were used as blank controls. Four scaffolds (n = 4) were analyzed for each experimental group and fluorescence values of each sample were measured in triplicate. To assess cell morphology after day 1 and 3 of cell culture, scaffolds were washed twice with PBS, fixed with 4% PFA for 20 min and then permeabilized with 0.1% Triton X-100 for 10 min. Afterwards, scaffolds were incubated with phalloidin (dilution 1:250, 2 $\mu\text{g}/\text{ml}$) for 45 min in the dark, washed twice with PBS and counterstained with DAPI (1.5 $\mu\text{g}/\text{ml}$) for 5 min. After washing twice with PBS, scaffolds were imaged by fluorescent microscopy.

4. RESULTS

4.1. ISOLATION AND CHARACTERIZATION OF PERIODONTAL LIGAMENT STEM CELLS

PDLSCs were successfully isolated from healthy human teeth collected from two healthy donors (20–28 years old) undergoing tooth extraction at Clínica Dentária Egas Moniz, Instituto Egas Moniz, under the approval of Ethical Committee of Instituto Egas Moniz. The tissue was harvested from the surface of the roots as represented in Figure 11. Both samples were enzymatically digested with a solution of 3 mg/mL collagenase type I and 4 mg/mL dispase, according to Mrozik protocol (Mrozik *et al.*, 2017), as described in section 3.1. After isolation, cells attached to the culture plate and displayed a fibroblast-like morphology similar to MSCs.

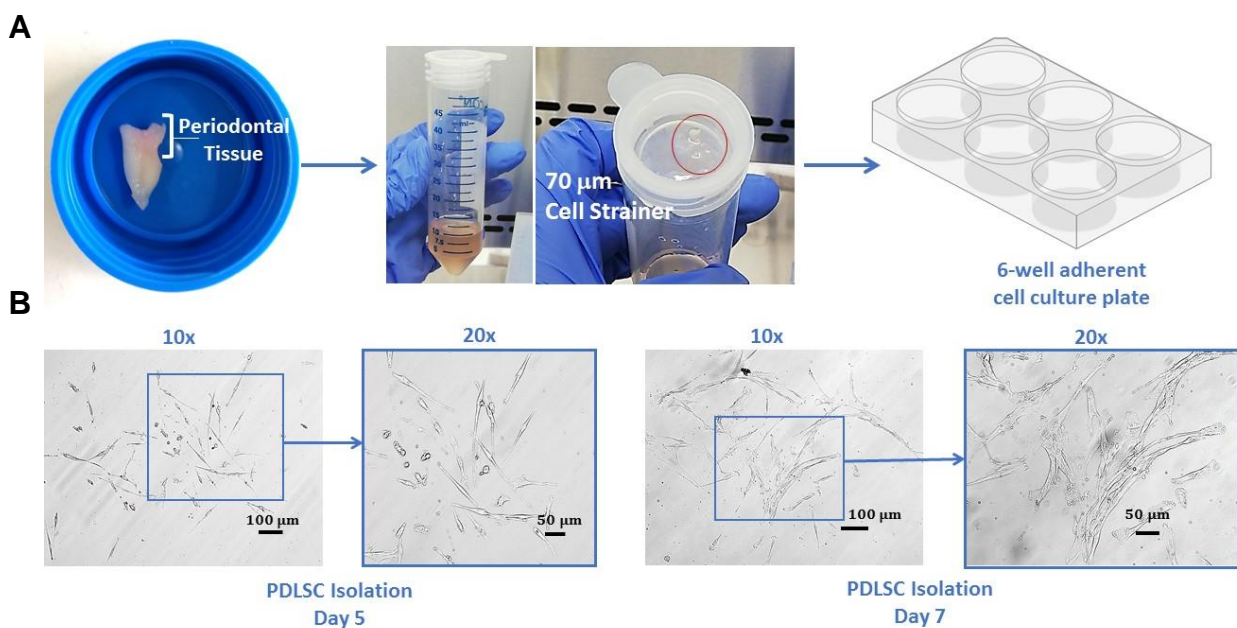


Figure 11. PDLSC isolation. **A)** Following tooth extraction, primary PDLSCs were isolated from periodontal tissue. The tissue was enzymatically digested, strained through a 70 µm cell strainer and cultured in 6-well adherent cell culture plates. **B)** Bright field images of PDLSC primary culture in expansion conditions (DMEM + 10% FBS + 1% A/A) after 5 and 7 days.

4.1.1. Expression of Mesenchymal Stromal Markers

4.1.1.1. Flow Cytometry

The immunophenotypic profile of PDLSCs from passage 1 to passage 7 was assessed by flow cytometry (Figure 12). Results demonstrated positive expression (> 80 %) of the MSC-associated markers CD29, CD44, CD73, CD90, and CD105. However, Stro-1 and CD106, were consistently negatively expressed by PDLSCs in passages 1-7.

PDSCs lack the expression of hematopoietic stem cell (HSC) markers and CD80, a co-stimulatory molecule essential for T-lymphocyte activation (Suvas *et al.*, 2002). Lastly, PDLSCs also exhibited positive expression for CD146 (also known as MUC18 and melanoma cell adhesion molecule, MCAM), an endothelial cell antigen also expressed at the surface of pericytes and previously used in the identification PDLSCs (Seo *et al.*, 2004). However, CD146 expression levels decreased with passaging.

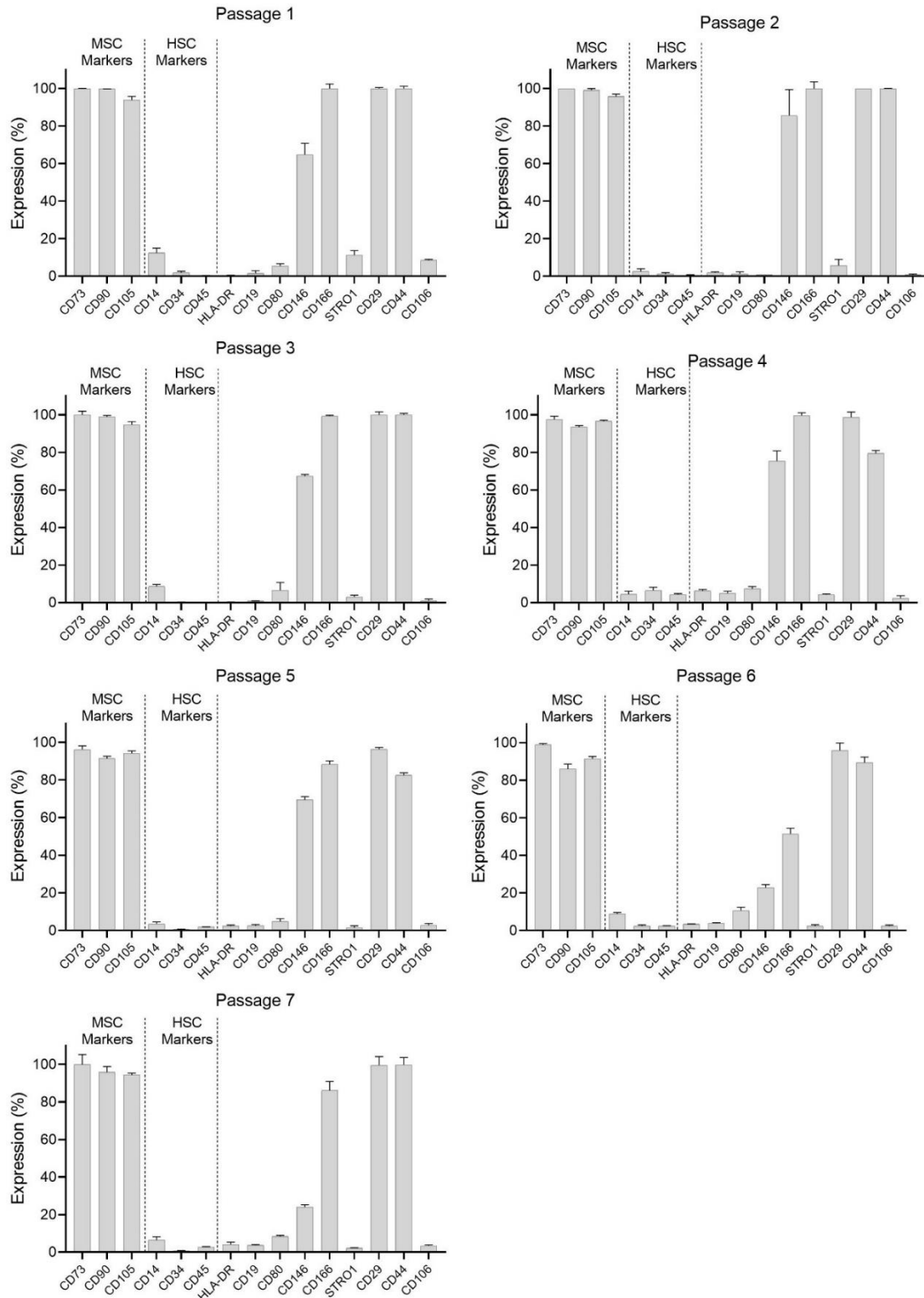


Figure 12. Characterization of PDLSCs by immunophenotypic analysis. Surface marker expression by PDLSCs cultured in expansion conditions from passage 1 to passage 7. Data are expressed as mean \pm SD (n=2 different donors).

4.1.1.2. Immunocytochemistry Analysis

As expected, immunocytochemistry assays (Figure 13) confirmed the expression of the common ECM and cytoskeleton proteins, such as laminin and fibronectin. Additionally, PDLSCs expressed Stro-1, a known MSC marker (Simmons and Torok-Storb, 1991); asporin, a protein associated with the PDL (Yamada, Kitamura and Murakami, 2008); osteocalcin and osteopontin, both osteogenic markers (Stein, Lian and Owen, 1990).

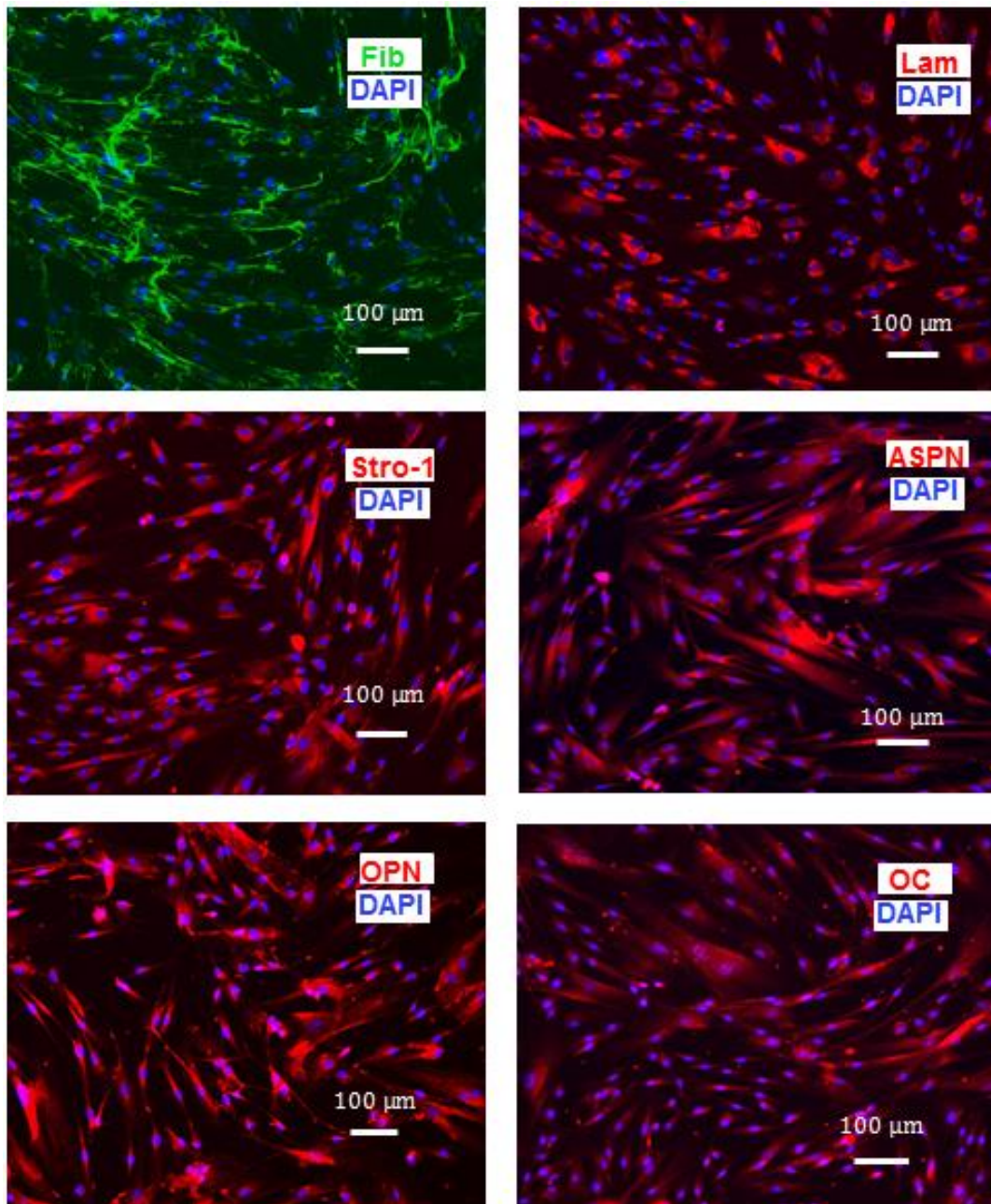


Figure 13. Characterization of PDLSCs by immunocytochemistry analysis. Immunofluorescent staining images of asporin (ASPN, red), fibronectin (Fib, green), laminin (Lam, red), STRO-1 (red), osteopontin (OPN, red) and osteocalcin (OC, red). Scale bar, 100 µm.

4.1.2. Multilineage Differentiation

After 21 days of differentiation, successful *in vitro* differentiation of PDLSCs into adipogenic, chondrogenic and osteogenic lineages (Figure 14) was confirmed. Adipogenic differentiation resulted in accumulation of lipid droplets, positively stained with Oil red O. Regarding osteogenic differentiation, ALP staining demonstrated lower levels of ALP synthesis, confirmed by the lower intensity of red stains. However, VK staining showed increased deposition of minerals, observed by the black deposits of minerals. Alizarin Red staining also confirmed the osteogenic differentiation of PDLSCs, presenting a mineralized ECM. Lastly, chondrogenic differentiation was confirmed by Alcian blue staining that confirmed the presence of GAGs.

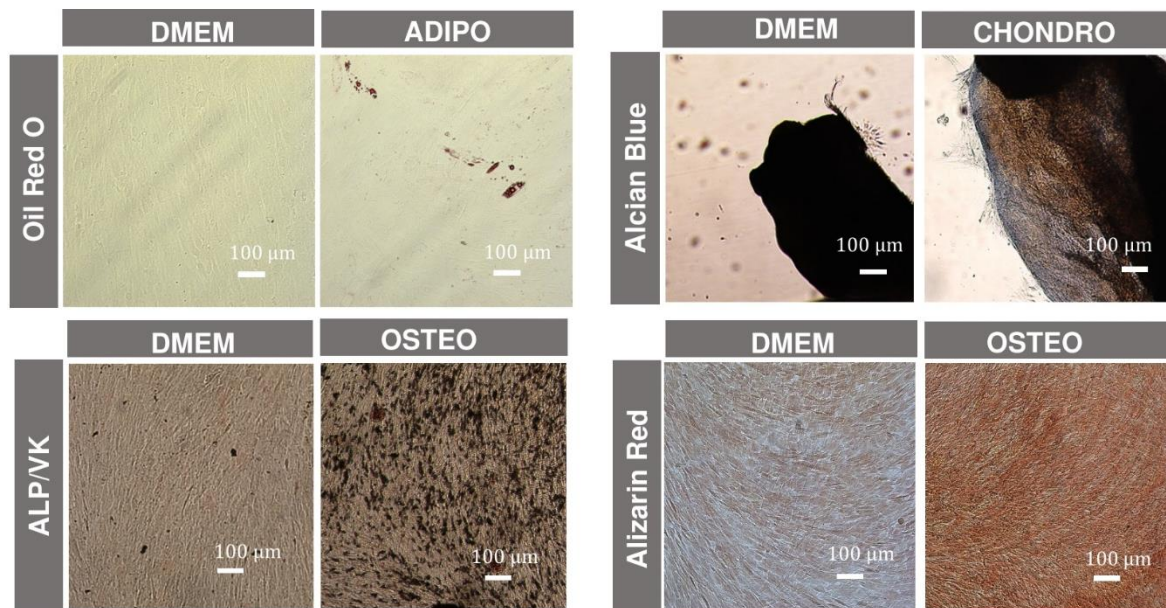


Figure 14. *In vitro* multilineage differentiation of PDLSCs. Adipogenic differentiation was detected by Oil red o staining showing the lipid vacuoles in red. Alcian blue stains proteoglycans in blue synthesized by chondrocytes. Alkaline phosphatase (ALP) and von Kossa (VK) stainings show ALP activity in red and mineralized extracellular matrix deposits in black. Alizarin red stains the calcium deposited in the extra-cellular matrix in red. As controls, all stainings were performed in PDLSCs cultured under expansion conditions (DMEM). Scale bar, 100 µm.

4.1.3. PDLSC Growth Kinetics

To evaluate the proliferative capacity of PDLSCs, cells were plated at three different cell seeding densities: 1.5×10^2 cells/cm², 1.5×10^3 cells/cm² and 3×10^3 cells/cm² (Figure 15) and counted at different timepoints (days 1, 3, 5, 7, 9 and 12, n=2, two donors). Cell seeding densities were chosen according to previous studies (Iwata *et al.*, 2010). The growth kinetics curves for PDLSCs cultured at 1.5×10^3 cells/cm² and 3×10^3 cells/cm² cells displayed similar behavior with an adaptation phase in the first 3 days followed by an exponential growth phase with a steep slope, stabilizing in day 9. When PDLSCs were seeded at 1.5×10^2 cells/cm², PDLSCs remained in the adaptation phase for 5 days and the results indicate that after 12 days of culture (Figure 16) the PDLSCs seeded at low density were still in exponential growth phase, reaching $(3.3 \pm 1.3) \times 10^5$ cells per well. Surprisingly, PDLSCs seeded at lower densities, presented higher population doublings after 12 days of culture (Figure 15 A and B).

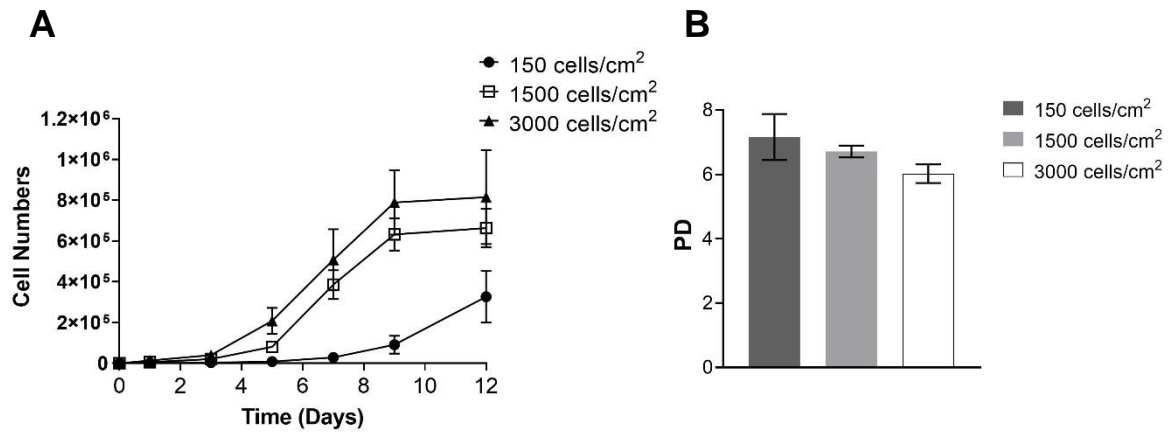


Figure 15. Proliferation of PDLSCs cultured in expansion conditions (DMEM + 10%FBS+ 1% A/A) seeded at 1.5×10^2 , 1.5×10^3 and 3.0×10^3 cells/cm² in 12-well plates. **A)** Growth curves of PDLSCs cultured at different cell seeding densities. **B)** Population doublings (PD) of PDLSCs cultured at different cell seeding densities after 12 days of culture. Data are expressed as mean \pm SD (n=2 donors).

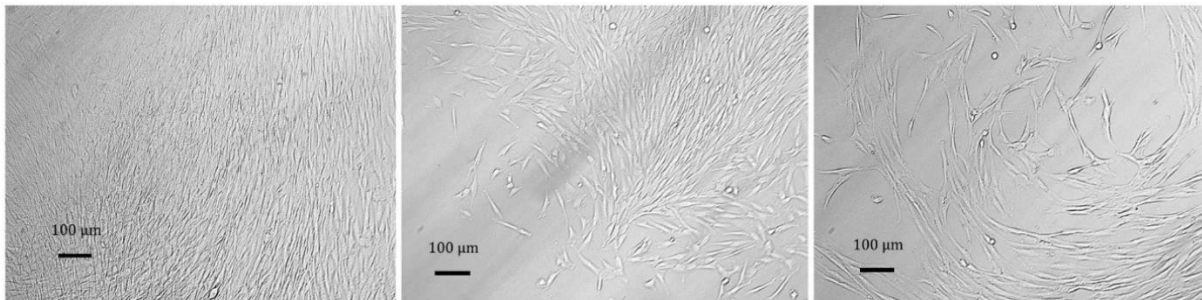


Figure 16. Bright field images depicting different zones of a 12-well plate bottom with PDLSC cultured for 12 days in expansion conditions (DMEM +10% FBS+ 1% A/A) at 1.5×10^2 cells/cm². Scale bar, 100 μ m.

4.2. COMPARISON OF MSCs DERIVED FROM ADIPOSE TISSUE, BONE MARROW AND PERIODONTAL LIGAMENT

Aiming to understand the differences between MSCs isolated from different sources: bone marrow, adipose tissue and periodontal ligament, comparative studies with BMMSCs, ATMSCs and PDLSCs were performed to assess phenotypical differences in cell surface marker expression, multilineage differentiation potential, growth kinetics and morphology. Overall, PDLSCs, BMMSCs and ATMSCs presented the typical MSC-associated properties, such as MSC-related surface marker expression and multilineage differentiation potential (Dominici *et al.*, 2006). Nonetheless, phenotypical differences between the three cell types were identified, particularly in cell surface marker expression, presence of specific proteins and cell growth kinetics

4.2.1. Expression of Mesenchymal Stromal Markers

4.2.1.1. Flow Cytometry

Immunophenotypic analysis of PDLSCs, BMMSCs and ATMSCs was assessed by flow cytometry (Figure 17). All samples displayed strongly positive expression (> 90 %) of MSC-associated cell surface markers CD29, CD44, CD73, CD90, CD105, and CD166 in passage 3. Interestingly, CD44 expression levels of PDLSCs remained significantly high (> 99.7 %), independently of passage number. However, CD44 expression levels of BMMSCs and ATMSCs decreased in passages 5 and 7 (expression levels ranged between 64.3-81.0 %).

Results showed that CD166 expression was positive (> 83.1 %) for PDLSCs and BMMSCs in passages 3, 5 and 7. However, for ATMSCs, CD166 expression levels showed a tendency to decrease with passaging, with (90.45 ± 0.33) % expression in passage 1 but (45.94 ± 2.65) % and (64.87 ± 5.12) % expression in passages 5 and 7, respectively. CD106 and Stro-1 expression levels were low (< 10 %) in all samples analyzed in passages 3, 5 and 7, independently of cell source. As expected, lack of expression of HSC-associated markers was also verified for PDLSCs, BMMSCs and ATMSCs in passages 3, 5 and 7. All samples displayed negative expression of known HSC-related markers, namely CD14, CD19, CD34, CD45 and HLA-DR. Additionally, the immune cell-related marker CD80 was negatively expressed by samples from all MSC sources.

Lastly, results showed that CD146, a marker previously used to identify PDLSCs (Seo *et al.*, 2004), was consistently positively expressed solely by PDLSCs in passages 3, 5 and 7. Despite this, results showed that CD146 expression by PDLSCs decreased with passaging (64.8 ± 0.91 % for passage 1, (47.4 ± 1.6) % for passage 5 and (24.1 ± 1.2) % for passage 7). CD146 expression was absent in BMMSCs and ATMSCs.

4.2.1.2. Immunocytochemistry Analysis

To further investigate differences in protein expression between PDLSCs, BMMSCs and ATMSCs, a comparative immunocytochemistry analysis was performed. Results depicted in Figure 18 confirmed the expression of the common ECM and cytoskeleton proteins, such as laminin and fibronectin, in all samples. Additionally, only PDLSCs expressed Stro-1 (a known MSC marker (Simmons and Torok-

Storb, 1991)), aspirin (a protein associated with the PDL (Yamada, Kitamura and Murakami, 2008)), osteocalcin and osteopontin (bone ECM proteins (Stein, Lian and Owen, 1990)). Interestingly, BMMSCs and ATMSCs did not express Stro-1, aspirin, osteocalcin and osteopontin.

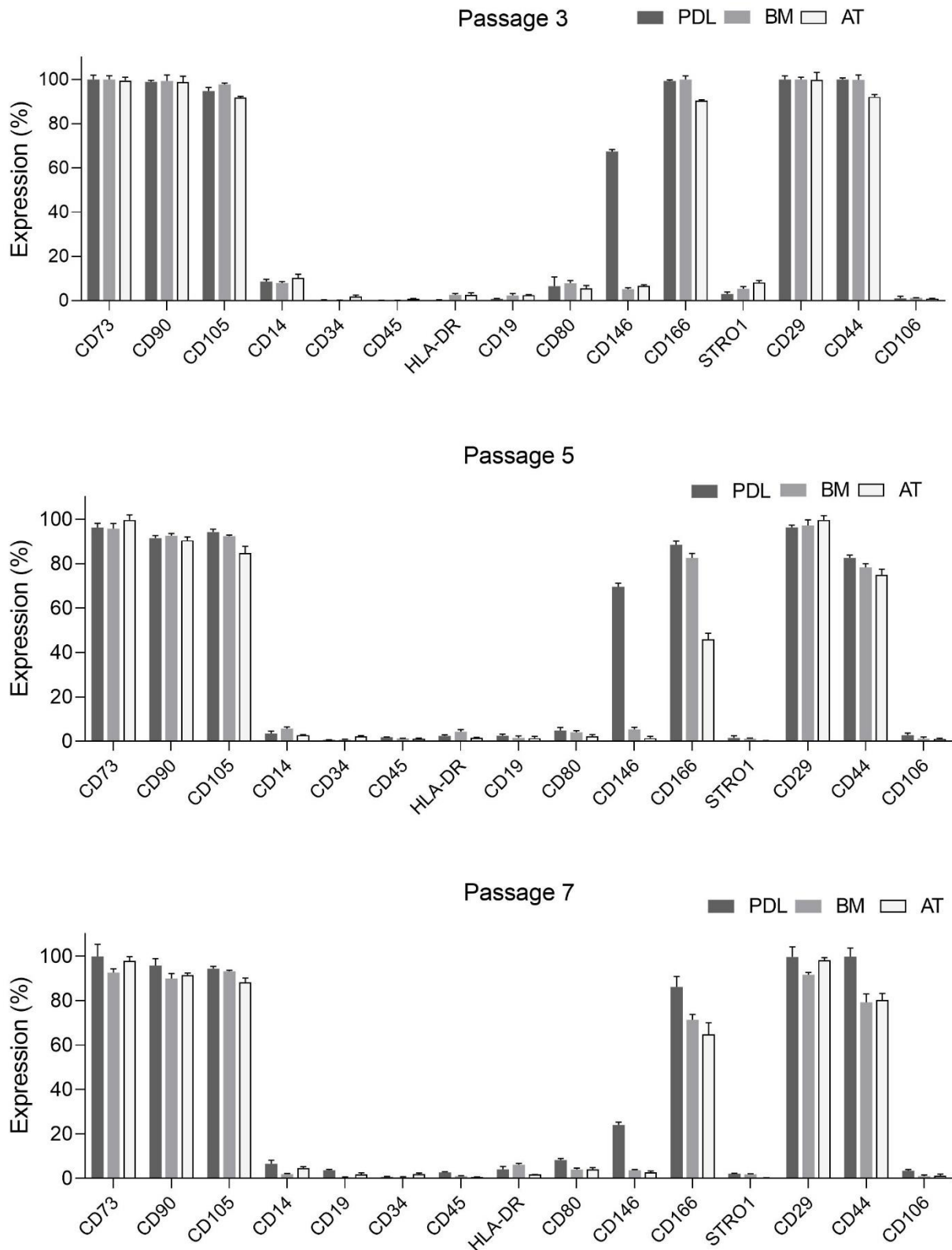


Figure 17. Immunophenotypic analysis of PDLSCs, ATMSCs and BMMSCs cultured in expansion conditions (DMEM + 10%FBS+ 1% A/A) at passages 3, 5 and 7 by flow cytometry. Data are expressed as mean \pm SD (n=2 donors).

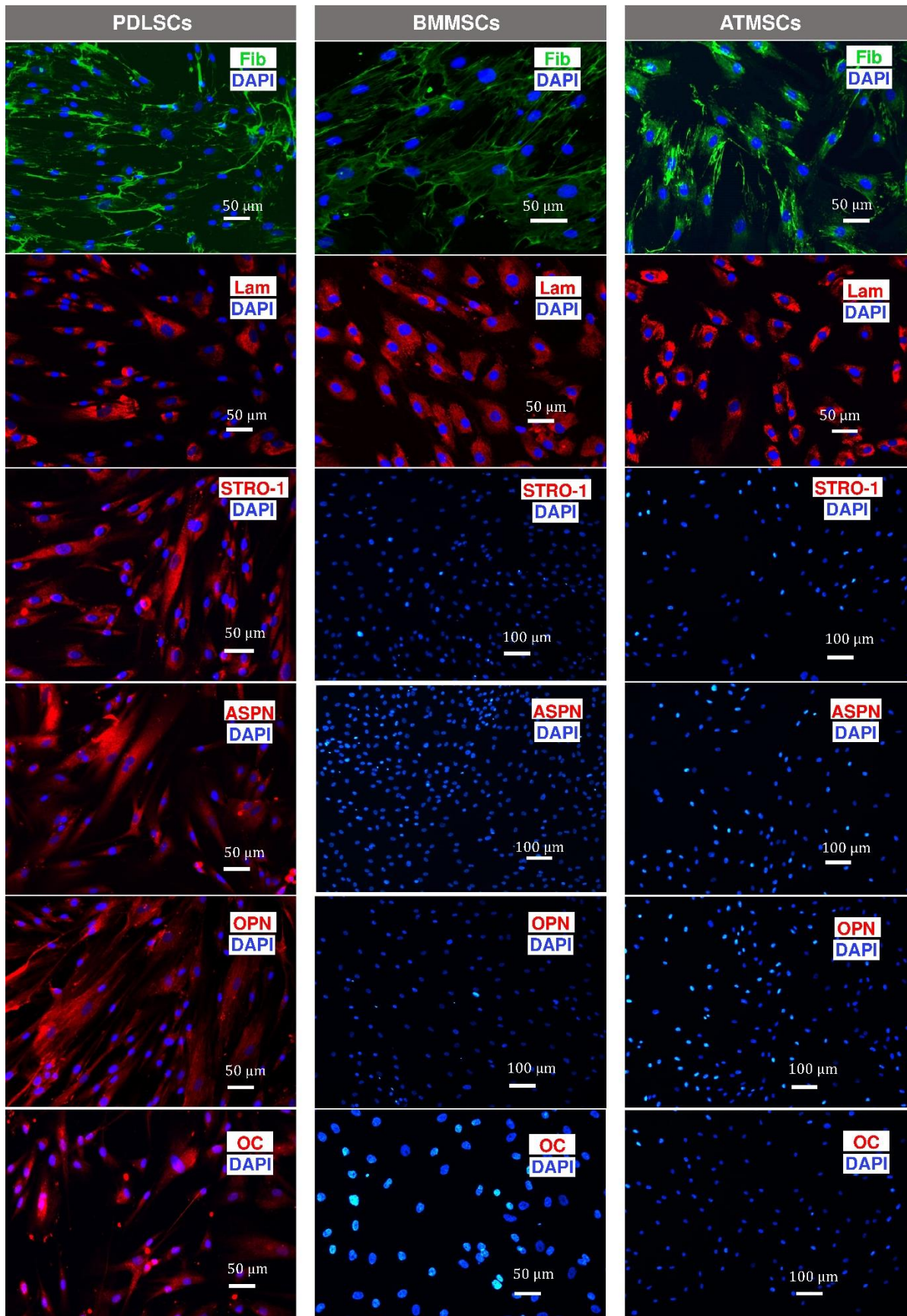


Figure 18. Comparison of immunofluorescent staining images for PDLSCs, BMMSCs and ATMSCs for the expression of fibronectin (Fib, green), laminin (Lam, red), stro-1 (STRO-1, red), asporin (ASP, red), osteopontin (OPN, red) and osteocalcin (OC, red). Nuclei were stained with DAPI (blue).

4.2.2. Multilineage Differentiation

After 21 days of differentiation in adipo-, chondro-, and osteogenic media, appropriate stainings confirmed the *in vitro* differentiation of PDLSCs, BMMSCs and ATMSCs into adipogenic, chondrogenic and osteogenic lineages (Figure 19). MSCs derived from PDL, BM and AT successfully differentiated into the three lineages.

Figure 19 revealed positive stainings of adipocytes, chondrocytes and osteoblasts with Oil red O, ALP/VK, and Alcian blue stainings, respectively. Cells cultured under expansion conditions (DMEM+ 10%FBS + 1% A/A medium) were used as negative controls. Regarding adipogenic differentiation, PDLSCs exhibited a lower amount of Oil Red O-stained liquid droplets compared with BMMSCs and ATMSCs, suggesting a decreased adipogenic potential. Nonetheless, Oil red O staining results does not allow clear comparison between the three different cell types. Further quantitative assays are necessary to assess PDLSC adipogenic differentiation capacity, such as adipogenic gene expression analysis. Furthermore, osteogenic differentiation stainings revealed that PDLSCs produced lower amount of ALP compared with BMMSCs and ATMSCs, however PDLSCs presented enhanced mineralization, observed by VK and Alizarin Red stainings (Figure 18).

4.2.3. Growth Kinetics and Morphology

To assess the proliferative capacity of MSCs from different sources (PDLSCs, BMMSCs and ATMSCs), cells were plated at 1.5×10^3 cells/cm² and 3×10^3 cells/cm² and counted at days 1, 3, 5, 7 and 9 after seeding (Figure 20, n=2 donors per cell type). Additionally, morphology of the PDLSCs, BMMSCs and ATMSCs was visualized under fluorescence microscopy (Figure 22). Overall, all cell types exhibited the typical MSC fibroblast-like morphology consisting of a spindle-shaped cell body, which was maintained by the cells throughout the *in vitro* culture period.

Interestingly, PDLSCs reached around $(7.9 \pm 1.6) \times 10^5$ cells at day 9 when seeded at 3×10^3 cells/cm², while BMMSCs and ATMSCs only reached $(0.54 \pm 0.22) \times 10^5$ and $(0.83 \pm 0.28) \times 10^5$ cells, respectively. When cells were seeded at 1.5×10^3 cells/cm², PDLSCs reached $(6.3 \pm 0.79) \times 10^5$ cells, while BMMSCs and ATMSCs presented $(0.29 \pm 0.21) \times 10^5$ and $(0.94 \pm 0.01) \times 10^5$ cells, respectively, at day 9. PDLSCs presented higher cell numbers compared to ATMSCs and BMMSCs (Figure 21 A). Additionally, ATMSCs presented generally higher cell numbers when compared to BMMSCs.

During the 9-day culture period, ATMSCs and PDLSCs exhibited similar cell growth behavior regardless of cell seeding density, since cells plated at 1.5×10^3 cells/cm² and 3×10^3 cells/cm² presented comparable growth kinetics. Seeding density appears to have a higher influence in BMMSC numbers. In fact, BMMSCs cultured at 1.5×10^3 cells/cm² exhibited consistently lower cell counts than BMMSCs seeded at 3×10^3 cells/cm² (Figure 20 and Figure 21 A). Moreover, as observed in Figure 21 B, PDLSCs were able to reach higher population doublings after 9 days of cell culture compared to BMMSCs and ATMSCs (6.0 ± 0.3 vs 2.1 ± 0.6 and 2.8 ± 0.5 for PDLSCs, BMMSCs and ATMSCs, respectively when cultured at 3×10^3 cells/cm²).

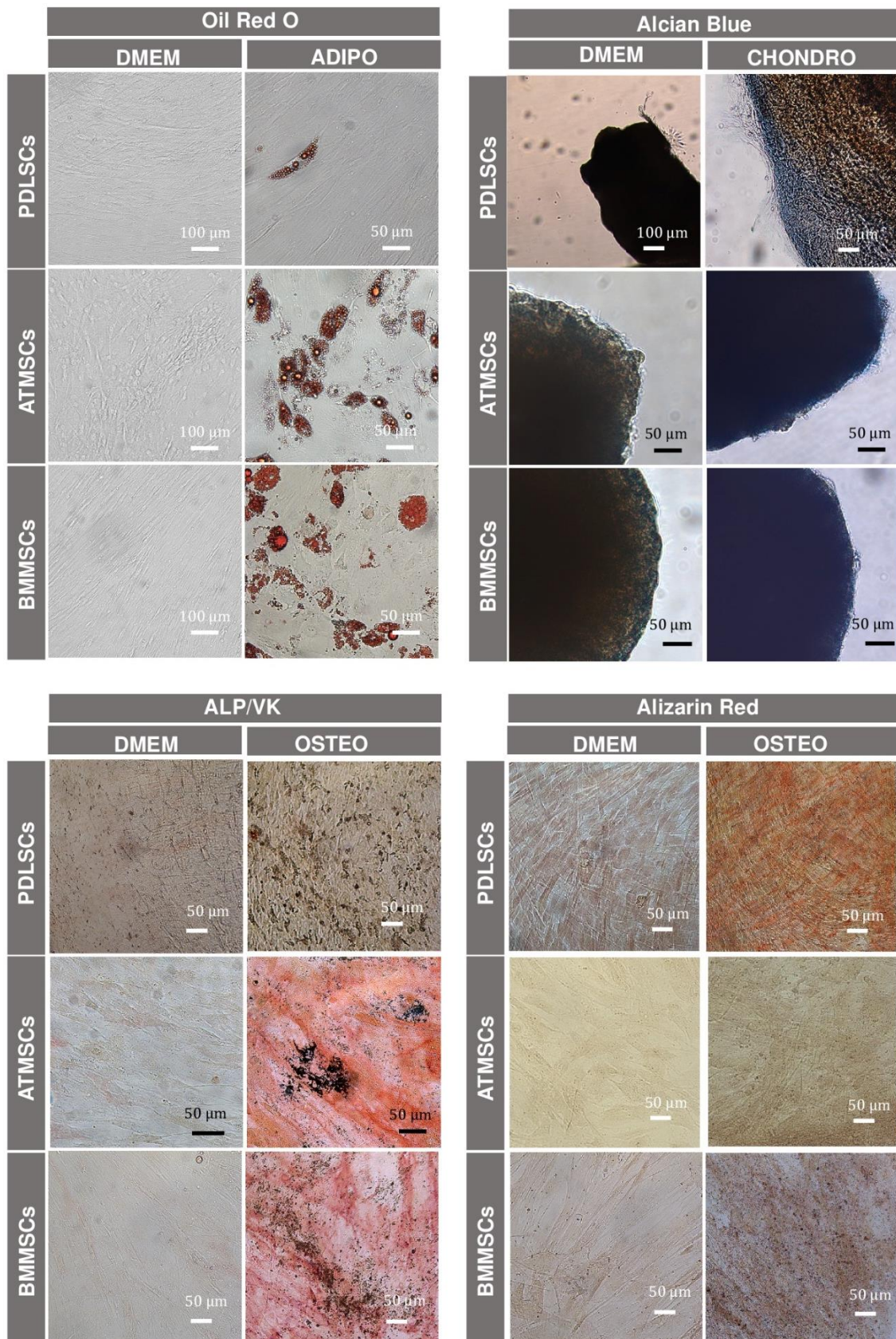


Figure 19. *In vitro* multilineage differentiation of PDLSCs, ATMSCs and BMMSCs. Adipogenic differentiation was detected with Oil red o staining showing the lipid vacuoles in red. Alcian blue stained sulfated glycosaminoglycans in blue. Alkaline phosphatase (ALP) and von Kossa (VK) stainings showed ALP activity in red and mineralized extracellular matrix deposits in black. Alizarin red stained calcium deposits in the extracellular matrix in red. As controls, all stainings were also performed in expansion conditions (DMEM).

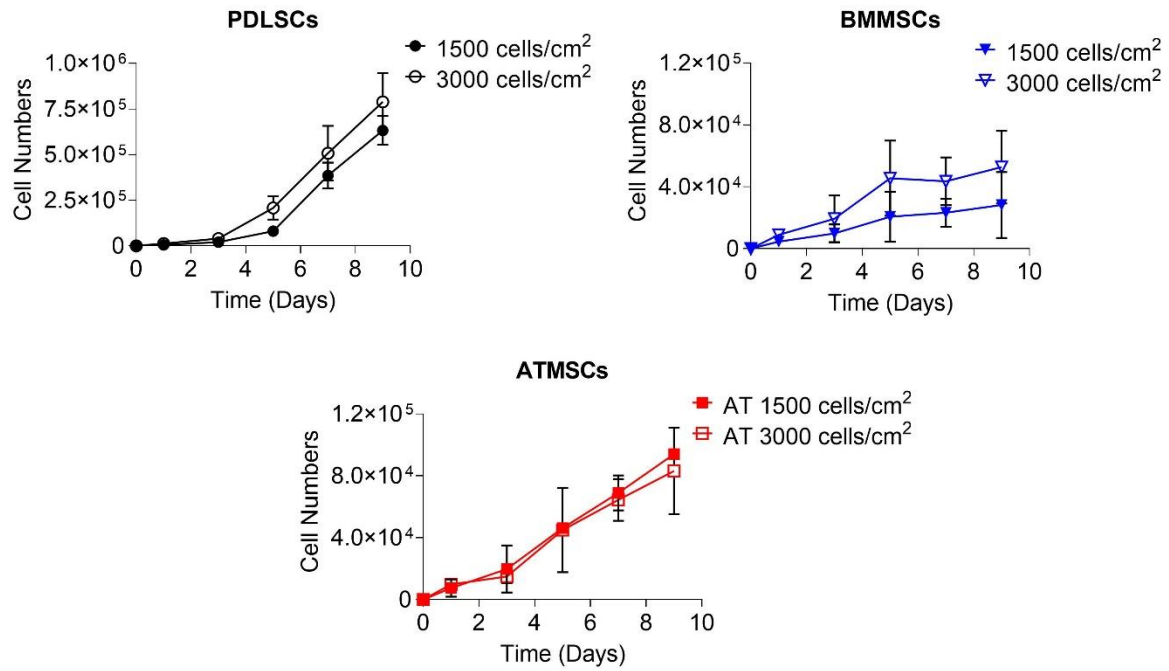


Figure 20. Growth curves for PDLSCs, BMMSCs and ATMSCs cultured in expansion conditions (DMEM + 10% FBS+ 1% A/A) for 9 days at two different cell seeding densities: 1.5×10^3 and 3.0×10^3 cells/cm². Data are expressed as mean \pm SD (n=2, two donors per cell type).

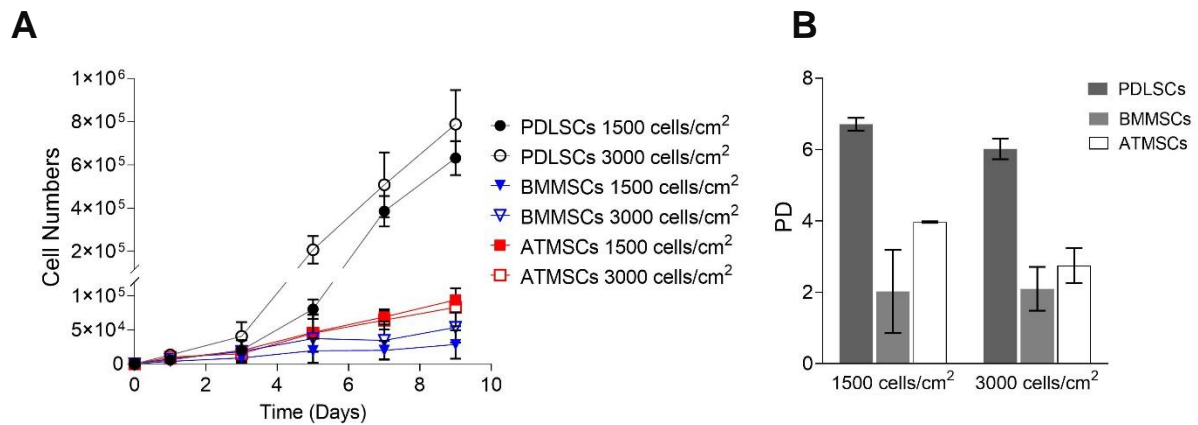


Figure 21. Proliferation of PDLSCs, ATMSCs and BMMSCs cultured in expansion conditions (DMEM + 10%FBS+ 1% A/A) seeded at 1.5×10^2 , 1.5×10^3 and 3.0×10^3 cells/cm² in 12-well plates. **A)** Growth curves of PDLSCs, ATMSCs and BMMSCs cultured at different cell seeding densities. **B)** Population doublings (PD) of PDLSCs, ATMSCs and BMMSCs cultured at different cell seeding densities. Data are expressed as mean \pm SD (n=2, two donors per cell type).

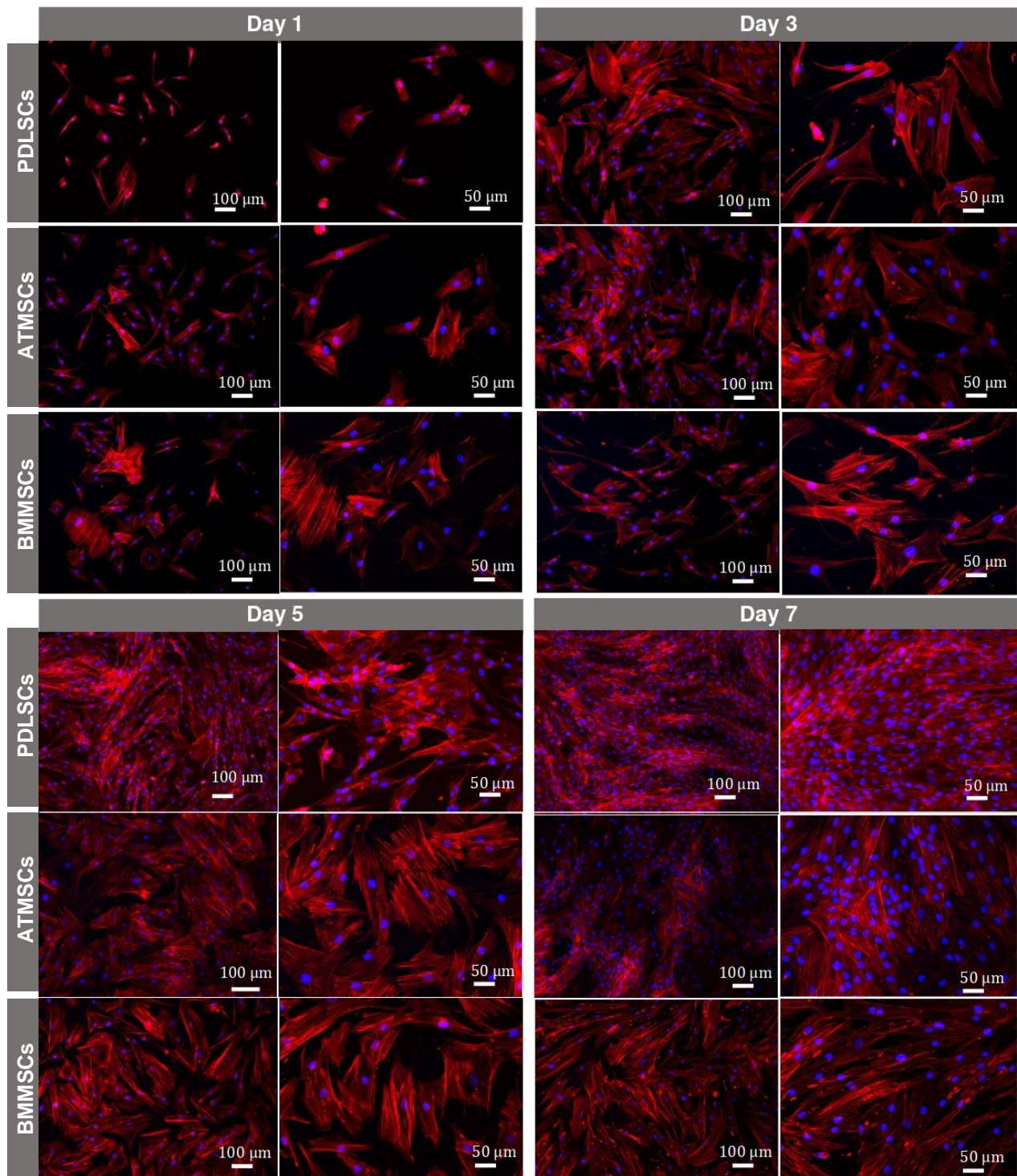


Figure 22. Morphology of PDLSCs, ATMSCs and BMMSCs at days 1, 3, 5 and 7 of culture in expansion conditions (DMEM + 10% FBS+ 1% A/A) at 3×10^3 cells/cm². Nuclei were stained with DAPI (blue) and cytoskeleton actin filaments were stained with phalloidin (red).

4.3. OSTEOGENIC POTENTIAL OF MSCs DERIVED FROM ADIPOSE TISSUE, BONE MARROW AND PERIODONTAL LIGAMENT

Previous results regarding multilineage differentiation of MSCs derived from different sources confirmed that PDLSCs, BMMSCs and ATMSCs were able to differentiate into an osteogenic lineage, confirmed by ALP, von Kossa and Alizarin Red stainings.

Aiming to quantitatively assess differences in osteogenic potential of MSCs isolated from different sources (PDLSCs, BMMSCs and ATMSCs), calcium content, ALP activity and osteogenic-related gene expression were analyzed after osteogenic differentiation. Additionally, after 21 days of osteogenic differentiation, immunocytochemistry analysis was also performed to confirm osteogenic differentiation of MSCs from different sources.

4.3.1. Calcium and Alkaline Phosphatase Activity Quantification

ECM mineralization during osteogenesis is characterized by the deposition of inorganic crystals on an organic matrix, (such as calcium) and ALP activity (Lian and Stein, 1995). In this work, calcium content and ALP activity were quantified (Figure 23) in PDLSCs, BMMSCs and ATMSCs cultured under osteogenic differentiation conditions after 21 days.

Results (Figure 23 A) showed that cells cultured under osteogenic differentiation conditions (OSTEO) presented higher calcium accumulation compared to cells cultured under expansion conditions (without osteogenic differentiation medium - DMEM). These differences confirmed the successful osteogenic differentiation of MSCs from different sources.

Interestingly, BMMSCs and ATMSCs did not present significant differences in calcium accumulation after 21 days of osteogenic differentiation (BMMSCs: $(9.2 \pm 1.2) \times 10^{-7} \mu\text{g} \cdot \mu\text{L}^{-1}$, ATMSCs: $(11.7 \pm 0.35) \times 10^{-7} \mu\text{g} \cdot \mu\text{L}^{-1}$). However, a significant enhancement in calcium accumulation was observed in MSCs derived from PDL compared to BMMSCs and ATMSCs ($(17.2 \pm 2.0) \times 10^{-7} \mu\text{g} \cdot \mu\text{L}^{-1}$) (Figure 23). These results demonstrated a higher mineralization capacity from PDLSCs.

Regarding ALP activity, results demonstrated that ALP activity of PDLSCs did not increase after osteogenic differentiation ($(1.4 \pm 0.13) \times 10^{-4} \mu\text{g} \cdot \mu\text{L}^{-1}$) (Figure 23 B). On the other hand, the ALP activity of BMMSCs and ATMSCs presented a significant increase after osteogenic differentiation (BMMSCs: $(3.1 \pm 0.26) \times 10^{-4} \mu\text{g} \cdot \mu\text{L}^{-1}$, ATMSCs: $(2.7 \pm 0.24) \times 10^{-4} \mu\text{g} \cdot \mu\text{L}^{-1}$).

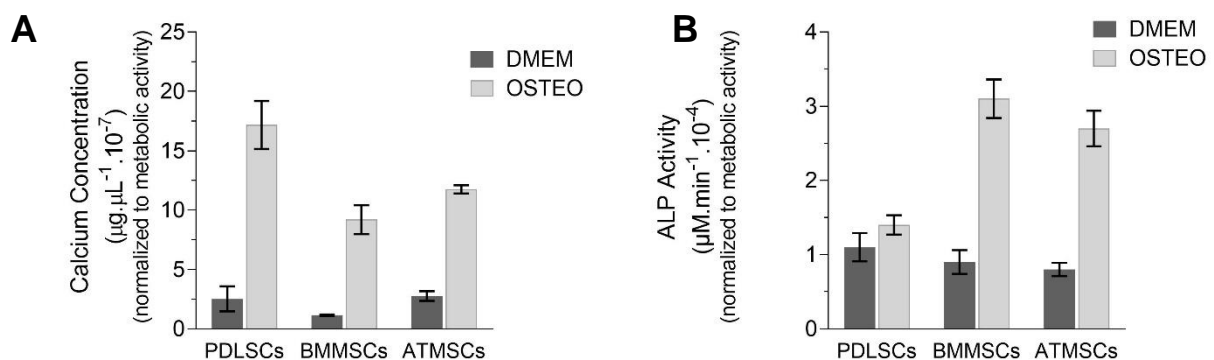


Figure 23. Quantitative assessment of calcium content and alkaline phosphatase (ALP) activity of PDLSCs, BMMSCs and ATMSCs cultured for 21 days under expansion (DMEM) and osteogenic differentiation (OSTEO) conditions, normalized to metabolic activity. **A)** Calcium concentration **B)** ALP activity. Data are expressed as mean \pm SD (n=3, two donors per cell type).

4.3.2. Gene Expression

After 21 days of culture under osteogenic differentiation conditions, gene expression levels of osteogenic/periodontal markers was evaluated by quantitative reverse transcription-polymerase chain reaction (qRT-PCR), such as runt-related transcription factor 2 (Runx2), collagen type I (Col I), alkaline phosphatase (ALP), osteopontin (OPN), osteocalcin (OC), cementum protein-1 (CEMP-1) and periostin (POSTN) (Figure 24). Cells isolated from different sources upregulated the expression of osteogenic gene markers compared to the control (undifferentiated cells at day 0), confirming the successful osteogenic differentiation of MSCs.

Results demonstrated that PDLSCs have greater osteogenic potential compared to MSCs derived from BM and AT, presenting enhanced upregulation of *Col I*, *Runx2*, *OC*, *CEMP-1* and *POSTN*. *OPN* and *ALP* gene expression of PDLSCs was significantly enhanced compared to ATMSCs, however these values were similar to BMMSCs. Lastly, results suggested that among the three cell types studied, ATMSCs presented the lowest osteogenic/periodontal potential, confirmed by the lower levels of osteogenic/periodontal gene expression compared to PDLSCs and BMMSCs, such as *OPN*, *OC* and *POSTN*.

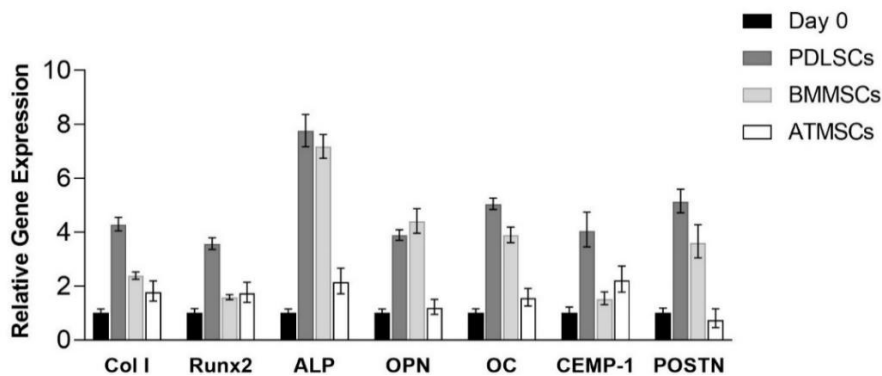


Figure 24. qRT-PCR analysis of PDLSCs, BMMSCs and ATMSCs after 21 days of osteogenic differentiation. Gene expression analysis of collagen I (Col I), runt-related transcription factor 2 (Runx2), alkaline phosphatase (ALP), osteopontin (OPN), osteocalcin (OC), cementum protein-1 (CEMP-1) and periostin (POSTN). Gene expression was normalized to the endogenous gene *GAPDH* and calculated as fold-change relative to the baseline expression of target gene measure in Day 0 experimental group (undifferentiated cells). Results are expressed as mean \pm SD (n=2, two donors per cell type).

4.3.3. Immunocytochemistry Analysis

After 21 days of osteogenic differentiation conditions, immunocytochemistry analysis of PDLSCs, BMMSCs and ATMSCs was performed. Results presented in Figure 25 confirmed the expression of the common ECM and cytoskeleton proteins, laminin and fibronectin in all samples. Additionally, MSCs derived from all sources stained positive for osteogenic and periodontal-related markers, namely osteocalcin, osteopontin and asporin, except in the case of ATMSCs that did not express asporin. Interestingly, cementum protein-1 was exclusively expressed by PDLSCs.

Overall, the results presented in this work confirmed that MSCs isolated from different sources were able to differentiate into an osteogenic lineage. However, significant changes were observed in the osteogenic commitment during differentiation of PDL-, bone marrow- and adipose tissue-derived stem cells, confirming that PDLSCs presented higher osteogenic/periodontal potential.

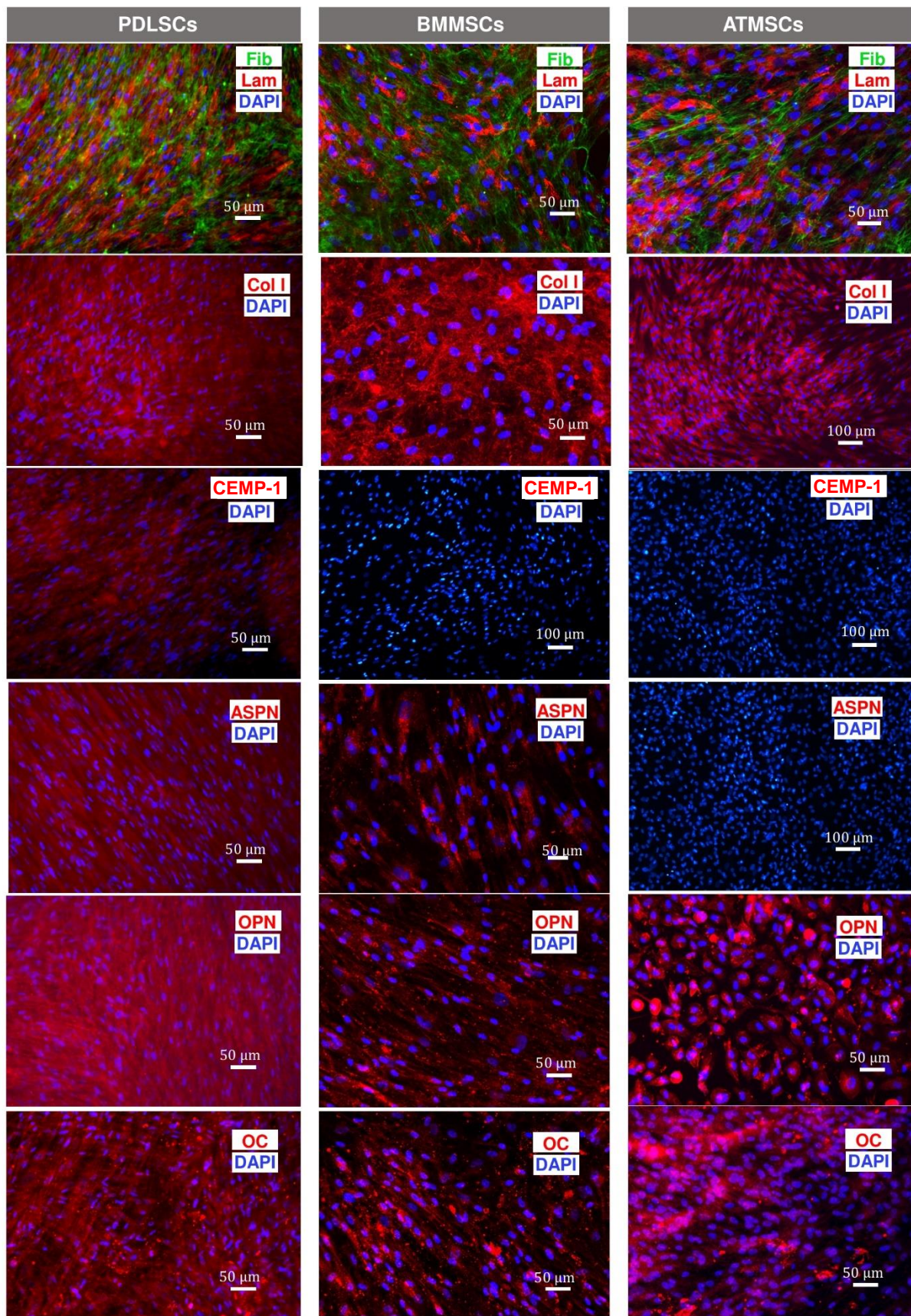


Figure 25. Immunocytochemistry analysis of PDLSCs, BMMSCs and ATMSCs cultured under osteogenic differentiation conditions for 21 days. Expression of fibronectin (Fib, green), laminin (Lam, red), collagen I (Col I, red), cementum protein-1 (CEMP-1, red), asporin (ASPN, red), osteopontin (OPN, red), and osteocalcin (OC, red).

4.4. PDLSC CULTURE ON 3D PRINTED PCL SCAFFOLDS

Aiming to investigate a suitable material for alveolar bone regeneration, PCL scaffolds with different pore sizes, namely 100 μm , 300 μm and 600 μm , were 3D printed using FDM technology and seeded with PDLSCs. Adhesion efficiency, proliferation and morphology studies were conducted and PDLSCs were successfully cultured for 10 days in the 3D printed PCL scaffolds.

4.4.1. Cell Proliferation

To study the effect of scaffold pore size in PDLSCs proliferation, cells were seeded onto 3D printed PCL scaffolds with different pore sizes, namely 100 μm , 300 μm and 600 μm . Cells were seeded at 5.0×10^4 cells/scaffold and cultured in expansion conditions (DMEM + 10% FBS + 1% A/A). Cell proliferation was assessed by quantitative evaluation of metabolic activity. PDLSCs remained viable for 10 days with cell numbers consistently increasing across all pore sizes (Figure 26 A). After 1 and 3 days of culture, cell numbers between the three different scaffolds were comparable, regardless of pore size. However, 7 days after seeding, the number of PDLSCs was notably higher in the 100 μm pore scaffolds when compared with the 300 μm and 600 μm pore scaffolds. After 10 days of culture, cell numbers were considerably higher for scaffolds with 100 μm and 300 μm pore sizes than in the 600 μm pore scaffold.

Cell adhesion was assessed at day 1 and the percentage of adhered cells (Figure 26 B) is comparable across the three pore sizes, presenting adherent cell percentages of $(19.4 \pm 2.17)\%$, $(18.5 \pm 1.34)\%$ and $(21.6 \pm 2.84)\%$ for scaffolds composed by 100, 300 and 600 μm pore sizes, respectively.

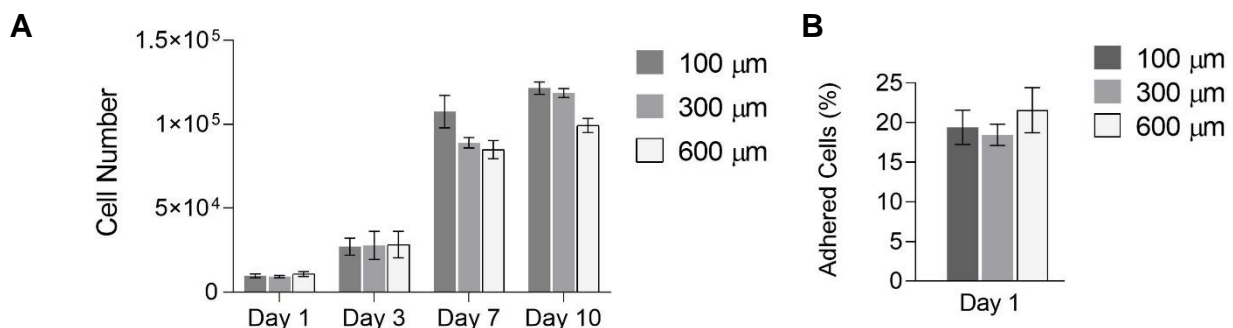


Figure 26. A. Proliferation of PDLSCs cultured for 10 days in expansion conditions (DMEM + 10% FBS + 1% A/A) on PCL scaffolds with different pore sizes (100 μm , 300 μm and 600 μm). **B.** Percentage of adhered PDLSCs (seeded at 5.0×10^4 cells/scaffold) after 1 day of culture with DMEM + 10% FBS+ 1% A/A on PCL scaffolds with different pore sizes. Data are expressed as mean \pm SD (n=4 scaffolds for each condition).

4.4.2. Cell Morphology

Morphology of PDLSCs seeded onto 3D printed PCL scaffolds with different pore sizes (Figure 27) was evaluated by DAPI/Phalloidin staining and visualized by fluorescent microscopy after 1 and 3 days of culture (Figure 28). Stainings demonstrated high proliferation on the scaffold surface, forming cell layers in all scaffolds. Moreover, images revealed that PDLSCs were well adhered to the scaffold surface independently of scaffold pore size.

Cell aggregates partially attached to the scaffold fibers were observed in all pore sizes due to the poor efficiency of cell seeding and the use of ultra-low attachment plates (Figure 27). Future studies will

include cell morphology assays at Day 10 to assess the proliferation of PDLSCs in PCL scaffolds with different pore sizes and to evaluate how PDLSCs interact with each other and with the structure of the scaffold.

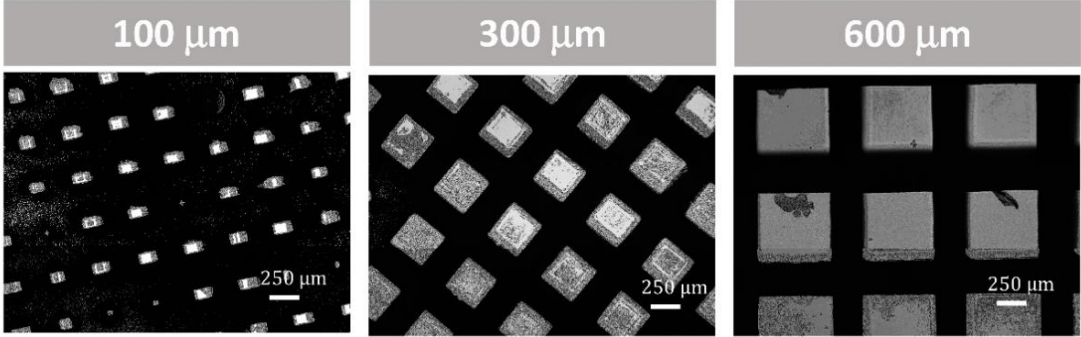


Figure 27. Bright field images of 3D printed polycaprolactone scaffolds after 1 day of PDLSC culture in expansion conditions (DMEM +10% FBS+ 1% A/A).

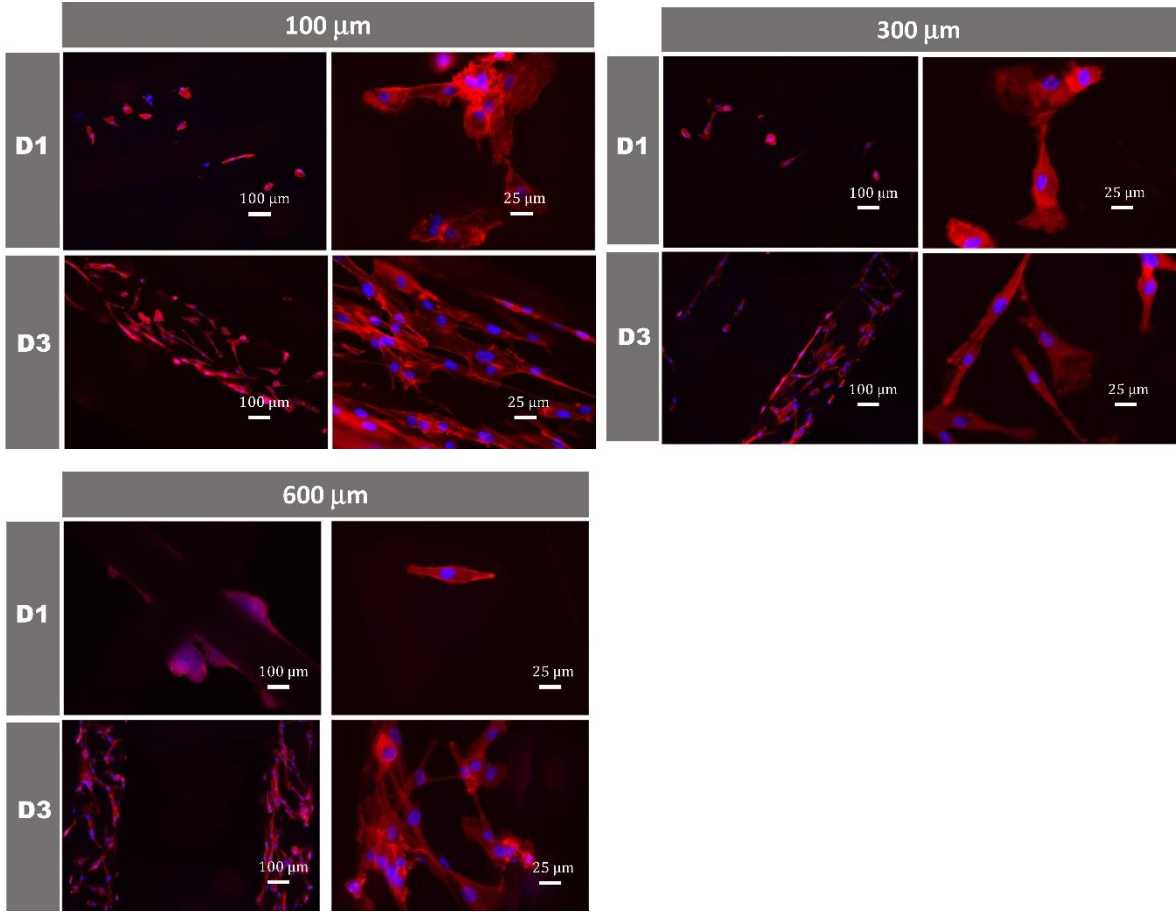


Figure 28. PDLS morphology in 3D printed polycaprolactone scaffolds with different pore sizes (100 μm, 300 μm and 600 μm) after 1 (D1) and 3 days (D3) of culture in expansion conditions (DMEM + 10% FBS+ 1% A/A). Nuclei were stained with DAPI (blue), and cytoskeleton actin filaments were stained with phalloidin (red).

5. DISCUSSION

5.1. ISOLATION AND CHARACTERIZATION OF PERIODONTAL LIGAMENT STEM CELLS (PDLSCs)

Aiming to characterize PDLSCs, immunophenotype analysis was performed by flow cytometry (Figure 12). Regarding MSC-related surface markers (Dominici *et al.*, 2006; Goodwin *et al.*, 2001; Karina Stewart *et al.*, 2003), results showed that PDLSCs were positive for CD29, CD44, CD73, CD90, CD105, according to previously reported studies (Nagatomo *et al.*, 2006; Lindroos *et al.*, 2008; Wada *et al.*, 2009; Iwata *et al.*, 2010; Shinagawa-Ohama *et al.*, 2017; Banavar *et al.*, 2020). Besides the common MSC-related surface markers identified by Domini and colleagues, we characterized PDLSCs using other surface markers such as CD166, CD106, CD80 and CD146. In fact, previous reports have shown that CD166 is a biomarker expressed by BMMSCs and lost during their development into differentiated phenotypes (Bruder *et al.*, 1997; Karina Stewart *et al.*, 2003). The positive expression of CD166 by PDLSCs (>99% in P1 through P5, and >50% for P6 and P7) is similar to previously reported expression levels for BMMSCs and PDLSCs (Banavar *et al.*, 2020). Despite other studies have reported the expression of CD106 by MSCs (Yang *et al.*, 2013), results showed that CD106 is absent in PDLSCs in all passages. Previous PDLSC immunophenotype studies also reported negative expression of CD106 (Wada *et al.*, 2009). As expected, and in agreement with previous studies (Iwata *et al.*, 2010; Lindroos *et al.*, 2008; Nagatomo *et al.*, 2006; Tamaki *et al.*, 2013; Vasandan *et al.*, 2014; Wada *et al.*, 2009), PDLSCs did not express HSC markers during passaging. However, we observed that PDLSCs exhibited a slightly higher expression level of CD14, ranging from 2.55 to 12.46%. Several factors can cause variability in expression of surface markers such as biological differences between donors, donor age and culture media composition variability (Y.-H. K. Yang *et al.*, 2018). Therefore, more biological replicates should be included in this study to further assess if PDLSCs tend to have higher CD14 expression in comparison with the remaining HSC markers selected for this study.

PDLSCs have been reported to possess immunomodulatory properties similar to BMMSCs (Wada *et al.*, 2009) and the negative expression of CD80, a T cell co-stimulatory molecule is in agreement with previous studies (Ding *et al.*, 2010; Xiaoyu Li *et al.*, 2020; Wada *et al.*, 2009) and suggests low immunogenicity. Moreover, previous studies have demonstrated that allogeneic PDLSCs prevent immune responses against activated T cells *in vitro*, trigger reconstruction of the PDL *in vivo* by blocking T cell activation, and successfully reduced the expression of a non-classical major histocompatibility complex-like glycoprotein (CD1b), resulting in significantly decreased T-cell proliferation (Ding *et al.*, 2010; Shin *et al.*, 2017; Wada *et al.*, 2009). The ability to modulate immune function of PDLSCs is a valuable advantage for cell transplantation therapies as the inflammatory condition in periodontitis inhibits the natural repair processes involving local cells, including stem, progenitor, and mature cells.

CD146, also known as the melanoma cell adhesion molecule (MCAM) or cell surface glycoprotein MUC18, is a cell surface marker previously applied in the identification PDLSCs (Saito *et al.*, 2013; Seo *et al.*, 2004) and commonly used as a marker for endothelial cells (Guezguez *et al.*, 2007). Several

studies demonstrated that CD146⁺ cell populations from numerous connective tissue sites exhibit MSC potential, including trilineage differentiation capacity (Baksh *et al.*, 2007; Covas *et al.*, 2008; Crisan *et al.*, 2008; Sorrentino *et al.*, 2008). Interestingly, results showed a high positive expression of CD146. However, a significant decrease in CD146 expression is observed after passage 5. Lastly, the values obtained for CD146 expression in this study are similar to previous reports found in literature (Ding *et al.*, 2010; Saito *et al.*, 2013; Wada *et al.*, 2009). Therefore, these results demonstrated that high passage numbers of PDLSCs can influence the immunophenotype of PDLSCs isolated from healthy donors.

Regarding immunocytochemistry analysis, PDLSCs were positive for laminin, fibronectin, Stro-1, asporin, osteocalcin and osteopontin (Figure 13). Additionally, PDLSCs spread, proliferate and secrete their own ECM, composed by laminin and fibronectin. Fibronectin is an important ECM component that plays critical roles in cell survival, proliferation, attachment and differentiation, while laminin is a glycoprotein and major structural component in the basal lamina with a critical role in cell adhesion, differentiation and migration (Linask and Lash, 1988; Marie, Hay and Saidak, 2014). Results showed that PDLSCs secreted abundant fibronectin with a fibrillar distribution and confirmed the presence of laminin.

Asporin, also known as periodontal ligament-associated protein-1 (PLAP-1) is a novel member of the small leucine-rich repeat proteoglycan family that is frequently expressed in human PDL tissue. Previous studies suggested that PLAP-1/asporin plays a specific role in the PDL as a negative regulator of differentiation and mineralization, preventing the cells present in the soft PDL from developing non-physiological mineralization (Yamada *et al.*, 2007; Yamada, Kitamura and Murakami, 2008). Interestingly, PDLSCs expressed proteins that are normally present in the bone ECM, such as osteocalcin and osteopontin, even when were not cultured under osteogenic differentiation conditions. These results supported previous studies (Lekic, Sodek and McCulloch, 1996; Basdra and Komposch, 1997; Nohutcu *et al.*, 1997) that report that PDL contains an heterogenous population of progenitor cells with osteogenic potential that participate in periodontal regeneration, since osteocalcin and osteopontin are predominantly expressed by osteogenic cells.

In addition to the MSC-related surface marker expression confirmed by flow cytometry and immunofluorescence, the MSC phenotype was confirmed by the successful PDLSC trilineage differentiation (adipogenic, chondrogenic and osteogenic differentiation) (Figure 14). After 21 days of *in vitro* differentiation, PDLSCs exhibited an osteogenic phenotype, as confirmed by the presence of Alizarin Red-positive mineral deposits, which indicate calcium accumulation. Chondrogenic potential of PDLSCs was confirmed by the positive Alcian blue staining of chondrocyte-specific matrix deposition. Finally, results confirmed the adipogenic differentiation of PDLSCs by the presence of Oil Red O-positive cells with stained lipid vacuoles. These results are in line with BMMSC and PDLSC characterization (Dominici *et al.*, 2006; Yang *et al.*, 2018; Seo *et al.*, 2004; Gay, Chen and MacDougall, 2007; Menicanin *et al.*, 2014; Vasandan *et al.*, 2014; Banavar *et al.*, 2020) when exposed to similar culture conditions.

Results demonstrated that PDLSCs exhibited high proliferative capacity reaching, after 12 days, $(7.9 \pm 1.6) \times 10^5$ and $(6.3 \pm 0.79) \times 10^5$ cells, when seeded at 1.5×10^3 cells/cm² and 3×10^3 cells/cm², respectively. In what concerns cell proliferation, cells cultured at higher cell densities (1.5×10^3 and 3×10^3 cells/cm²) presented significantly higher cell numbers in comparison to cells culture at a lower cell

seeding density (1.5×10^2 cells/cm²). PDLSCs cultured at higher densities (1.5 and 3×10^3 cells/cm²) presented similar growth kinetic curves with an adaptation period of 3 days followed by an exponential growth phase until day 9. PDLSCs grown in a lower density (1.5×10^2 cells/cm²) remained in the adaptation phase for a longer period, as the exponential growth phase begun only after day 5. No plateau was reached in the growth curve for PDLSCs cultured in low density, suggesting that at day 12 of culture these cells were still in exponential growth phase. The results herein presented (Figure 15) are in accordance with reports found in literature (Iwata *et al.*, 2010). Interestingly, PDLSCs exhibited high proliferative ability even when seeded at a low density (1.5×10^2 cells/cm²), reaching $(3.3 \pm 1.3) \times 10^5$ cells after 12 days of culture. Moreover, population doublings tended to decrease with cell density (Figure 15 B), supporting previous results that suggest PDLSCs cultured at lower densities exhibit higher proliferation rates. In fact, this high proliferative capacity presented by PDLSCs can be considered as an advantage regarding their expansion for therapeutic applications, opening the possibility to obtain more cells and to perform more experiments at the same time from the same source of primary cells despite low harvest yields. Additionally, PDLSCs growth may be promoted by cell contact, since cells cultured at a lower cell seeding density (1.5×10^2 cells/cm²) presented dispersed confluent areas with PDLSCs growing in distinct colonies across the surface of the plate. In fact, as depicted in Figure 16, after 12 days, PDLSCs cultured at 1.5×10^2 cells/cm² still presented dispersed cells, despite the existence of high confluent regions.

5.2. COMPARISON OF PERIODONTAL LIGAMENT STEM CELLS WITH MSCs DERIVED FROM ADIPOSE TISSUE AND BONE MARROW

To assess differences among MSCs derived from different sources, cell surface expression profiles of PDLSCs, BMMSCs and ATMSCs were analyzed and compared by flow cytometry (Figure 17). As expected, and in line with previous reports, PDLSCs (Nagatomo *et al.*, 2006; Lindroos *et al.*, 2008; Wada *et al.*, 2009; Iwata *et al.*, 2010; Shinagawa-Ohama *et al.*, 2017; Banavar *et al.*, 2020), BMMSCs (Tamaki *et al.*, 2013; Wang *et al.*, 2017; Xu *et al.*, 2017; Mohamed-Ahmed *et al.*, 2018) and ATMSCs (Strem *et al.*, 2005; Xu *et al.*, 2017; Mohamed-Ahmed *et al.*, 2018; Petrenko *et al.*, 2020) presented a positive expression of MSC-related markers CD29, CD44, CD73, CD90, CD105. CD44 is a cell adhesion molecule that is generally expressed by MSCs (Jones *et al.*, 2002; Mafi *et al.*, 2011), playing a key role in migration of MSCs into damaged tissues. BMMSCs and ATMSCs have been reported to present similar levels of expression of CD44 in early passages (passage 3 or lower) (Mitchell *et al.*, 2006; Iwata *et al.*, 2010; Tamaki *et al.*, 2013; Petrenko *et al.*, 2020). Moreover, reports have shown that BMMSCs cultured in similar expansion conditions (with DMEM media + 10% FBS + 1% A/A) maintained a strongly positive expression of CD44 in all passages between passage 3 and 8 (> 96.6%) (Yang *et al.*, 2018). For ATMSCs, no comparable studies were found on CD44 expression in passages 5 and higher. Thus, additional flow cytometry experiments with more donors from all sources are necessary to understand if CD44 expression of BMMSC and ATMSCs is negatively affected by passaging, while PDLSCs remain consistently positive for CD44 in early and late passages.

Furthermore, ATMSCs showed a higher variation in CD166 expression levels when compared with PDLSCs and BMMSCs. ATMSC CD166 expression levels varied between (45.9 ± 2.7)% and (90.5 ± 0.3)%, while PDLSCs presented CD166 expression levels between (86.1 ± 4.8)% and (99.3 ± 0.4)%. BMMSCs presented CD166 expression levels between (71.3 ± 2.4)% and (99.9 ± 1.6)%. As mentioned above, results found in literature regarding immunophenotypic analysis of human BMMSCs and ATMSCs mostly consider early passages, hence, further experiments with more donors are needed to better understand variations in ATMSCs expression levels of CD166 through passaging.

CD106, also known as vascular cell adhesion molecule-1 (VCAM-1), is a cell-cell adhesion molecule known to be critical for T cell activation and leukocyte recruitment to the inflammation site, therefore, playing an important role in evoking effective immune responses (Burkly *et al.*, 1991; Carter and Wicks, 2001). Moreover, studies showed that CD106 is critical for MSC-mediated immunosuppression (Ren *et al.*, 2010; Yang *et al.*, 2013). In the context of MSC-based therapies that target immunomodulation, these studies suggested that CD106 expression promotes immunoregulatory responses. The results herein presented showed that CD106 expression was absent in all samples and passages analyzed. Nonetheless, previous reports showed that CD106 expression for BMMSCs ranged from 14% to 60% (Bühring *et al.*, 2009; Wada *et al.*, 2009; Yang *et al.*, 2013, 2018). Variation in CD106 expression reports may be attributed to the heterogenous nature of MSC populations as previous studies also indicate that CD106⁺ and CD106⁻ cells coexist in MSC populations and both populations possess multipotent capacity (Yang *et al.*, 2013). Furthermore, the work herein presented showed that Stro-1 is negatively expressed by MSCs derived from PDL, BM and AT with consistently low expression levels in passages 3, 5 and 7 (< 11.3%). Stro-1 is a well-known marker for MSCs, despite this, many limitations in its potential have been identified. It is unclear whether Stro-1 expression correlates with multipotency and it has also been revealed to be unsuitable as a sole marker to identify MSCs (Lin *et al.*, 2011; Lv *et al.*, 2014). Additionally, Stro-1 is not universally expressed by MSCs derived from different sources. Previous studies showed significantly variable Stro-1 expression in BMMSCs, with expression values ranging from 2% to 80% indicating that the exact proportion of Stro-1⁺ cells is markedly donor dependent (Simmons and Torok-Storb, 1991; Stewart *et al.*, 1999; Bühring *et al.*, 2009; Iwata *et al.*, 2010; Mohamed-Ahmed *et al.*, 2018). Regarding Stro-1 expression of ATMSCs, reports are fewer and not in accordance regarding Stro-1 expression (Strem *et al.*, 2005; Lin *et al.*, 2008; Iwata *et al.*, 2010; Mohamed-Ahmed *et al.*, 2018). Stro-1 was used for the selection of PDLSCs by Seo and colleagues during isolation, demonstrating that Stro-1⁺ cells have the potential to regenerate periodontal tissues *in vivo* (Seo *et al.*, 2004). Despite this, the potential of Stro-1 as a specific marker for PDLSCs is limited as evidences showed that (i) heterogeneous unsorted PDLSCs also promote periodontal tissue formation (Dangaria *et al.*, 2011b; Yu *et al.*, 2013); (ii) Stro-1⁺ cells are usually found in low numbers in primary PDLSCs populations (Trubiani *et al.*, 2005; Gay, Chen and MacDougall, 2007; Itaya *et al.*, 2009; Iwata *et al.*, 2010); and (iii) expanded Stro-1⁺ cells are not superior in proliferation, colony forming unit or mineralization capacity, when compared to primary PDLSCs (Yan *et al.*, 2014). Overall, the results presented in this work confirmed that Stro-1 is not a suitable marker to distinguish between MSCs derived from different sources. Moreover, this work supported the fact that MSC properties of PDLSCs are not dependent on positive expression of Stro-1.

Regarding CD146 expression, both BMMSCs and ATMSCs exhibited negative expression of CD146 in all passages (< 7%). Interestingly, PDLSC expression of CD146 was positive, presenting expression values of (67.4 ± 0.9)% in passage 3 and (69.5 ± 1.6)% in passage 5. However, expression of CD146 by PDLSCs decreased with passaging, reaching expression values of (24.1 ± 1.2)% in passage 7. These results were in line with previous reports of CD146 expression by PDLSCs (Seo *et al.*, 2004) and suggested that CD146 expression could be used as a marker of PDLSCs. Nonetheless, more donors are required to confirm the differences observed in CD146 expression between PDLSCs, BMMSCs and ATMSCs.

Immunocytochemistry analysis of PDLSCs, BMMSCs and ATMSCs confirmed the presence of commonly expressed ECM molecules laminin and fibronectin (Figure 18). Interestingly, Stro-1, a previously mentioned MSC-associated marker, was exclusively expressed by PDLSCs. As discussed above, previous reports have suggested that Stro-1 expression by BMMSCs is markedly donor dependent, thus, negative immunofluorescent staining could be explained by donor variability. Contrary to the results presented in this work, previous immunocytochemistry studies have reported the expression of Stro-1 in ATMSCs (Ning *et al.*, 2006; Zannettino *et al.*, 2008; Lin *et al.*, 2011). However, results showed preferential perivascular Stro-1 expression within adipose tissue (Zannettino *et al.*, 2008) and a Stro-1 expression pattern highly specific for endothelial cells in arterioles and capillaries (Lin *et al.*, 2011). As previously mentioned, Stro-1 has been reported as being absent and present on human ATMSCs, and the Stro-1's endothelial localization observed in some studies has not been understood yet. In fact, differences in Stro-1 antibody sources and detection methods (flow cytometry vs immunohistochemistry) have been discussed to understand the controversy concerning ATMSC Stro-1 expression (Gimble, Katz and Bunnell, 2007).

Overall, comparative analysis of PDLSCs, BMMSCs and ATMSCs revealed phenotypic similarities regarding expression of MSC-related markers, contributing to the establishment of PDLSCs as a novel source of MSCs. Despite this, differences in PDLSC expression, such as positive immunofluorescence stainings of asporin, osteopontin and osteocalcin, which were negatively stained in BMMSCs and ATMSCs, were observed. Staining for osteopontin and osteocalcin was strongly positive in the PDLSCs without osteogenic differentiation medium, suggesting a higher potential to differentiate into an osteogenic lineage. Nevertheless, additional comparative studies are necessary to assess if phenotype differences between PDLSCs and MSCs derived from other sources have an impact in cells function and potential.

As expected, multipotency of PDLSCs, BMMSCs and ATMSCs was confirmed with positive stainings for trilineage differentiation (Figure 19). The qualitative nature of *in vitro* stainings for osteo-, adipo- and chondrogenic differentiation does not allow an accurate assessment of disparities in differentiation potential. However, it is relevant to note, the significant difference in lipid accumulation when comparing PDLSCs with BMMSCs or ATMSCs. PDLSCs produced lower amounts of red stained lipid vacuoles after adipogenic differentiation. These results suggested that PDLSCs did not respond to adipogenic stimuli as strongly as BMMSCs and ATMSCs. A number of studies have successfully conducted trilineage differentiation of cells derived from PDL, BM and AT (Zuk *et al.*, 2002; Gay, Chen and MacDougall, 2007; Mohamed-Ahmed *et al.*, 2018).

Comparison of PDLSCs, BMMSCs and ATMSCs growth curves revealed substantial differences in proliferation between each cell type (Figure 20). BMMSCs and ATMSCs exhibited similar growth patterns, maintaining close to steady slopes during the 9-day proliferation period. Despite this, ATMSCs reached higher cell numbers in all timepoints. This evidence supported results from other studies, that reported that ATMSCs presented similar or greater rates of proliferation than BMMSCs (Shafiee *et al.*, 2011; LI *et al.*, 2014; Mohamed-Ahmed *et al.*, 2018). Moreover, comparison between the three cell types revealed differences in proliferation patterns. PDLSCs exhibited an initial 5-day period of lower growth rate followed by a significant increase, evidenced by a clear change in growth curve slopes before and after the 5th day of culture. As stated by previous studies (Iwata *et al.*, 2010; Tamaki *et al.*, 2013), PDLSCs exhibited significantly increased proliferation capacity reaching higher final cell numbers (counted at day 9) than BMMSC and ATMSC.

Cell seeding density appears to have a higher influence in BMMSCs expansion, in comparison with PDLSCs and ATMSCs. BMMSCs cultured at 1.5×10^3 cells/cm² reached lower cell numbers in every timepoint than BMMSCs seeded at 3×10^3 cells/cm², while PDLSCs and ATMSCs reached comparable cell numbers, regardless of seeding density. Besides PDLSC higher rate of proliferation compared with BMMSCs and ATMSCs, PDLSCs also presented higher cell population doublings (Figure 21 B), regardless of seeding density. Furthermore, morphology assays supported the results discussed above, suggesting that PDLSCs exhibited higher proliferation. After 7 days of culture, PDLSCs were completely confluent, contrary to ATMSCs and BMMSCs, as observed by DAPI staining (Figure 22).

5.3. OSTEOGENIC POTENTIAL OF MSCs DERIVED FROM ADIPOSE TISSUE, BONE MARROW AND PERIODONTAL LIGAMENT

Osteogenic differentiation is characterized by three different stages: (i) cell proliferation and ECM biosynthesis, (ii) ECM development, maturation and organization, and (iii) ECM mineralization (Lian and Stein, 1995). Osteogenic differentiation involves selective expression of transcription factors and osteogenic genes. ECM has a significant role during osteogenic differentiation. In fact, during osteogenesis, a mature collagenous ECM is formed in which minerals, such as calcium, are deposited (Lian and Stein, 1995).

Results presented in Figure 23 demonstrated that calcium content was considerably higher in PDLSCs, BMMSCs and ATMSCs cultured in osteogenic differentiation conditions compared with cells cultured in expansion conditions (DMEM + 10% FBS + 1% A/A). This result suggested a successful mineralization, which is characteristic of later stages of osteogenic differentiation, along with the development of a bone tissue-like structure (Lian and Stein, 1995). Interestingly, although calcium amount was similar for differentiated BMMSCs and ATMSCs, a significant higher amount of calcium was observed in differentiated PDLSCs, suggesting an enhancement of osteogenic potential by MSCs derived from PDL. In fact, the role of PDLSCs in osteogenic differentiation has been widely studied *in vitro* and *in vivo*. Reports showed that cells from PDL have a phenotype characteristic of osteoblast-like cells (Nojima *et al.*, 1990; Basdra and Komposch, 1997). Moreover, studies demonstrated that a population of PDLSCs migrated from PDL remnants, upregulated osteogenic marker genes,

differentiated into osteoblasts and generated new bone following tooth extraction (Yuan *et al.*, 2018). Thus, we believe that PDLSCs may contain subpopulations of unique stem cells with a higher osteogenic potential, responsible for alveolar bone remodeling/regeneration. Therefore, the enhancement of calcium deposition by PDLSCs observed in this study could be a consequence of the higher osteogenic potential presented by these cells. This is in line with previous reports that MSCs preferentially differentiate into cells of the same tissue origin (Guneta *et al.*, 2016; Xu *et al.*, 2017; Mohamed-Ahmed *et al.*, 2018).

Results demonstrated that ALP activity of PDLSCs did not increase after osteogenic differentiation. On the other hand, the ALP activity of BMMSCs and ATMSCs presented a significant increase after osteogenic differentiation. In fact, these results are in accordance with ALP staining results, confirming the low ALP activity of PDLSCs. Yu and colleagues (Yu and Philippe, 2015) have shown that PDLSCs are composed by a heterogeneous population of cells, presenting ALP⁺ and ALP⁻ cells. They found that both ALP⁺ and ALP⁻ cells showed similar osteogenic potential with no observable difference in the amount of mineral deposits after osteogenic differentiation (Yu *et al.*, 2016). Therefore, the lack of ALP activity observed in this work might be due to the presence of a population of ALP⁻ cells. It is important to highlight that the lower levels of ALP activity of PDLSCs did not compromise the osteogenic differentiation of these cells, as observed by the enhancement of mineralization and upregulation of osteogenic marker genes. However, isolation of PDLSCs from different donors is required to understand the low levels of ALP activity observed by PDLSCs. Interestingly, the low levels of ALP activity of PDLSCs might be related to the decreased adipogenic potential presented by PDLSCs. In fact, ALP is involved in the control of intracellular lipid accumulation in preadipocyte maturation, thus, absence of ALP may prevent formation of lipids in cells (Ali *et al.*, 2006, 2013).

Moreover, qRT-PCR results confirmed effective osteogenic differentiation of MSCs after 21 days under osteogenic differentiation conditions, independently of the tissue of origin (Figure 24). Generally, PDLSCs, BMMSCs and ATMSCs exhibited upregulation of one of the principal transcriptional regulators of osteogenic differentiation (*Runx2*) and of several osteogenic/periodontal genes (*Col 1*, *ALP*, *OPN*, *OC*, *CEMP-1* and *POSTN*). Interestingly, after osteogenic induction, ATMSCs presented lower relative expression of osteogenic genes and downregulated *POSTN* gene expression, compared to BMMSCs and PDLSCs. Overall, these results suggested that ATMSCs possess lower osteogenic capacity compared with PDLSCs and BMMSCs. This is supported by previous comparative studies focusing on osteogenic differentiation that reported limited osteogenic differentiation potential of ATMSCs compared to BMMSCs regarding ALP activity, calcium content and expression of early and late osteogenic genes (Shafiee *et al.*, 2011; Woo, Hwang and Shim, 2016; Xu *et al.*, 2017; Mohamed-Ahmed *et al.*, 2018).

Differences in differentiation potential presented by cells may be the result of the conditions and cellular environment in which each cell type was isolated, genetic variations or other factors that remain unidentified. The epigenetic mechanism is a process that regulates heritable alterations in gene expression without changing the DNA sequence through methylation and histone modifications (Gibney and Nolan, 2010). Interestingly, reports showed that epigenetic regulation of MSCs is closely involved in osteogenic differentiation (Eslaminejad, Fani and Shahhoseini, 2013), therefore, differences in

epigenetic status among the three cell types derived from different tissues may also contribute to the differences observed regarding osteogenic differentiation potential.

Gene expression results also showed that *ALP* gene expression is considerably upregulated in differentiated PDLSCs and BMMSCs. This is consistent with osteogenic differentiation as ALP activity increases and reaches a peak during matrix maturation (Lian and Stein, 1995). Additionally, both cell types exhibited considerable upregulation of late osteogenic marker genes, *OC* and *OPN*. Osteocalcin and osteopontin are non-collagenous proteins (Olszta *et al.*, 2007) that play key roles in the biological and mechanical functions of bone. Studies showed that these two proteins are produced during bone formation, in the mineralization stage, and are involved in ECM organization, coordinating cell-matrix and mineral-matrix interactions (Stein, Lian and Owen, 1990).

RUNX2 (also known as core-binding factor alpha, *CBFa1*) is the master regulator of osteoblast differentiation, being a marker for osteogenic gene expression and function (Lian and Stein, 2003; Bruderer, R. Richards, *et al.*, 2014; Thiagarajan, Abu-Awwad and Dixon, 2017). *RUNX2* regulates downstream genes that determine the osteogenic phenotype and controls the expression of osteogenic marker genes such as *Col I*, *ALP*, *OPN*, and *OC* (Birmingham *et al.*, 2012; Hayrapetyan, Jansen and van den Beucken, 2015). Furthermore, *RUNX2* is known to be crucial for the commitment of MSCs to the osteogenic lineage (Bruderer, R. G. Richards, *et al.*, 2014). Overall, these studies revealed that *RUNX2* is specifically required to trigger the initial osteogenic gene regulatory network, making it a suitable marker for early stages of osteogenic differentiation. Interestingly, in this study, *RUNX2* upregulation is considerably higher in PDLSCs compared with BMMSCs and ATMSCs after 21 days of osteogenic differentiation.

After 21 days of osteogenic differentiation, closer analysis of gene expression levels revealed higher upregulation of *Col I* and *CEMP-1* in PDLSCs compared with BMMSCs and ATMSCs. Collagen I is the most abundant protein in bone ECM and is pivotal for matrix mineralization (Lian and Stein, 1995). In fact, the higher expression level of *Col I* presented by PDLSCs is consistent with previous reports indicating that, during osteogenic differentiation, PDLSCs possess better collagen forming capacity when compared with BMMSCs (Li *et al.*, 2019). *CEMP-1* has been identified as a novel cementum-specific protein and is strongly expressed by cementoblasts and their progenitors (Kadokura *et al.*, 2019), including cells located near the blood vessels in the PDL (Arzate *et al.*, 1992). Combined with the expression of *CEMP-1* observed by immunocytochemistry analysis of differentiated PDLSCs (Figure 25), enhanced upregulation of *CEMP-1* gene expression in osteogenic differentiated PDLSCs suggested that PDLSCs may comprise a subpopulation of cementum progenitor cells, as previously proposed in earlier reports by McCulloch & Melcher in 1983 and further supported by recent studies (Torii *et al.*, 2015; Shinagawa-Ohama *et al.*, 2017).

Periostin is a matricellular protein with a fundamental role in bone and tooth tissue development and repair. Originally, periostin was proposed as a specific-osteoblast marker (Takeshita *et al.*, 1993) but is currently known to be expressed in various collagen-rich fibrous connective tissues subjected to constant mechanical stress, such as PDL, heart valves and tendons (Merle and Garnerio, 2012). Periostin acts as an important protein for tissue integrity and maturity and has a key role as a modulator of PDL hemostasis (Romanos *et al.*, 2014). Reports found in literature showed that periostin has several

functions in the PDL, namely, remodeling of collagen matrix (Kii *et al.*, 2006) and maintenance of the integrity of the PDL in response to mechanical stresses (Rios *et al.*, 2005). Moreover, previous studies showed that TNF- α and bacterial virulence factors (*P. gingivalis* lipopolysaccharide) decreased periostin expression in human PDL fibroblasts, suggesting that periostin expression variations could be a contributing factor of periodontal disease progression (Padial-Molina *et al.*, 2013). Considering its role in osteoblast adhesion, differentiation and survival (Horiuchi *et al.*, 1999; Romanos *et al.*, 2014), periostin expression was expected to be observed in PDLSCs, BMMSCs and ATMSCs cultured under osteogenic differentiation conditions. Interestingly, periostin (*POSTN*) gene expression was upregulated in PDLSCs and BMMSCs but downregulated in ATMSCs. This supported the hypothesis stated above that osteogenic potential is lower in ATMSCs. After 21 days of osteogenic differentiation, PDLSCs presented higher *POSTN* gene expression levels compared with BMMSCs. Considering periostin functions in the PDL, it is not surprising that PDLSCs expressed higher levels of periostin when cultured under osteogenic differentiation conditions, since PDLSCs reside in the PDL.

Immunofluorescence results after 21 days of osteogenic differentiation indicated a successful differentiation for the three cell types, regardless of their tissue of origin (Figure 25). As expected, common ECM proteins laminin and fibronectin were positively stained in all samples. Additionally, positive stainings for osteopontin and osteocalcin, both osteogenic markers (Stein, Lian and Owen, 1990) were observed in PDLSCs, BMMSCs and ATMSCs. Periodontal-related marker (Yamada *et al.*, 2007), asporin, was observed in PDLSCs and BMMSCs. As mentioned above, type I collagen synthesis is pivotal in osteogenic differentiation to allow the establishment of a robust ECM and its subsequent mineralization. Thus, the strongly positive Col I staining present in all samples confirmed the successful osteogenic differentiation.

Regarding cementum protein-1, only differentiated PDLSCs demonstrated a positive staining. Previous studies reported CEMP-1 expression in osteogenic differentiated PDLSCs (Komaki *et al.*, 2012), however, it is still not clear if cementoblasts and osteoblasts arise from a common progenitor because both of these cell types share features of mineral-forming capacity and gene expression.

Overall, PDLSCs presented an enhanced osteogenic potential compared to BMMSCs and ATMSCs, showing promising results for periodontal TE applications.

5.4. PDLSC CULTURE ON 3D PRINTED PCL SCAFFOLDS

3D printed scaffold-based approaches have shown great promise in periodontal TE/RM, namely in alveolar bone regeneration. Design of scaffolds for periodontal TE applications requires understanding the relationship between structure and biological function. Here, we evaluated the impact of pore size in PDLSCs proliferation. The results presented herein showed that PDLSCs can be successfully cultured in 3D printed PCL scaffolds with pore sizes of 100 μm , 300 μm and 600 μm (Figure 26). Pore sizes of 100, 300 and 600 μm , were chosen according to physiological and structural characteristics of cement, alveolar bone and PDL, respectively. Moreover, latest studies have reported similar pore sizes aiming to regenerate soft and hard tissues (C. H. Lee *et al.*, 2014). PCL is a widely used biomaterial for TE known to be biocompatible, biodegradable and non-toxic (Dwivedi *et al.*, 2020). Previous studies

reported successful culture of BMSCs and PDLSCs in scaffolds composed by PCL alone or combined with other polymers (Alves da Silva *et al.*, 2010; Xue *et al.*, 2017; Peng *et al.*, 2018; Silva, Carvalho, *et al.*, 2020; Silva, Moura, *et al.*, 2020; Smaida *et al.*, 2020). As expected, the results herein presented demonstrated that PDLSCs are able to proliferate for 10 days in 3D printed PCL scaffolds. Regardless of pore size, metabolic activity assay revealed an increase in cell numbers with culture time. Despite comparable cell numbers across the different scaffolds after 3 days, the 600 μm pore scaffolds seemed the least favorable for PDLSC proliferation, with lower cell numbers after 7 and 10 days when compared with the scaffolds with 100 μm and 300 μm pore sizes. Moreover, a closer analysis of cell numbers after 7 days suggested that the 100 μm pore size may favor higher proliferation rates. Nonetheless, after 10 days, the number of cells in the 100 μm - and 300 μm pore scaffolds was comparable. In fact, Ashworth and colleagues have demonstrated that a pore size of 100 μm was found to be necessary to ensure an even distribution of PDLSCs across a collagen scaffold (Ashworth *et al.*, 2018). Independently of PCL scaffold pore size, average percentage of adhered cells was similar for all the scaffolds. DAPI/Phalloidin staining confirmed PDLSC adhesion onto the PCL scaffolds regardless of pore size (Figure 28).

Future studies are necessary to optimize PDLSC adhesion in order to develop scalable scaffold-based alveolar bone regeneration therapies, since higher adhesion efficiency is required. Pore size should, therefore, be carefully optimized in the design of scaffolds for periodontal regeneration, in particular focusing on alveolar bone regeneration, aiming to obtain a rapid and efficient response of PDLSCs, producing a mineralized ECM to form new bone tissue.

Overall, this work showed promising results for the implementation of PDLSCs in scaffold-based periodontal TE/RM. PDLSCs can successfully adhere and proliferate in PCL 3D printed scaffolds with pore sizes ranging between 100 μm and 600 μm . Additionally, results suggested lower pore sizes (100 μm and 300 μm) favor higher proliferation rates. Furthermore, osteogenic differentiation assays, such as calcium quantification and qRT-PCR analysis, should be performed to further understand the impact of pore size in periodontal/osteogenic differentiation of PDLSCs.

6. CONCLUSIONS

MSCs have shown promising results in RM clinical applications. Despite this, limitations still remain, such as accessibility to MSC-source tissues like bone-marrow and adipose tissue. Thus, invasive surgical procedures are required to collect the cells, subjecting the donor to significant pain and trauma.

Periodontal tissue is easily accessible with non-invasive procedures. This tissue can be harvested during standard dental scaling and root planning, making it an attractive potential source of MSCs. The work carried out in this MSc thesis provided additional evidence that PDL harbors a population of highly proliferative, multipotent stem cells that express the MSC phenotype (PDLSCs) as defined by the minimal criteria proposed by the ISCT. Moreover, this work contributed to the establishment of a standard, effective and reproducible protocol for the isolation and identification of PDLSCs at SCERG laboratory (iBB-IST, Portugal). Additionally, PDLSCs were also successfully preserved in liquid/vapor nitrogen tanks allowing for the creation of a cell bank for further studies of PDLSC properties and potential applications.

Comparison of PDLSCs with MSCs derived from alternative well-established sources, namely, adipose tissue and bone marrow, suggested that PDLSCs belong to a unique population of MSCs. The results herein presented showed that in addition to MSC-related surface marker expression and multilineage differentiation capacity, PDLSCs also positively expressed CD146. Immunofluorescent staining revealed that only PDLSCs presented osteogenic marker expression (osteopontin) while cultured in expansion conditions. Furthermore, cell growth kinetics studies showed that PDLSCs demonstrated a significantly higher proliferation rate compared to BMMSCs and ATMSCs. Despite this, it is important to note that further studies are necessary to find PDLSC-specific markers that facilitate identification of this population.

Osteogenic differentiation was successfully induced in PDLSCs, BMMSCs, and ATMSCs. Interestingly, quantitative assessment of differentiation potential indicates that PDLSCs may have a higher predisposition for osteogenic differentiation with higher calcium deposition and increased upregulation of osteogenic marker genes, such as *Col 1* and *Runx2* compared to BMMSCs and ATMSCs. Moreover, differentiated PDLSCs presented higher expression of CEMP-1 showed by immunofluorescent stainings and enhanced upregulation of *CEMP-1* gene compared with ATMSCs and BMMSCs, suggesting that PDLSCs may comprise a subpopulation of cementum progenitor cells. In the context of periodontal tissue regeneration, early response to osteogenic induction and unique cementogenic properties can constitute two significant advantages in periodontium regeneration. PDLSC-based therapies could potentially involve PDLSC delivery into the root defect and induce dental-root repair/regeneration through *de novo* cellular cementum formation. Despite this, it is still unclear if osteoblasts and cementoblasts arise from the same progenitor, and further studies are needed to clarify if PDLSCs possess innate cementogenic potential.

Aggressive periodontitis can lead to severe periodontal tissue damage and consequential alveolar bone resorption. Therefore, periodontal tissue regeneration requires coordinated hard (alveolar bone and cementum) and soft tissue (PDL) regeneration. For this, alveolar space needs to be maintained

during periodontal regeneration, which can potentially be achieved with the use of a stiff biodegradable scaffold. The emergence of 3D printing technology allows for the creation of patient specific scaffolds made by biocompatible synthetic polymers, such as PCL.

PDLSCs have been reported to have an important role in periodontal wound healing and regeneration, thus supporting the hypothesis that PDLSC might have an enhanced osteogenic potential to promote alveolar bone regeneration, as observed in this work. We believe that PDLSCs might secrete key signaling molecules and recruit progenitor cells to the repair site. Thus, PDLSC delivery by 3D printed PCL scaffolds might be a successful bioengineering strategy for periodontal tissue regeneration, allowing for the maintenance of alveolar space while simultaneously promoting the regeneration of alveolar bone.

In this MSc thesis, PDLSCs were successfully cultured in 3D printed PCL scaffolds with 100 μm , 300 μm and 600 μm pore sizes. Cell metabolic activity results suggested that 100 μm and 300 μm pore sizes favored higher proliferation rates.

Overall, the results indicated that PDLSCs are a population of cells that exhibit MSC-like phenotype and present higher osteogenic potential than other well-established MSC sources for TE/RM applications. Moreover, results confirmed that 3D printed PCL scaffolds are suitable for PDLSC proliferation, contributing to the development of novel scaffold-based therapeutic approaches to periodontal tissue regeneration.

7. FUTURE WORK

The development of a scaffold-based therapy combined with the delivery of MSCs to promote alveolar bone tissue regeneration could contribute to significant advancements in periodontal tissue regeneration field. To achieve such goals, further characterization of PDLSCs is necessary to identify reliable PDLSC-specific markers. Moreover, additional investigation of osteogenic differentiation mechanisms in PDLSCs should be carried out to further understand PDLSC functions in alveolar bone regeneration.

Future work should include higher number of donors of PDLSCs to evaluate the impact of donor variability.

The next steps towards the development of a new scaffold-based therapy for periodontal tissue regeneration must include further optimization of PCL scaffold pore size to determine the most favorable pore size for PDLSC proliferation and osteogenic differentiation. Furthermore, scaffold cell seeding efficiency should be optimized to improve PDLSC adhesion to PCL scaffolds. Osteogenesis is pivotal for alveolar bone regeneration, thus, *in vitro* and *in vivo* assessment of PDLSC osteogenic differentiation capacity in 3D printed PCL scaffolds should also be conducted. Additionally, PCL slow biodegradation could be advantageous for the delivery of other molecules, such as growth factors or anti-inflammatory drugs. Thus, future studies should focus on the investigation of compounds that favor alveolar bone regeneration and that can be used in combination with a PCL scaffold without compromising PDLSC properties and therapeutic functions.

Finally, periodontal tissue regeneration can only be fully achieved with coordinated regeneration of PDL, cementum and alveolar bone. Thus, multiphasic scaffold approaches should also be explored. These multiphasic scaffolds should have each layer/phase designed to guide a specific target tissue regeneration. For example, a complex scaffold with an alveolar bone phase with FDM 3D printed scaffold, an intermediate phase with a fibrous material to aid in PDL regeneration, and a third thin phase to promote new cementum formation.

8. REFERENCES

- Abudula, T. *et al.* (2020) 'Sustainable drug release from polycaprolactone coated chitin-lignin gel fibrous scaffolds', *Scientific Reports*, 10(1), p. 20428. doi: 10.1038/s41598-020-76971-w.
- Agrawal, C. M. and Ray, R. B. (2001) 'Biodegradable polymeric scaffolds for musculoskeletal tissue engineering', *Journal of Biomedical Materials Research*, 55(2), pp. 141–150. doi: 10.1002/1097-4636(200105)55:2<141::AID-JBM1000>3.0.CO;2-J.
- Ali, A. *et al.* (2013) 'Lipid accumulation and alkaline phosphatase activity in human preadipocytes isolated from different body fat depots', *Journal of Endocrinology, Metabolism and Diabetes of South Africa*, 18(1), pp. 58–64. doi: 10.1080/22201009.2013.10872304.
- Ali, A. T. *et al.* (2006) 'The relationship between alkaline phosphatase activity and intracellular lipid accumulation in murine 3T3-L1 cells and human preadipocytes', *Analytical Biochemistry*, 354(2), pp. 247–254. doi: 10.1016/j.ab.2006.04.028.
- Alves da Silva, M. L. *et al.* (2010) 'Cartilage Tissue Engineering Using Electrospun PCL Nanofiber Meshes and MSCs', *Biomacromolecules*, 11(12), pp. 3228–3236. doi: 10.1021/bm100476r.
- in 't Anker, P. S. *et al.* (2004) 'Isolation of Mesenchymal Stem Cells of Fetal or Maternal Origin from Human Placenta', *Stem Cells*, 22(7), pp. 1338–1345. doi: 10.1634/stemcells.2004-0058.
- Arzate, H. *et al.* (1992) 'Production of a monoclonal antibody to an attachment protein derived from human cementum', *The FASEB Journal*, 6(11), pp. 2990–2995. doi: 10.1096/fasebj.6.11.1644261.
- Ashworth, J. C. *et al.* (2018) 'Optimising collagen scaffold architecture for enhanced periodontal ligament fibroblast migration', *Journal of Materials Science: Materials in Medicine*, 29(11), p. 166. doi: 10.1007/s10856-018-6175-9.
- Ausenda, F. *et al.* (2019) 'New Perspectives in the Use of Biomaterials for Periodontal Regeneration', *Materials*, 12(13), p. 2197. doi: 10.3390/ma12132197.
- Baldwin, P. *et al.* (2019) 'Autograft, Allograft, and Bone Graft Substitutes: Clinical Evidence and Indications for Use in the Setting of Orthopaedic Trauma Surgery', *Journal of Orthopaedic Trauma*, 33(4), pp. 203–213. doi: 10.1097/BOT.0000000000001420.
- Banavar, S. R. *et al.* (2020) 'Establishing a technique for isolation and characterization of human periodontal ligament derived mesenchymal stem cells', *The Saudi Dental Journal*. doi: 10.1016/j.sdentj.2020.04.007.
- Bartholomew, A. *et al.* (2002) 'Mesenchymal stem cells suppress lymphocyte proliferation in vitro and prolong skin graft survival in vivo', *Experimental Hematology*, 30(1), pp. 42–48. doi: 10.1016/S0301-472X(01)00769-X.
- Bartnikowski, M., Vaquette, C. and Ivanovski, S. (2020) 'Workflow for highly porous resorbable custom 3D printed scaffolds using medical grade polymer for large volume alveolar bone regeneration', *Clinical Oral Implants Research*, 31(5), pp. 431–441. doi: 10.1111/clr.13579.
- Bartold, P. M., Shi, S. and Gronthos, S. (2006) 'Stem cells and periodontal regeneration', *Periodontology 2000*, 40(1), pp. 164–172. doi: 10.1111/j.1600-0757.2005.00139.x.
- Basdra, E. K. and Komposch, G. (1997) 'Osteoblast-like properties of human periodontal ligament cells: an in vitro analysis.', *European journal of orthodontics*, 19(6), pp. 615–21. doi:

10.1093/ejo/19.6.615.

Bergstrom, J. (2014) 'Smoking rate and periodontal disease prevalence: 40-year trends in Sweden 1970-2010', *Journal of Clinical Periodontology*, 41(10), pp. 952–957. doi: 10.1111/jcpe.12293.

Berkovitz, B. K. (2004) 'Periodontal ligament: structural and clinical correlates.', *Dental update*, 31(1), pp. 46–50, 52, 54. doi: 10.12968/denu.2004.31.1.46.

Berkovitz, B. K. B. (1990) 'The structure of the periodontal ligament: an update', *The European Journal of Orthodontics*, 12(1), pp. 51–76. doi: 10.1093/ejo/12.1.51.

Bhatt, R. A. and Rozental, T. D. (2012) 'Bone Graft Substitutes', *Hand Clinics*, 28(4), pp. 457–468. doi: 10.1016/j.hcl.2012.08.001.

Birmingham, E. *et al.* (2012) 'Osteogenic differentiation of mesenchymal stem cells is regulated by osteocyte and osteoblast cells in a simplified bone niche', *European Cells and Materials*, 23, pp. 13–27. doi: 10.22203/eCM.v023a02.

Bosshardt, D. D. (2005) 'Are Cementoblasts a Subpopulation of Osteoblasts or a Unique Phenotype?', *Journal of Dental Research*, 84(5), pp. 390–406. doi: 10.1177/154405910508400501.

Bosshardt, D. D. and Sculean, A. (2009) 'Does periodontal tissue regeneration really work?', *Periodontology 2000*, 51(1), pp. 208–219. doi: 10.1111/j.1600-0757.2009.00317.x.

Brito, M. V. (2013) 'Osteocalcin expression in periodontal ligament when inducing orthodontic forces', *Revista Odontológica Mexicana*, 17(3), pp. 150–153.

Bruderer, M., Richards, R. G., *et al.* (2014) 'Role and regulation of RUNX2 in osteogenesis.', *European cells & materials*, 28, pp. 269–86. doi: 10.22203/ecm.v028a19.

Bruderer, M., Richards, R., *et al.* (2014) 'Role and regulation of RUNX2 in osteogenesis', *European Cells and Materials*, 28, pp. 269–286. doi: 10.22203/eCM.v028a19.

Bühning, H.-J. *et al.* (2009) 'Phenotypic characterization of distinct human bone marrow-derived MSC subsets.', *Annals of the New York Academy of Sciences*, 1176, pp. 124–34. doi: 10.1111/j.1749-6632.2009.04564.x.

Burkly, L. C. *et al.* (1991) 'Signaling by vascular cell adhesion molecule-1 (VCAM-1) through VLA-4 promotes CD3-dependent T cell proliferation', *European Journal of Immunology*, 21(11), pp. 2871–2875. doi: 10.1002/eji.1830211132.

Buser, D. *et al.* (1998) 'Evaluation of filling materials in membrane-protected bone defects. A comparative histomorphometric study in the mandible of miniature pigs.', *Clinical Oral Implants Research*, 9(3), pp. 137–150. doi: 10.1034/j.1600-0501.1998.090301.x.

Cai, X. *et al.* (2015) 'Influence of bone marrow-derived mesenchymal stem cells pre-implantation differentiation approach on periodontal regeneration in vivo', *Journal of Clinical Periodontology*, 42(4), pp. 380–389. doi: 10.1111/jcpe.12379.

Carmagnola, D. *et al.* (2017) 'Engineered Scaffolds and Cell-Based Therapy for Periodontal Regeneration', *Journal of Applied Biomaterials & Functional Materials*, 15(4), pp. e303–e312. doi: 10.5301/jabfm.5000389.

Carter, R. A. and Wicks, I. P. (2001) 'Vascular cell adhesion molecule 1 (CD106): A multifaceted regulator of joint inflammation', *Arthritis & Rheumatism*, 44(5), pp. 985–994. doi: 10.1002/1529-0131(200105)44:5<985::AID-ANR176>3.0.CO;2-P.

Carvalho, M. S. *et al.* (2021) 'Bone Matrix Non-Collagenous Proteins in Tissue Engineering: Creating New Bone by Mimicking the Extracellular Matrix', *Polymers*, 13(7), p. 1095. doi: 10.3390/polym13071095.

Chai, Y. *et al.* (2000) 'Fate of the mammalian cranial neural crest during tooth and mandibular morphogenesis.', *Development (Cambridge, England)*, 127(8), pp. 1671–9. Available at: <http://www.ncbi.nlm.nih.gov/pubmed/10725243>.

Chen, L., Qu, J. and Xiang, C. (2019) 'The multi-functional roles of menstrual blood-derived stem cells in regenerative medicine', *Stem Cell Research & Therapy*, 10(1), p. 1. doi: 10.1186/s13287-018-1105-9.

Chen, S. C. *et al.* (2006) 'Location of putative stem cells in human periodontal ligament', *Journal of Periodontal Research*, 41(6), pp. 547–553. doi: 10.1111/j.1600-0765.2006.00904.x.

Chen, Y.-L. *et al.* (2008) 'Periodontal regeneration using ex vivo autologous stem cells engineered to express the BMP-2 gene: an alternative to alveoloplasty', *Gene Therapy*, 15(22), pp. 1469–1477. doi: 10.1038/gt.2008.131.

Chiego, D. (2019) *Essentials of Oral Histology and Embryology: A Clinical Approach*.

Cho, M. II and Garant, P. R. (2000) 'Development and general structure of the periodontium', *Periodontology 2000*, 24(1), pp. 9–27. doi: 10.1034/j.1600-0757.2000.2240102.x.

Costa, P. F. *et al.* (2014) 'Advanced tissue engineering scaffold design for regeneration of the complex hierarchical periodontal structure', *Journal of Clinical Periodontology*, 41(3), pp. 283–294. doi: 10.1111/jcpe.12214.

Coura, G. S. *et al.* (2008) 'Human periodontal ligament: a niche of neural crest stem cells.', *Journal of periodontal research*, 43(5), pp. 531–6. doi: 10.1111/j.1600-0765.2007.01065.x.

D'Aiuto, F. *et al.* (2004) 'Gene polymorphisms in pro-inflammatory cytokines are associated with systemic inflammation in patients with severe periodontal infections', *Cytokine*, 28(1), pp. 29–34. doi: 10.1016/j.cyto.2004.06.005.

Dangaria, S. J. *et al.* (2009) 'Extracellular matrix-mediated differentiation of periodontal progenitor cells', *Differentiation*, 78(2–3), pp. 79–90. doi: 10.1016/j.diff.2009.03.005.

Dangaria, S. J. *et al.* (2011a) 'Differentiation of Neural-Crest-Derived Intermediate Pluripotent Progenitors into Committed Periodontal Populations Involves Unique Molecular Signature Changes, Cohort Shifts, and Epigenetic Modifications', *Stem Cells and Development*, 20(1), pp. 39–52. doi: 10.1089/scd.2010.0180.

Dangaria, S. J. *et al.* (2011b) 'Successful Periodontal Ligament Regeneration by Periodontal Progenitor Preseeding on Natural Tooth Root Surfaces', *Stem Cells and Development*, 20(10), pp. 1659–1668. doi: 10.1089/scd.2010.0431.

Dapeng, L. *et al.* (2014) 'Erk1/2 signalling is involved in the differentiation of periodontal ligament stem cells to Schwann cells in dog', *Archives of Oral Biology*, 59(5), pp. 487–491. doi: 10.1016/j.archoralbio.2014.02.010.

Do, L. G. *et al.* (2008) 'Smoking-attributable periodontal disease in the Australian adult population', *Journal of Clinical Periodontology*, 35(5), pp. 398–404. doi: 10.1111/j.1600-051X.2008.01223.x.

Dominici, M. *et al.* (2006) 'Minimal criteria for defining multipotent mesenchymal stromal cells. The

International Society for Cellular Therapy position statement', *Cytotherapy*, 8(4), pp. 315–317. doi: 10.1080/14653240600855905.

Le Douarin, N. M., Ziller, C. and Couly, G. F. (1993) 'Patterning of neural crest derivatives in the avian embryo: in vivo and in vitro studies.', *Developmental biology*, 159(1), pp. 24–49. doi: 10.1006/dbio.1993.1219.

Dwivedi, R. *et al.* (2020) 'Polycaprolactone as biomaterial for bone scaffolds: Review of literature', *Journal of Oral Biology and Craniofacial Research*, 10(1), pp. 381–388. doi: 10.1016/j.jobcr.2019.10.003.

Eke, P. I. *et al.* (2016) 'Risk Indicators for Periodontitis in US Adults: NHANES 2009 to 2012', *Journal of Periodontology*, 87(10), pp. 1174–1185. doi: 10.1902/jop.2016.160013.

Elsalanty, M. E. and Genecov, D. G. (2009) 'Bone Grafts in Craniofacial Surgery', *Craniofacial Trauma & Reconstruction*, 2(3–4), pp. 125–134. doi: 10.1055/s-0029-1215875.

Engelberg, I. and Kohn, J. (1991) 'Physico-mechanical properties of degradable polymers used in medical applications: A comparative study', *Biomaterials*, 12(3), pp. 292–304. doi: 10.1016/0142-9612(91)90037-B.

Eslaminejad, M. B., Fani, N. and Shahhoseini, M. (2013) 'Epigenetic regulation of osteogenic and chondrogenic differentiation of mesenchymal stem cells in culture.', *Cell journal*, 15(1), pp. 1–10. Available at: <http://www.ncbi.nlm.nih.gov/pubmed/23700555>.

Fang, S. *et al.* (2019) 'The role of pulmonary mesenchymal cells in airway epithelium regeneration during injury repair', *Stem Cell Research & Therapy*, 10(1), p. 366. doi: 10.1186/s13287-019-1452-1.

Fehranbat, M. and Popowics, T. (2015) *Illustrated Dental Embryology, Histology, and Anatomy*. 4th edn. Philadelphia: Saunders.

Friedenstein, A. J., Chailakhjan, R. K. and Lalykina, K. S. (1970) 'The development of fibroblast colonies in monolayer cultures of guinea-pig bone marrow and spleen cells.', *Cell and tissue kinetics*, 3(4), pp. 393–403. doi: 10.1111/j.1365-2184.1970.tb00347.x.

Friedenstein, A. J., Gorskaja, J. F. and Kulagina, N. N. (1976) 'Fibroblast precursors in normal and irradiated mouse hematopoietic organs.', *Experimental hematology*, 4(5), pp. 267–74. Available at: <http://www.ncbi.nlm.nih.gov/pubmed/976387>.

Friedenstein, A. J., Piatetzky-Shapiro, I. I. and Petrakova, K. V (1966) 'Osteogenesis in transplants of bone marrow cells.', *Journal of embryology and experimental morphology*, 16(3), pp. 381–90. Available at: <http://www.ncbi.nlm.nih.gov/pubmed/5336210>.

Galli, M. *et al.* (2021) 'Current and future trends in periodontal tissue engineering and bone regeneration', *Plastic and Aesthetic Research*, 2021. doi: 10.20517/2347-9264.2020.176.

Gargett, C. E. *et al.* (2009) 'Isolation and culture of epithelial progenitors and mesenchymal stem cells from human endometrium.', *Biology of reproduction*, 80(6), pp. 1136–45. doi: 10.1095/biolreprod.108.075226.

Gavasane, A. J. (2014) 'Synthetic Biodegradable Polymers Used in Controlled Drug Delivery System: An Overview', *Clinical Pharmacology & Biopharmaceutics*, 3(2). doi: 10.4172/2167-065X.1000121.

Gay, I., Chen, S. and MacDougall, M. (2007) 'Isolation and characterization of multipotent human

periodontal ligament stem cells', *Orthodontics & Craniofacial Research*, 10(3), pp. 149–160. doi: 10.1111/j.1601-6343.2007.00399.x.

Giannobile, W. V. (2014) 'Commentary: Treatment of Periodontitis: Destroyed Periodontal Tissues Can Be Regenerated Under Certain Conditions', *Journal of Periodontology*, 85(9), pp. 1151–1154. doi: 10.1902/jop.2014.140254.

Gibney, E. R. and Nolan, C. M. (2010) 'Epigenetics and gene expression', *Heredity*, 105(1), pp. 4–13. doi: 10.1038/hdy.2010.54.

Gimble, J. M., Katz, A. J. and Bunnell, B. A. (2007) 'Adipose-Derived Stem Cells for Regenerative Medicine', *Circulation Research*, 100(9), pp. 1249–1260. doi: 10.1161/01.RES.0000265074.83288.09.

Goh, B. T. *et al.* (2015) 'Novel 3D polycaprolactone scaffold for ridge preservation - a pilot randomised controlled clinical trial', *Clinical Oral Implants Research*, 26(3), pp. 271–277. doi: 10.1111/clr.12486.

Goodwin, H. S. *et al.* (2001) 'Multilineage differentiation activity by cells isolated from umbilical cord blood: expression of bone, fat, and neural markers.', *Biology of blood and marrow transplantation : journal of the American Society for Blood and Marrow Transplantation*, 7(11), pp. 581–8. doi: 10.1053/bbmt.2001.v7.pm11760145.

Gordon, S. and Martinez, F. O. (2010) 'Alternative Activation of Macrophages: Mechanism and Functions', *Immunity*, 32(5), pp. 593–604. doi: 10.1016/j.immuni.2010.05.007.

Gottlow, J. *et al.* (1986) 'New attachment formation in the human periodontium by guided tissue regeneration Case reports', *Journal of Clinical Periodontology*, 13(6), pp. 604–616. doi: 10.1111/j.1600-051X.1986.tb00854.x.

Gould, T. R. L., Melcher, A. H. and Brunette, D. M. (1980) 'Migration and division of progenitor cell populations in periodontal ligament after wounding', *Journal of Periodontal Research*, 15(1), pp. 20–42. doi: 10.1111/j.1600-0765.1980.tb00258.x.

Gronthos, S. *et al.* (2003) 'Telomerase Accelerates Osteogenesis of Bone Marrow Stromal Stem Cells by Upregulation of CBFA1, Osterix, and Osteocalcin', *Journal of Bone and Mineral Research*, 18(4), pp. 716–722. doi: 10.1359/jbmr.2003.18.4.716.

Grzesik, W. J. and Narayanan, A. S. (2002) 'Cementum and Periodontal Wound Healing and Regeneration', *Critical Reviews in Oral Biology & Medicine*, 13(6), pp. 474–484. doi: 10.1177/154411130201300605.

Guillotin, B. *et al.* (2010) 'Laser assisted bioprinting of engineered tissue with high cell density and microscale organization', *Biomaterials*, 31(28), pp. 7250–7256. doi: 10.1016/j.biomaterials.2010.05.055.

Guneta, V. *et al.* (2016) 'Comparative study of adipose-derived stem cells and bone marrow-derived stem cells in similar microenvironmental conditions', *Experimental Cell Research*, 348(2), pp. 155–164. doi: 10.1016/j.yexcr.2016.09.012.

Handa, K. *et al.* (2002) 'Progenitor cells from dental follicle are able to form cementum matrix in vivo.', *Connective tissue research*, 43(2–3), pp. 406–8. doi: 10.1080/03008200290001023.

Hayrapetyan, A., Jansen, J. A. and van den Beucken, J. J. J. P. (2015) 'Signaling pathways involved in osteogenesis and their application for bone regenerative medicine.', *Tissue engineering. Part B, Reviews*, 21(1), pp. 75–87. doi: 10.1089/ten.TEB.2014.0119.

- Henneman, S., Von den Hoff, J. W. and Maltha, J. C. (2008) 'Mechanobiology of tooth movement', *The European Journal of Orthodontics*, 30(3), pp. 299–306. doi: 10.1093/ejo/cjn020.
- Hollister, S. J. (2009) 'Scaffold Design and Manufacturing: From Concept to Clinic', *Advanced Materials*, 21(32–33), pp. 3330–3342. doi: 10.1002/adma.200802977.
- Horch, H.-H. *et al.* (2006) 'Synthetic, pure-phase beta-tricalcium phosphate ceramic granules (Cerasorb®) for bone regeneration in the reconstructive surgery of the jaws', *International Journal of Oral and Maxillofacial Surgery*, 35(8), pp. 708–713. doi: 10.1016/j.ijom.2006.03.017.
- Horiuchi, K. *et al.* (1999) 'Identification and characterization of a novel protein, periostin, with restricted expression to periosteum and periodontal ligament and increased expression by transforming growth factor beta.', *Journal of bone and mineral research : the official journal of the American Society for Bone and Mineral Research*, 14(7), pp. 1239–49. doi: 10.1359/jbmr.1999.14.7.1239.
- Hu, J. *et al.* (2016) 'Periodontal regeneration in swine after cell injection and cell sheet transplantation of human dental pulp stem cells following good manufacturing practice.', *Stem cell research & therapy*, 7(1), p. 130. doi: 10.1186/s13287-016-0362-8.
- Huang, C.-Y. C. *et al.* (2009) 'Plasticity of stem cells derived from adult periodontal ligament.', *Regenerative medicine*, 4(6), pp. 809–21. doi: 10.2217/rme.09.55.
- Hubbell, J. A. (2003) 'Materials as morphogenetic guides in tissue engineering', *Current Opinion in Biotechnology*, 14(5), pp. 551–558. doi: 10.1016/j.copbio.2003.09.004.
- Hutmacher, D. W. *et al.* (2001) 'Mechanical properties and cell cultural response of polycaprolactone scaffolds designed and fabricated via fused deposition modeling', *Journal of Biomedical Materials Research*, 55(2), pp. 203–216. doi: 10.1002/1097-4636(200105)55:2<203::AID-JBM1007>3.0.CO;2-7.
- Hynes, K. *et al.* (2012) 'Clinical utility of stem cells for periodontal regeneration', *Periodontology 2000*, 59(1), pp. 203–227. doi: 10.1111/j.1600-0757.2012.00443.x.
- in 't Anker, P. S. *et al.* (2003) 'Amniotic fluid as a novel source of mesenchymal stem cells for therapeutic transplantation', *Blood*, 102(4), pp. 1548–1549. doi: 10.1182/blood-2003-04-1291.
- Itaya, T. *et al.* (2009) 'Characteristic changes of periodontal ligament-derived cells during passage', *Journal of Periodontal Research*, 44(4), pp. 425–433. doi: 10.1111/j.1600-0765.2008.01137.x.
- Ivanovski, S. *et al.* (2014) 'Multiphasic Scaffolds for Periodontal Tissue Engineering', *Journal of Dental Research*, 93(12), pp. 1212–1221. doi: 10.1177/0022034514544301.
- Iwata, T. *et al.* (2010) 'Validation of human periodontal ligament-derived cells as a reliable source for cytotherapeutic use', *Journal of Clinical Periodontology*, 37(12), pp. 1088–1099. doi: 10.1111/j.1600-051X.2010.01597.x.
- Iwata, T. *et al.* (2015) 'Cell sheet engineering and its application for periodontal regeneration.', *Journal of tissue engineering and regenerative medicine*, 9(4), pp. 343–56. doi: 10.1002/term.1785.
- Ji, Y.-M. *et al.* (2010) 'Dental Stem Cell Therapy with Calcium Hydroxide in Dental Pulp Capping', *Tissue Engineering Part A*, 16(6), pp. 1823–1833. doi: 10.1089/ten.tea.2009.0054.
- Jiang, N. *et al.* (2016) 'Periodontal Ligament and Alveolar Bone in Health and Adaptation: Tooth Movement.', *Frontiers of oral biology*, 18, pp. 1–8. doi: 10.1159/000351894.
- Jin, Q.-M. *et al.* (2003) 'Cementum engineering with three-dimensional polymer scaffolds', *Journal of Biomedical Materials Research*, 67A(1), pp. 54–60. doi: 10.1002/jbm.a.10058.

- Jones, E. A. *et al.* (2002) 'Isolation and characterization of bone marrow multipotential mesenchymal progenitor cells', *Arthritis & Rheumatism*, 46(12), pp. 3349–3360. doi: 10.1002/art.10696.
- de Jong, T. *et al.* (2017) 'The intricate anatomy of the periodontal ligament and its development: Lessons for periodontal regeneration', *Journal of Periodontal Research*, 52(6), pp. 965–974. doi: 10.1111/jre.12477.
- Jung, I.-H. *et al.* (2013) 'Optimal Medium Formulation for the Long-Term Expansion and Maintenance of Human Periodontal Ligament Stem Cells', *Journal of Periodontology*, 84(10), pp. 1434–1444. doi: 10.1902/jop.2013.120541.
- Kadokura, H. *et al.* (2019) 'Establishment of a Primary Culture System of Human Periodontal Ligament Cells that Differentiate into Cementum Protein 1-expressing Cementoblast-like Cells.', *In vivo (Athens, Greece)*, 33(2), pp. 349–352. doi: 10.21873/invivo.11480.
- Kaku, M. *et al.* (2012) 'Identification and characterization of neural crest-derived cells in adult periodontal ligament of mice', *Archives of Oral Biology*, 57(12), pp. 1668–1675. doi: 10.1016/j.archoralbio.2012.04.022.
- Kämmerer, P. W. *et al.* (2017) 'Guided Bone Regeneration Using Collagen Scaffolds, Growth Factors, and Periodontal Ligament Stem Cells for Treatment of Peri-Implant Bone Defects In Vivo', *Stem Cells International*, 2017, pp. 1–9. doi: 10.1155/2017/3548435.
- Kato, A. *et al.* (2015) 'Combination of Root Surface Modification with BMP-2 and Collagen Hydrogel Scaffold Implantation for Periodontal Healing in Beagle Dogs', *The Open Dentistry Journal*, 9(1), pp. 52–59. doi: 10.2174/1874210601509010052.
- Kawanabe, N. *et al.* (2010) 'Isolation of multipotent stem cells in human periodontal ligament using stage-specific embryonic antigen-4', *Differentiation*, 79(2), pp. 74–83. doi: 10.1016/j.diff.2009.10.005.
- Khalil, S., Nam, J. and Sun, W. (2005) 'Multi-nozzle deposition for construction of 3D biopolymer tissue scaffolds', *Rapid Prototyping Journal*, 11(1), pp. 9–17. doi: 10.1108/13552540510573347.
- Kii, I. *et al.* (2006) 'Periostin is an extracellular matrix protein required for eruption of incisors in mice.', *Biochemical and biophysical research communications*, 342(3), pp. 766–772. doi: 10.1016/j.bbrc.2006.02.016.
- Kim, S.-H. *et al.* (2009) 'Alveolar Bone Regeneration by Transplantation of Periodontal Ligament Stem Cells and Bone Marrow Stem Cells in a Canine Peri-Implant Defect Model: A Pilot Study', *Journal of Periodontology*, 80(11), pp. 1815–1823. doi: 10.1902/jop.2009.090249.
- Kinane, D. F., Stathopoulou, P. G. and Papapanou, P. N. (2017) 'Periodontal diseases', *Nature Reviews Disease Primers*, 3(1), p. 17038. doi: 10.1038/nrdp.2017.38.
- Koch, L. *et al.* (2010) 'Laser Printing of Skin Cells and Human Stem Cells', *Tissue Engineering Part C: Methods*, 16(5), pp. 847–854. doi: 10.1089/ten.tec.2009.0397.
- Kolk, A. *et al.* (2012) 'Current trends and future perspectives of bone substitute materials – From space holders to innovative biomaterials', *Journal of Cranio-Maxillofacial Surgery*, 40(8), pp. 706–718. doi: 10.1016/j.jcms.2012.01.002.
- Komaki, M. *et al.* (2012) 'Cementum protein 1 (CEMP1) induces a cementoblastic phenotype and reduces osteoblastic differentiation in periodontal ligament cells', *Journal of Cellular Physiology*, 227(2), pp. 649–657. doi: 10.1002/jcp.22770.

- Krampera, M. (2011) 'Mesenchymal stromal cell "licensing": a multistep process', *Leukemia*, 25(9), pp. 1408–1414. doi: 10.1038/leu.2011.108.
- Kumar, G. S. (2019) *Orban's Oral Histology and Embryology*. 15th edn. Elsevier.
- Lalla, E. and Papapanou, P. N. (2011) 'Diabetes mellitus and periodontitis: a tale of two common interrelated diseases', *Nature Reviews Endocrinology*, 7(12), pp. 738–748. doi: 10.1038/nrendo.2011.106.
- Lauritano, D. et al. (2020) 'Nanomaterials for Periodontal Tissue Engineering: Chitosan-Based Scaffolds. A Systematic Review', *Nanomaterials*, 10(4), p. 605. doi: 10.3390/nano10040605.
- Lee, C. H. et al. (2014) 'Three-Dimensional Printed Multiphase Scaffolds for Regeneration of Periodontium Complex', *Tissue Engineering Part A*, 20(7–8), pp. 1342–1351. doi: 10.1089/ten.tea.2013.0386.
- Lee, J. S. et al. (2014) 'Transdifferentiation of human periodontal ligament stem cells into pancreatic cell lineage', *Cell Biochemistry and Function*, 32(7), pp. 605–611. doi: 10.1002/cbf.3057.
- Lekic, P. and McCulloch, C. A. G. (1996) 'Periodontal ligament cell populations: The central role of fibroblasts in creating a unique tissue', *Anatomical Record*, 245(2), pp. 327–341. doi: 10.1002/(SICI)1097-0185(199606)245:2<327::AID-AR15>3.0.CO;2-R.
- Lekic, P., Sodek, J. and McCulloch, C. A. G. (1996) 'Osteopontin and bone sialoprotein expression in regenerating rat periodontal ligament and alveolar bone', *The Anatomical Record*, 244(1), pp. 50–58. doi: 10.1002/(SICI)1097-0185(199601)244:1<50::AID-AR5>3.0.CO;2-J.
- Li, J. et al. (2019) 'Osteogenic capacity and cytotherapeutic potential of periodontal ligament cells for periodontal regeneration in vitro and in vivo', *PeerJ*, 7, p. e6589. doi: 10.7717/peerj.6589.
- Li, X. et al. (2014) 'Comprehensive characterization of four different populations of human mesenchymal stem cells as regards their immune properties, proliferation and differentiation', *International Journal of Molecular Medicine*, 34(3), pp. 695–704. doi: 10.3892/ijmm.2014.1821.
- Li, Yuan et al. (2021) 'Biomechanical and biological responses of periodontium in orthodontic tooth movement: up-date in a new decade', *International Journal of Oral Science*, 13(1), p. 20. doi: 10.1038/s41368-021-00125-5.
- Lian, J. B. and Stein, G. S. (1995) 'Development of the osteoblast phenotype: molecular mechanisms mediating osteoblast growth and differentiation.', *The Iowa orthopaedic journal*, 15, pp. 118–40. Available at: <http://www.ncbi.nlm.nih.gov/pubmed/7634023>.
- Lian, J. and Stein, G. (2003) 'Runx2/Cbfa1: A Multifunctional Regulator of Bone Formation', *Current Pharmaceutical Design*, 9(32), pp. 2677–2685. doi: 10.2174/1381612033453659.
- Lin, G. et al. (2008) 'Defining Stem and Progenitor Cells within Adipose Tissue', *Stem Cells and Development*, 17(6), pp. 1053–1063. doi: 10.1089/scd.2008.0117.
- Lin, G. et al. (2011) 'Tissue Distribution of Mesenchymal Stem Cell Marker Stro-1', *Stem Cells and Development*, 20(10), pp. 1747–1752. doi: 10.1089/scd.2010.0564.
- Linask, K. K. and Lash, J. W. (1988) 'A role for fibronectin in the migration of avian precardiac cells', *Developmental Biology*, 129(2), pp. 315–323. doi: 10.1016/0012-1606(88)90378-8.
- Lindroos, B. et al. (2008) 'Characterisation of human dental stem cells and buccal mucosa fibroblasts', *Biochemical and Biophysical Research Communications*, 368(2), pp. 329–335. doi:

10.1016/j.bbrc.2008.01.081.

Liu, H. W. *et al.* (1997) 'A Collagenous Cementum-Derived Attachment Protein Is a Marker for Progenitors of the Mineralized Tissue-Forming Cell Lineage of the Periodontal Ligament', *Journal of Bone and Mineral Research*, 12(10), pp. 1691–1699. doi: 10.1359/jbmr.1997.12.10.1691.

Liu, J. *et al.* (2015) 'Concise Reviews: Characteristics and Potential Applications of Human Dental Tissue-Derived Mesenchymal Stem Cells', *STEM CELLS*, 33(3), pp. 627–638. doi: 10.1002/stem.1909.

Liu, J. *et al.* (2019) 'Macrophage polarization in periodontal ligament stem cells enhanced periodontal regeneration', *Stem Cell Research & Therapy*, 10(1), p. 320. doi: 10.1186/s13287-019-1409-4.

Liu, Q. *et al.* (2006) 'Expression of Scleraxis in human periodontal ligament cells and gingival fibroblasts.', *Zhonghua kou qiang yi xue za zhi = Zhonghua kouqiang yixue zazhi = Chinese journal of stomatology*, 41(9), pp. 556–8. doi: 17129431.

Liu, Y. *et al.* (2008) 'Periodontal Ligament Stem Cell-Mediated Treatment for Periodontitis in Miniature Swine', *STEM CELLS*, 26(4), pp. 1065–1073. doi: 10.1634/stemcells.2007-0734.

Luan, X. *et al.* (2006) 'Dental follicle progenitor cell heterogeneity in the developing mouse periodontium.', *Stem cells and development*, 15(4), pp. 595–608. doi: 10.1089/scd.2006.15.595.

Lv, F.-J. *et al.* (2014) 'Concise Review: The Surface Markers and Identity of Human Mesenchymal Stem Cells', *STEM CELLS*, 32(6), pp. 1408–1419. doi: 10.1002/stem.1681.

M. Kaplan, J., E. Youd, M. and A. Lodie, T. (2011) 'Immunomodulatory Activity of Mesenchymal Stem Cells', *Current Stem Cell Research & Therapy*, 6(4), pp. 297–316. doi: 10.2174/157488811797904353.

Maeda, H. *et al.* (2011) 'Periodontal Ligament Stem Cells', in *Stem Cells in Clinic and Research*. IntechOpen, pp. 619–636. doi: 10.5772/23749.

Mafi, P. *et al.* (2011) 'Adult mesenchymal stem cells and cell surface characterization - a systematic review of the literature.', *The open orthopaedics journal*, 5(Suppl 2), pp. 253–60. doi: 10.2174/1874325001105010253.

Mancini, L., Fratini, A. and Marchetti, E. (2021) 'Periodontal Regeneration', *Encyclopedia*, 1(1), pp. 87–98. doi: 10.3390/encyclopedia1010011.

Marie, P. J., Hay, E. and Saidak, Z. (2014) 'Integrin and cadherin signaling in bone: role and potential therapeutic targets', *Trends in Endocrinology & Metabolism*, 25(11), pp. 567–575. doi: 10.1016/j.tem.2014.06.009.

Di Martino, A., Sittering, M. and Risbud, M. V (2005) 'Chitosan: a versatile biopolymer for orthopaedic tissue-engineering.', *Biomaterials*, 26(30), pp. 5983–90. doi: 10.1016/j.biomaterials.2005.03.016.

McCulloch, C. A. G. *et al.* (1987) 'Paravascular cells in endosteal spaces of alveolar bone contribute to periodontal ligament cell populations', *The Anatomical Record*, 219(3), pp. 233–242. doi: 10.1002/ar.1092190304.

McCulloch, C. A. G., Lekic, P. and McKee, M. D. (2000) 'Role of physical forces in regulating the form and function of', *Periodontology 2000*, 24, pp. 56–72.

McCulloch, C. A. G. and Melcher, A. H. (1983) 'Cell density and cell generation in the periodontal ligament of mice', *American Journal of Anatomy*, 167(1), pp. 43–58. doi: 10.1002/aja.1001670105.

Meisel, R. *et al.* (2004) 'Human bone marrow stromal cells inhibit allogeneic T-cell responses by indoleamine 2,3-dioxygenase-mediated tryptophan degradation', *Blood*, 103(12), pp. 4619–4621. doi:

10.1182/blood-2003-11-3909.

Melcher, A. H. (1985) 'Cells of periodontium: their role in the healing of wounds.', *Annals of the Royal College of Surgeons of England*, 67(2), pp. 130–1. Available at: <http://www.ncbi.nlm.nih.gov/pubmed/3977253>.

Menicanin, D. *et al.* (2014) 'Periodontal-Ligament-Derived Stem Cells Exhibit the Capacity for Long-Term Survival, Self-Renewal, and Regeneration of Multiple Tissue Types in Vivo', *Stem Cells and Development*, 23(9), pp. 1001–1011. doi: 10.1089/scd.2013.0490.

Merle, B. and Garnero, P. (2012) 'The multiple facets of periostin in bone metabolism', *Osteoporosis International*, 23(4), pp. 1199–1212. doi: 10.1007/s00198-011-1892-7.

Michalowicz, B. S. *et al.* (2000) 'Evidence of a Substantial Genetic Basis for Risk of Adult Periodontitis', *Journal of Periodontology*, 71(11), pp. 1699–1707. doi: 10.1902/jop.2000.71.11.1699.

Mitchell, J. B. *et al.* (2006) 'Immunophenotype of human adipose-derived cells: temporal changes in stromal-associated and stem cell-associated markers.', *Stem cells (Dayton, Ohio)*, 24(2), pp. 376–85. doi: 10.1634/stemcells.2005-0234.

Mitsiadis, T. A. and Graf, D. (2009) 'Cell fate determination during tooth development and regeneration', *Birth Defects Research Part C: Embryo Today: Reviews*, 87(3), pp. 199–211. doi: 10.1002/bdrc.20160.

Mohamed-Ahmed, S. *et al.* (2018) 'Adipose-derived and bone marrow mesenchymal stem cells: a donor-matched comparison', *Stem Cell Research & Therapy*, 9(1), p. 168. doi: 10.1186/s13287-018-0914-1.

Mooney, D. J. and Vandenburgh, H. (2008) 'Cell delivery mechanisms for tissue repair.', *Cell stem cell*, 2(3), pp. 205–13. doi: 10.1016/j.stem.2008.02.005.

Mrozik, K. *et al.* (2017) 'A Method to Isolate, Purify, and Characterize Human Periodontal Ligament Stem Cells', in, pp. 413–427. doi: 10.1007/978-1-4939-6685-1_24.

Murphy, C. M., Haugh, M. G. and O'Brien, F. J. (2010) 'The effect of mean pore size on cell attachment, proliferation and migration in collagen–glycosaminoglycan scaffolds for bone tissue engineering', *Biomaterials*, 31(3), pp. 461–466. doi: 10.1016/j.biomaterials.2009.09.063.

Nagamura-Inoue, T. (2014) 'Umbilical cord-derived mesenchymal stem cells: Their advantages and potential clinical utility', *World Journal of Stem Cells*, 6(2), p. 195. doi: 10.4252/wjsc.v6.i2.195.

Nagatomo, K. *et al.* (2006) 'Stem cell properties of human periodontal ligament cells', *Journal of Periodontal Research*, 41(4), pp. 303–310. doi: 10.1111/j.1600-0765.2006.00870.x.

Nakamura, S. *et al.* (2019) 'Acceleration of bone regeneration of horizontal bone defect in rats using collagen-binding basic fibroblast growth factor combined with collagen scaffolds', *Journal of Periodontology*, 90(9), pp. 1043–1052. doi: 10.1002/JPER.18-0674.

Nanci, A. (2017) *Ten Cate's Oral Histology Development, Structure, and Function ANTONIO NANCI, PhD (McGill), PhD Honoris causa (University of Messina)*. 9th edn, E. 9th edn. Elsevier Health Sciences.

Nanci, A. and Bosshardt, D. D. (2006) 'Structure of periodontal tissues in health and disease.', *Periodontology 2000*, 40, pp. 11–28. doi: 10.1111/j.1600-0757.2005.00141.x.

Ng, T. K. *et al.* (2015) 'Transdifferentiation of periodontal ligament-derived stem cells into retinal

ganglion-like cells and its microRNA signature', *Scientific Reports*, 5(1), p. 16429. doi: 10.1038/srep16429.

Di Nicola, M. *et al.* (2002) 'Human bone marrow stromal cells suppress T-lymphocyte proliferation induced by cellular or nonspecific mitogenic stimuli', *Blood*, 99(10), pp. 3838–3843. doi: 10.1182/blood.V99.10.3838.

Ning, H. *et al.* (2006) 'Neuron-like differentiation of adipose tissue-derived stromal cells and vascular smooth muscle cells', *Differentiation*, 74(9–10), pp. 510–518. doi: 10.1111/j.1432-0436.2006.00081.x.

Nociti, F. H., Casati, M. Z. and Duarte, P. M. (2015) 'Current perspective of the impact of smoking on the progression and treatment of periodontitis', *Periodontology 2000*, 67(1), pp. 187–210. doi: 10.1111/prd.12063.

Nohutcu, R. M. *et al.* (1997) 'Expression of extracellular matrix proteins in human periodontal ligament cells during mineralization in vitro.', *Journal of periodontology*, 68(4), pp. 320–7. doi: 10.1902/jop.1997.68.4.320.

Nojima, N. *et al.* (1990) 'Fibroblastic cells derived from bovine periodontal ligaments have the phenotypes of osteoblasts', *Journal of Periodontal Research*, 25(3), pp. 179–185. doi: 10.1111/j.1600-0765.1990.tb01041.x.

Nyman, S. *et al.* (1982) 'New attachment following surgical treatment of human periodontal disease', *Journal of Clinical Periodontology*, 9(4), pp. 290–296. doi: 10.1111/j.1600-051X.1982.tb02095.x.

Obregon, F. *et al.* (2015) 'Three-Dimensional Bioprinting for Regenerative Dentistry and Craniofacial Tissue Engineering', *Journal of Dental Research*, 94(9_suppl), pp. 143S-152S. doi: 10.1177/0022034515588885.

Okubo, N. *et al.* (2010) 'Vascular Cell-Like Potential of Undifferentiated Ligament Fibroblasts to Construct Vascular Cell-Specific Marker-Positive Blood Vessel Structures in a PI3K Activation-Dependent Manner', *Journal of Vascular Research*, 47(5), pp. 369–383. doi: 10.1159/000277724.

Olszta, M. J. *et al.* (2007) 'Bone structure and formation: A new perspective', *Materials Science and Engineering: R: Reports*, 58(3–5), pp. 77–116. doi: 10.1016/j.mser.2007.05.001.

Padial-Molina, M. *et al.* (2013) 'Tumor Necrosis Factor- α and Porphyromonas gingivalis Lipopolysaccharides Decrease Periostin in Human Periodontal Ligament Fibroblasts', *Journal of Periodontology*, 84(5), pp. 694–703. doi: 10.1902/jop.2012.120078.

Park, C. H. *et al.* (2012) 'Tissue engineering bone-ligament complexes using fiber-guiding scaffolds', *Biomaterials*, 33(1), pp. 137–145. doi: 10.1016/j.biomaterials.2011.09.057.

Park, J.-Y., Jeon, S. H. and Choung, P.-H. (2011) 'Efficacy of Periodontal Stem Cell Transplantation in the Treatment of Advanced Periodontitis', *Cell Transplantation*, 20(2), pp. 271–286. doi: 10.3727/096368910X519292.

Pelaez, D. *et al.* (2017) 'Cardiomyogenesis of periodontal ligament-derived stem cells by dynamic tensile strain', *Cell and Tissue Research*, 367(2), pp. 229–241. doi: 10.1007/s00441-016-2503-x.

Peng, C. *et al.* (2018) 'Response of hPDLSCs on 3D printed PCL/PLGA composite scaffolds in vitro', *Molecular Medicine Reports*. doi: 10.3892/mmr.2018.9076.

Perinelli, D. R. *et al.* (2018) 'Chitosan-based nanosystems and their exploited antimicrobial activity', *European Journal of Pharmaceutical Sciences*, 117, pp. 8–20. doi: 10.1016/j.ejps.2018.01.046.

Petrenko, Y. *et al.* (2020) 'A Comparative Analysis of Multipotent Mesenchymal Stromal Cells derived from Different Sources, with a Focus on Neuroregenerative Potential', *Scientific Reports*, 10(1), p. 4290. doi: 10.1038/s41598-020-61167-z.

Pieri, F. *et al.* (2009) 'Effect of Mesenchymal Stem Cells and Platelet-Rich Plasma on the Healing of Standardized Bone Defects in the Alveolar Ridge: A Comparative Histomorphometric Study in Minipigs', *Journal of Oral and Maxillofacial Surgery*, 67(2), pp. 265–272. doi: 10.1016/j.joms.2008.06.036.

Pihlstrom, B. L., Michalowicz, B. S. and Johnson, N. W. (2005) 'Periodontal diseases.', *Lancet (London, England)*, 366(9499), pp. 1809–20. doi: 10.1016/S0140-6736(05)67728-8.

Pispa, J. and Thesleff, I. (2003) 'Mechanisms of ectodermal organogenesis', *Developmental Biology*, 262(2), pp. 195–205. doi: 10.1016/S0012-1606(03)00325-7.

Pöschke, A. *et al.* (2018) 'Molecular Characteristics of the Equine Periodontal Ligament', *Frontiers in Veterinary Science*, 4. doi: 10.3389/fvets.2017.00235.

Preshaw, P. M., Seymour, R. A. and Heasman, P. A. (2004) 'Current Concepts in Periodontal Pathogenesis', *Dental Update*, 31(10), pp. 570–578. doi: 10.12968/denu.2004.31.10.570.

Qiu, J. *et al.* (2020) 'Enhancement of periodontal tissue regeneration by conditioned media from gingiva-derived or periodontal ligament-derived mesenchymal stem cells: a comparative study in rats', *Stem Cell Research & Therapy*, 11(1), p. 42. doi: 10.1186/s13287-019-1546-9.

Ren, G. *et al.* (2010) 'Inflammatory Cytokine-Induced Intercellular Adhesion Molecule-1 and Vascular Cell Adhesion Molecule-1 in Mesenchymal Stem Cells Are Critical for Immunosuppression', *The Journal of Immunology*, 184(5), pp. 2321–2328. doi: 10.4049/jimmunol.0902023.

Rios, H. *et al.* (2005) 'Periostin Null Mice Exhibit Dwarfism, Incisor Enamel Defects, and an Early-Onset Periodontal Disease-Like Phenotype', *Molecular and Cellular Biology*, 25(24), pp. 11131–11144. doi: 10.1128/MCB.25.24.11131-11144.2005.

Roberts, T. T. and Rosenbaum, A. J. (2012) 'Bone grafts, bone substitutes and orthobiologics', *Organogenesis*, 8(4), pp. 114–124. doi: 10.4161/org.23306.

Romanos, G. E. *et al.* (2014) 'PERIOSTIN: role in formation and maintenance of dental tissues.', *Journal of cellular physiology*, 229(1), pp. 1–5. doi: 10.1002/jcp.24407.

Sant, S. *et al.* (2011) 'Hybrid PGS-PCL microfibrinous scaffolds with improved mechanical and biological properties', *Journal of Tissue Engineering and Regenerative Medicine*, 5(4), pp. 283–291. doi: 10.1002/term.313.

dos Santos, F. *et al.* (2009) 'Ex vivo expansion of human mesenchymal stem cells: A more effective cell proliferation kinetics and metabolism under hypoxia', *Journal of Cellular Physiology*, p. n/a-n/a. doi: 10.1002/jcp.21987.

Sanz, M. *et al.* (2010) 'European workshop in periodontal health and cardiovascular disease--scientific evidence on the association between periodontal and cardiovascular diseases: a review of the literature', *European Heart Journal Supplements*, 12(Suppl B), pp. B3–B12. doi: 10.1093/eurheartj/suq003.

Sculean, A. *et al.* (2015) 'Biomaterials for promoting periodontal regeneration in human intrabony defects: a systematic review', *Periodontology 2000*, 68(1), pp. 182–216. doi: 10.1111/prd.12086.

Seo, B. *et al.* (2004) 'Investigation of multipotent postnatal stem cells from human periodontal

ligament', pp. 149–155. doi: 10.1016/S0140-6736(04)16627-0.

Shafiee, A. *et al.* (2011) 'A comparison between osteogenic differentiation of human unrestricted somatic stem cells and mesenchymal stem cells from bone marrow and adipose tissue', *Biotechnology Letters*, 33(6), pp. 1257–1264. doi: 10.1007/s10529-011-0541-8.

Shi, Y. *et al.* (2018) 'Immunoregulatory mechanisms of mesenchymal stem and stromal cells in inflammatory diseases', *Nature Reviews Nephrology*, 14(8), pp. 493–507. doi: 10.1038/s41581-018-0023-5.

Shimauchi, H. *et al.* (2013) 'Possible functional scaffolds for periodontal regeneration', *Japanese Dental Science Review*, 49(4), pp. 118–130. doi: 10.1016/j.jdsr.2013.05.001.

Shinagawa-Ohama, R. *et al.* (2017) 'Heterogeneous Human Periodontal Ligament-Committed Progenitor and Stem Cell Populations Exhibit a Unique Cementogenic Property Under In Vitro and In Vivo Conditions', *Stem Cells and Development*, 26(9), pp. 632–645. doi: 10.1089/scd.2016.0330.

Shue, L., Yufeng, Z. and Mony, U. (2012) 'Biomaterials for periodontal regeneration', *Biomatter*, 2(4), pp. 271–277. doi: 10.4161/biom.22948.

Siddiqui, N. *et al.* (2018) 'PCL-Based Composite Scaffold Matrices for Tissue Engineering Applications', *Molecular Biotechnology*, 60(7), pp. 506–532. doi: 10.1007/s12033-018-0084-5.

Silva, B. S. e *et al.* (2017) 'Epithelial rests of Malassez: from latent cells to active participation in orthodontic movement', *Dental Press Journal of Orthodontics*, 22(3), pp. 119–125. doi: 10.1590/2177-6709.22.3.119-125.sar.

Silva, J. C., Carvalho, M. S., *et al.* (2020) 'Extracellular matrix decorated polycaprolactone scaffolds for improved mesenchymal stem/stromal cell osteogenesis towards a patient-tailored bone tissue engineering approach', *Journal of Biomedical Materials Research Part B: Applied Biomaterials*, 108(5), pp. 2153–2166. doi: 10.1002/jbm.b.34554.

Silva, J. C., Moura, C. S., *et al.* (2020) 'Extruded Bioreactor Perfusion Culture Supports the Chondrogenic Differentiation of Human Mesenchymal Stem/Stromal Cells in 3D Porous Poly(ϵ -Caprolactone) Scaffolds', *Biotechnology Journal*, 15(2), p. 1900078. doi: 10.1002/biot.201900078.

Simmons, P. J. and Torok-Storb, B. (1991) 'Identification of stromal cell precursors in human bone marrow by a novel monoclonal antibody, STRO-1.', *Blood*, 78(1), pp. 55–62. Available at: <http://www.ncbi.nlm.nih.gov/pubmed/2070060>.

Sims, M. R. (1975) 'Oxytalan-vascular relationships observed in histologic examination of the periodontal ligaments of man and mouse.', *Archives of oral biology*, 20(11), pp. 713–6. doi: 10.1016/0003-9969(75)90040-0.

Smaida, R. *et al.* (2020) 'Potential Implantable Nanofibrous Biomaterials Combined with Stem Cells for Subchondral Bone Regeneration', *Materials*, 13(14), p. 3087. doi: 10.3390/ma13143087.

Smith, A. (2006) 'A glossary for stem-cell biology', *Nature*, 441(1060). doi: 10.1038/nature04954.

Sommer (2010) 'Neural crest-derived stem cells', in *StemBook*, pp. 1–20. doi: 10.3824/stembook.1.51.1.

Soskolne, W. A. and Klinger, A. (2001) 'The Relationship Between Periodontal Diseases and Diabetes: An Overview', *Annals of Periodontology*, 6(1), pp. 91–98. doi: 10.1902/annals.2001.6.1.91.

de Sousa, E. *et al.* (2014) 'Synovial fluid and synovial membrane mesenchymal stem cells: latest

discoveries and therapeutic perspectives', *Stem Cell Research & Therapy*, 5(5), p. 112. doi: 10.1186/scrt501.

Stein, G. S., Lian, J. B. and Owen, T. A. (1990) 'Relationship of cell growth to the regulation of tissue-specific gene expression during osteoblast differentiation.', *FASEB journal : official publication of the Federation of American Societies for Experimental Biology*, 4(13), pp. 3111–23. doi: 10.1096/fasebj.4.13.2210157.

Stewart, K. *et al.* (1999) 'Further characterization of cells expressing STRO-1 in cultures of adult human bone marrow stromal cells.', *Journal of bone and mineral research : the official journal of the American Society for Bone and Mineral Research*, 14(8), pp. 1345–56. doi: 10.1359/jbmr.1999.14.8.1345.

Strem, B. M. *et al.* (2005) 'Multipotential differentiation of adipose tissue-derived stem cells', *The Keio Journal of Medicine*, 54(3), pp. 132–141. doi: 10.2302/kjm.54.132.

Strydom, H. *et al.* (2012) 'The oxytalan fibre network in the periodontium and its possible mechanical function.', *Archives of oral biology*, 57(8), pp. 1003–11. doi: 10.1016/j.archoralbio.2012.06.003.

Sukpaita, T. *et al.* (2019) 'In Vivo Bone Regeneration Induced by a Scaffold of Chitosan/Dicarboxylic Acid Seeded with Human Periodontal Ligament Cells', *International Journal of Molecular Sciences*, 20(19), p. 4883. doi: 10.3390/ijms20194883.

Suvas, S. *et al.* (2002) 'Distinct Role of CD80 and CD86 in the Regulation of the Activation of B Cell and B Cell Lymphoma', *Journal of Biological Chemistry*, 277(10), pp. 7766–7775. doi: 10.1074/jbc.M105902200.

Takeshita, S. *et al.* (1993) 'Osteoblast-specific factor 2: cloning of a putative bone adhesion protein with homology with the insect protein fasciclin I.', *The Biochemical journal*, 294 (Pt 1, pp. 271–8. doi: 10.1042/bj2940271.

Tamaki, Y. *et al.* (2013) 'In vitro analysis of mesenchymal stem cells derived from human teeth and bone marrow', *Odontology*, 101(2), pp. 121–132. doi: 10.1007/s10266-012-0075-0.

Tang, G. *et al.* (2020) 'Recent Advances of Chitosan-Based Injectable Hydrogels for Bone and Dental Tissue Regeneration', *Frontiers in Bioengineering and Biotechnology*, 8. doi: 10.3389/fbioe.2020.587658.

Taylor, G. W. (2001) 'Bidirectional Interrelationships Between Diabetes and Periodontal Diseases: An Epidemiologic Perspective', *Annals of Periodontology*, 6(1), pp. 99–112. doi: 10.1902/annals.2001.6.1.99.

Techawattanawisal, W. *et al.* (2007) 'Isolation of multipotent stem cells from adult rat periodontal ligament by neurosphere-forming culture system', *Biochemical and Biophysical Research Communications*, 357(4), pp. 917–923. doi: 10.1016/j.bbrc.2007.04.031.

Thiagarajan, L., Abu-Awwad, H. A.-D. M. and Dixon, J. E. (2017) 'Osteogenic Programming of Human Mesenchymal Stem Cells with Highly Efficient Intracellular Delivery of RUNX2', *STEM CELLS Translational Medicine*, 6(12), pp. 2146–2159. doi: 10.1002/sctm.17-0137.

Tomokiyo, A. *et al.* (2018) 'Detection, Characterization, and Clinical Application of Mesenchymal Stem Cells in Periodontal Ligament Tissue', *Stem Cells International*, 2018, pp. 1–9. doi: 10.1155/2018/5450768.

- Tomokiyo, A., Wada, N. and Maeda, H. (2019) 'Periodontal Ligament Stem Cells: Regenerative Potency in Periodontium', *Stem Cells and Development*, 28(15), pp. 974–985. doi: 10.1089/scd.2019.0031.
- Torii, D. *et al.* (2015) 'Cementogenic potential of multipotential mesenchymal stem cells purified from the human periodontal ligament', *Odontology*, 103(1), pp. 27–35. doi: 10.1007/s10266-013-0145-y.
- Tran, H. L. B. *et al.* (2014) 'Various methods for isolation of multipotent human periodontal ligament cells for regenerative medicine', *In Vitro Cellular & Developmental Biology - Animal*, 50(7), pp. 597–602. doi: 10.1007/s11626-014-9748-z.
- Trubiani, O. *et al.* (2005) 'Morphological and Cytofluorimetric Analysis of Adult Mesenchymal Stem Cells Expanded Ex Vivo from Periodontal Ligament', *International Journal of Immunopathology and Pharmacology*, 18(2), pp. 213–221. doi: 10.1177/039463200501800204.
- Trubiani, O. *et al.* (2010) 'Expression profile of the embryonic markers nanog, OCT-4, SSEA-1, SSEA-4, and frizzled-9 receptor in human periodontal ligament mesenchymal stem cells', *Journal of Cellular Physiology*, 225(1), pp. 123–131. doi: 10.1002/jcp.22203.
- Uccelli, A., Moretta, L. and Pistoia, V. (2008) 'Mesenchymal stem cells in health and disease', *Nature Reviews Immunology*, 8(9), pp. 726–736. doi: 10.1038/nri2395.
- Vasandan, A. B. *et al.* (2014) 'Functional differences in mesenchymal stromal cells from human dental pulp and periodontal ligament', *Journal of Cellular and Molecular Medicine*, 18(2), pp. 344–354. doi: 10.1111/jcmm.12192.
- Wada, N. *et al.* (2009) 'Immunomodulatory properties of human periodontal ligament stem cells', *Journal of Cellular Physiology*, 219(3), pp. 667–676. doi: 10.1002/jcp.21710.
- Wang, X. *et al.* (2017) 'Expression of CD44 standard form and variant isoforms in human bone marrow stromal cells', *Saudi Pharmaceutical Journal*, 25(4), pp. 488–491. doi: 10.1016/j.jsps.2017.04.011.
- Woo, D.-H., Hwang, H. S. and Shim, J. H. (2016) 'Comparison of adult stem cells derived from multiple stem cell niches', *Biotechnology Letters*, 38(5), pp. 751–759. doi: 10.1007/s10529-016-2050-2.
- Woo, H. N. *et al.* (2021) 'The recent advances in scaffolds for integrated periodontal regeneration', *Bioactive Materials*, 6(10), pp. 3328–3342. doi: 10.1016/j.bioactmat.2021.03.012.
- Xu, J. *et al.* (2009) 'Multiple Differentiation Capacity of STRO-1 + /CD146 + PDL Mesenchymal Progenitor Cells', *Stem Cells and Development*, 18(3), pp. 487–496. doi: 10.1089/scd.2008.0113.
- Xu, L. *et al.* (2017) 'Tissue source determines the differentiation potentials of mesenchymal stem cells: a comparative study of human mesenchymal stem cells from bone marrow and adipose tissue', *Stem Cell Research & Therapy*, 8(1), p. 275. doi: 10.1186/s13287-017-0716-x.
- Xu, T. *et al.* (2005) 'Inkjet printing of viable mammalian cells', *Biomaterials*, 26(1), pp. 93–99. doi: 10.1016/j.biomaterials.2004.04.011.
- Xu, X. *et al.* (2013) 'Gingivae contain neural-crest- and mesoderm-derived mesenchymal stem cells', *Journal of Dental Research*, 92(9), pp. 825–832. doi: 10.1177/0022034513497961.
- Xu, X. *et al.* (2019) 'Concise Review: Periodontal Tissue Regeneration Using Stem Cells: Strategies and Translational Considerations', *STEM CELLS Translational Medicine*, 8(4), pp. 392–403. doi: 10.1002/sctm.18-0181.

- Xue, R. *et al.* (2017) 'Polycaprolactone nanofiber scaffold enhances the osteogenic differentiation potency of various human tissue-derived mesenchymal stem cells', *Stem Cell Research & Therapy*, 8(1), p. 148. doi: 10.1186/s13287-017-0588-0.
- Yamada, S. *et al.* (2007) 'PLAP-1/Asporin, a Novel Negative Regulator of Periodontal Ligament Mineralization', *Journal of Biological Chemistry*, 282(32), pp. 23070–23080. doi: 10.1074/jbc.M611181200.
- Yamada, S. *et al.* (2014) 'Characterization of a Novel Periodontal Ligament-specific Periostin Isoform', *Journal of Dental Research*, 93(9), pp. 891–897. doi: 10.1177/0022034514543015.
- Yamada, S., Kitamura, M. and Murakami, S. (2008) 'PLAP-1: A novel molecule regulating homeostasis of periodontal tissues', *Japanese Dental Science Review*, 44(2), pp. 137–144. doi: 10.1016/j.jdsr.2008.07.002.
- Yamada, Y. *et al.* (2004) 'Autogenous Injectable Bone for Regeneration with Mesenchymal Stem Cells and Platelet-Rich Plasma: Tissue-Engineered Bone Regeneration', *Tissue Engineering*, 10(5–6), pp. 955–964. doi: 10.1089/1076327041348284.
- Yamaguchi, M. and Mishima, H. (2021) 'The Role of RANKL and Involvement of Cementum in Orthodontic Root Resorption', *Applied Sciences*, 11(16), p. 7244. doi: 10.3390/app11167244.
- Yan, X.-Z. *et al.* (2014) 'Human Periodontal Ligament Derived Progenitor Cells: Effect of STRO-1 Cell Sorting and Wnt3a Treatment on Cell Behavior', *BioMed Research International*, 2014, pp. 1–10. doi: 10.1155/2014/145423.
- Yang, Y.-H. K. *et al.* (2018) 'Changes in phenotype and differentiation potential of human mesenchymal stem cells aging in vitro', *Stem Cell Research & Therapy*, 9(1), p. 131. doi: 10.1186/s13287-018-0876-3.
- Yang, Y. and El Haj, A. J. (2006) 'Biodegradable scaffolds – delivery systems for cell therapies', *Expert Opinion on Biological Therapy*, 6(5), pp. 485–498. doi: 10.1517/14712598.6.5.485.
- Yang, Z. X. *et al.* (2013) 'CD106 Identifies a Subpopulation of Mesenchymal Stem Cells with Unique Immunomodulatory Properties', *PLoS ONE*. Edited by A. Vergani, 8(3), p. e59354. doi: 10.1371/journal.pone.0059354.
- Yoshizawa, T. *et al.* (2004) 'Homeobox protein MSX2 acts as a molecular defense mechanism for preventing ossification in ligament fibroblasts.', *Molecular and cellular biology*, 24(8), pp. 3460–72. doi: 10.1128/MCB.24.8.3460-3472.2004.
- Yu, N. *et al.* (2013) 'Enhanced periodontal tissue regeneration by periodontal cell implantation', *Journal of Clinical Periodontology*, 40(7), pp. 698–706. doi: 10.1111/jcpe.12113.
- Yu, Z. and Philippe, G. (2015) 'Differential Properties of Human ALP+ Periodontal Ligament Stem Cells vs Their ALP- Counterparts', *Journal of Stem Cell Research & Therapy*, 05(07). doi: 10.4172/2157-7633.1000292.
- Yuan, X. *et al.* (2018) 'A Wnt-Responsive PDL Population Effectuates Extraction Socket Healing.', *Journal of dental research*, 97(7), pp. 803–809. doi: 10.1177/0022034518755719.
- Zang, S. *et al.* (2019) 'Injectable chitosan/ β -glycerophosphate hydrogels with sustained release of BMP-7 and ornidazole in periodontal wound healing of class III furcation defects', *Materials Science and Engineering: C*, 99, pp. 919–928. doi: 10.1016/j.msec.2019.02.024.

Zannettino, A. C. W. *et al.* (2008) 'Multipotential human adipose-derived stromal stem cells exhibit a perivascular phenotype in vitro and in vivo', *Journal of Cellular Physiology*, 214(2), pp. 413–421. doi: 10.1002/jcp.21210.

Zein, I. *et al.* (2002) 'Fused deposition modeling of novel scaffold architectures for tissue engineering applications', *Biomaterials*, 23(4), pp. 1169–1185. doi: 10.1016/S0142-9612(01)00232-0.

Zhai, Q. *et al.* (2019) 'Dental stem cell and dental tissue regeneration', *Frontiers of Medicine*, 13(2), pp. 152–159. doi: 10.1007/s11684-018-0628-x.

Zhang, X., Fan, W. and Liu, T. (2020) 'Fused deposition modeling 3D printing of polyamide-based composites and its applications', *Composites Communications*, 21, p. 100413. doi: 10.1016/j.coco.2020.100413.

Zhao, R. *et al.* (2021) 'Bone Grafts and Substitutes in Dentistry: A Review of Current Trends and Developments', *Molecules*, 26(10), p. 3007. doi: 10.3390/molecules26103007.

Ziegler, N. *et al.* (2010) 'Mechano-transduction in periodontal ligament cells identifies activated states of MAP-kinases p42/44 and p38-stress kinase as a mechanism for MMP-13 expression', *BMC Cell Biology*, 11(1), p. 10. doi: 10.1186/1471-2121-11-10.

Zuk, P. A. *et al.* (2002) 'Human Adipose Tissue Is a Source of Multipotent Stem Cells', *Molecular Biology of the Cell*. Edited by M. Raff, 13(12), pp. 4279–4295. doi: 10.1091/mbc.e02-02-0105.